AD_____

Award Number: W81XWH-09-1-0300

TITLE: The Mechanism of Action of Unique Small Molecules that Inhibit the Pim Protein Kinase Blocking Prostate Cancer Cell Growth

PRINCIPAL INVESTIGATOR: Andrew S. Kraft, M.D.

CONTRACTING ORGANIZATION: Medical University of South Carolina
Charleston, SC 29425

REPORT DATE: May 2012

TYPE OF REPORT: Revised Final

PREPARED FOR: U.S. Army Medical Research and Materiel Command
Fort Detrick, Maryland 21702-5012

DISTRIBUTION STATEMENT: Approved for Public Release;
Distribution Unlimited

The views, opinions and/or findings contained in this report are those of the author(s) and should not be construed as an official Department of the Army position, policy or decision unless so designated by other documentation.

REPORT DOCUMENTATION PAGE

Form Approved
OMB No. 0704-0188

Public reporting burden for this collection of information is estimated to average 1 hour per response, including the time for reviewing instructions, searching existing data sources, gathering and maintaining the data needed, and completing and reviewing this collection of information. Send comments regarding this burden estimate or any other aspect of this collection of information, including suggestions for reducing this burden to Department of Defense, Washington Headquarters Services, Directorate for Information Operations and Reports (0704-0188), 1215 Jefferson Davis Highway, Suite 1204, Arlington, VA 22202-4302. Respondents should be aware that notwithstanding any other provision of law, no person shall be subject to any penalty for failing to comply with a collection of information if it does not display a currently valid OMB control number. **PLEASE DO NOT RETURN YOUR FORM TO THE ABOVE ADDRESS.**

1. REPORT DATE	2. REPORT TYPE	3. DATES COVERED
May 2012	Revised Final	1 May 2009 - 30 April 2012

4. TITLE AND SUBTITLE
The Mechanism of Action of Unique Small Molecules that Inhibit the Pim Protein Kinase Blocking Prostate Cancer Cell Growth

5a. CONTRACT NUMBER

5b. GRANT NUMBER
W81XWH-09-1-0300

5c. PROGRAM ELEMENT NUMBER

6. AUTHOR(S)

Andrew S. Kraft, M.D.

E-Mail: kraft@musc.edu

5d. PROJECT NUMBER

5e. TASK NUMBER

5f. WORK UNIT NUMBER

7. PERFORMING ORGANIZATION NAME(S) AND ADDRESS(ES)

Medical University of South Carolina
Charleston, SC 29425

8. PERFORMING ORGANIZATION REPORT NUMBER

9. SPONSORING / MONITORING AGENCY NAME(S) AND ADDRESS(ES)
U.S. Army Medical Research and Materiel Command
Fort Detrick, Maryland 21702-5012

10. SPONSOR/MONITOR'S ACRONYM(S)

11. SPONSOR/MONITOR'S REPORT NUMBER(S)

12. DISTRIBUTION / AVAILABILITY STATEMENT
Approved for public release; distribution unlimited

13. SUPPLEMENTARY NOTES

14. ABSTRACT:

The Pim protein kinase is over expressed in prostate cancer. To clarify the role of this protein in regulating prostate cancer growth we have investigated its mechanism of action. We have examined the ability of small molecule inhibitors of this kinase to combine with other agents and have developed two rationally developed dual therapies. First, because overexpression of Bcl-2 family members is implicated in chemotherapeutic resistance in prostate cancer, we investigated the cooperative effects of Pim kinase inhibition with ABT-737, a small molecule antagonist of Bcl-2 family members. Strikingly, the addition of ABT-737 to Pim inhibitors triggered a robust apoptosis of prostate cancer cells in vitro and in vivo. Second, we demonstrate that inhibition of AKT in prostate cancer cell lines not only induces the expression of multiple RTKs, but increases the protein levels of serine threonine protein kinase Pim-1. Pim-1 activity is identified as essential in the feedback regulation of RTK levels by AKT inhibition. Both tissue culture and animal experiments demonstrate that the combination of AKT and Pim inhibitors provides synergistic inhibition of tumor growth. Thus Pim inhibitor has potential activity to treat this cancer.

15. SUBJECT TERMS
Pim Kinases, Prostate Cancer, Cell Cycle, Kinase Inhibitors, SKP-2

16. SECURITY CLASSIFICATION OF:			17. LIMITATION OF ABSTRACT	18. NUMBER OF PAGES	19a. NAME OF RESPONSIBLE PERSON
U					USAMRMC
a. REPORT	b. ABSTRACT	c. THIS PAGE	UU	82	19b. TELEPHONE NUMBER *(include area code)*
U	U	U			

Standard Form 298 (Rev. 8-98)
Prescribed by ANSI Std. Z39.18

Table of Contents

	Page
Introduction……..…….…..	**4**
Body…….	**4**
Key Research Accomplishments…….…….	**8**
Reportable Outcomes……	**9**
Conclusion……	**10**
Appendix……	**12**

INTRODUCTION (Subject, purpose, and scope)

The overexpression of the serine/threonine Pim protein kinase in normal or cancerous prostate cells stimulates the growth of these cells. Pim is over expressed in human prostate cancer, and its level may parallel the onset of metastatic disease. In animal models the expression of the c-Myc protein is associated with increased Pim protein levels. Thus, data from tissue culture, human and animal prostate cancer implicates the Pim protein in prostate tumorigenesis. In this application we suggest that Pim regulates the levels of the cell cycle inhibitor p27. We have hypothesized that this decrease will coordinate with elevated c-Myc in tumor cells to drive tumor growth. Our laboratory has developed novel benzylidene thiazolidine-2, 4 diones, (D5, SMI-4a) that inhibit the activity of Pim kinase. These agents reverse Pim activity and allow the level of p27 to rise. This protein will then function to inhibit tumor growth. The first goal of this grant was to understand the mechanism by which Pim protein kinases regulate p27. We have completed this work and published the mechanism in the Journal of Biological Chemistry (see reportable outcomes) in which we detail the ability of Pim to phosphorylate both Skp-2 and Cdc27. The second goal of this work is to determine the mechanism by which Pim controls the levels of c-Myc and whether c-Myc content parallels the level of Pim protein kinase. We have examined this question in a paper in the Proceedings of the National Academy of Sciences in which we demonstrate that the knock-out of all Pim protein kinases decreases the levels of c-Myc protein (see reportable outcomes). Finally, the third goal of this proposal was to evaluate the anti-tumor activity of the Pim protein kinases and decipher whether inhibition of one or more isoforms was necessary to inhibit tumor growth. We have completed this goal and submitted a publication to Journal of Experimental Medicine (see reportable outcomes).

BODY

Our research efforts have focused on the Statement of Work, and in an attempt to bring together data that will satisfy the needs of a peer reviewed publication. The results of these experiments are documented in the enclosed paper and have been submitted to the Journal of Biologic Chemistry. Rather than separating these tasks into individual goals for simplicity we have combined this description.

Task 2(a, b) in year 1 and Task 1 and 2 (a, b) in year 2. (Reportable outcomes: J Biol Chem 285 (38): 29128-29137, 2010) we have found that the overexpression of active Pim1 protein kinase but not kinase dead decreases the level of p27 protein. To evaluate the mechanism we have focused our attention on the Skp2 protein which bind directly to p27 and activates the E3 ligase which ubiquinates p27 leading to its degradation. We demonstrate that knocking down Pim-1 kinase increases Skp-2 and decreases p27 levels. Similarly, we find that inhibition of Pim kinases with increasing doses of our small molecule Pim kinase inhibitor, SMI-4a [called in the past D5], decreases the level of Skp-2 and increases p27 protein. In tissue culture, overexpression of Pim-1 in normal mouse prostate epithelial cells increased Skp-2 levels while decreasing p27 protein. Experiments carried out in which the half-life of the Skp-2 protein was evaluated by adding cycloheximide to cells demonstrated that the expression of Pim-1 markedly increased the half-life of Skp-2 protein. These results suggest that the regulation of Skp-2 by

Pim-1 decreases p27 levels. This effect is inhibited by SMI-4a, the Pim kinase inhibitors we have developed.

To evaluate how Pim and Skp-2 may interact we examined whether these proteins could coimmunoprecipitate. Both kinases active and dead Pims will bind directly to the Skp-2 protein. Immunoprecipitating Pim-1 from serum stimulated cells demonstrates that Pim and Skp-2 associate in a cell cycle dependent manner. To evaluate how Pim-1 might affect the half-life of the Skp-2 protein we evaluated whether Pim-1 could regulate the ubiquination of Skp-2. We find that if a tagged Skp-2 and 6xHis-ubiquitin plasmids are transfected into cells along with Pim-1 that the ubiquination of Skp-2 is inhibited, explaining the increased levels of this protein. In addition, we find that Pim-1 can phosphorylate Skp-2 and the addition of our inhibitor, SMI-4a, can block the Pim-1 to modify the Skp-2 protein. Together these results suggest that the Pim protein kinase binds to Skp-2 and inhibits its ubiquination possibly in part secondary to the ability of Pim-1 to phosphorylate Skp-2.

We have used GST fusion proteins to evaluate the phosphorylation of Skp2. Skp-2 is thought to be phosphorylated on serine 64 and 72. We have defined a new phosphorylation site on this protein that is modified by Pim-1. If this site is mutated in Skp-2 it partially decreases the phosphorylation of this protein. This result suggests that Skp-2 is a target of Pim and that 417 and potentially other sites are phosphorylated. Expanding this experimental approach mutation of S64 or S72 also inhibits Pim phosphorylation of Skp-2. Our small molecule Pim inhibitor, SMI-4a, blocks the Pim-induced phosphorylation of this protein. To evaluate the potential effects of these phosphorylations on the half-life of this protein each of these three sites was mutated, transfected into cells, which were then treated with cycloheximide and the half-life of the protein examined by Western blotting. We find that each of these phosphorylation mutants shortens the half-life of these proteins. Another approach to examining the importance of these phosphorylation sites is to cotransfect Skp-2 and p27. If Skp-2 is active then p27 levels will be lowered. We find in *Figure 13c* that mutation of T417 and to a greater extent S64 but not S72 affects the level of p27. In conclusion, Pim phosphorylates Skp-2 on S64, S72, and T417 and this phosphorylation regulates the half-life of Skp-2 and thus the levels of p27. Our Pim inhibitors block this phosphorylation and thus would raise the levels of p27.

To discern how Pim might regulate Skp-2 ubiquination, we examined in detail the APC/C complex either Cdc20 or Cdc27. This E3 ligase is regulated by. We find that the addition of Pim-1 to cells dissociates the Cdc27 regulator protein from the APC/C complex, and knocking Pim-1 down using siRNA increases the amount of this protein. We find that Pim-1 is capable of phosphorylating Cdc27 but not Cdc20 both *in vitro* and when over expressed in cells.

Based on the interaction between and Pim-1 protein kinase and Skp-2 we have transfected either one or both of these proteins into prostate cells and examined the levels of p27 and the location of cells in the cell cycle. We find that cells expressing both proteins have the lowest levels of p27, the fewest cells in G1 and the most cells in the G2 phase of the cell cycle. This result is highly significant. Our small molecule inhibitor of Pim-1 (SMI-4a) can block the ability of Skp-2 or serum to drive cells into the G2 phase of the cell cycle and stimulate an increase in p27. We include a model for how the Pim kinase can regulate the levels of Skp-2. Pim-1 can phosphorylate both Skp-2 and CDC27 and lead to their destruction. This combined effect can be

inhibited by SMI-4a. Our novel Pim inhibitor can be developed as a compound that increases the levels of p27, blocks progression through the cell cycle, and inhibits tumor growth.

Task 3 completed in year 3. (Reportable outcome - Proceedings of the National Academy of Sciences. 108:528-533, 2011) This task asked us to evaluate the interaction between the c-Myc protein and Pim kinase using our unique small molecule Pim inhibitor, SMI-4a. To evaluate this interaction, we have chosen to step back from the complicated prostate cancer models usually employed in Pim research, and attempt to initially simplify this analysis using MEFs from animals that are missing all of the 3 Pim kinase isoforms. Because there is no Pim kinase activity the biology of these cells mimics the effect of a small molecule Pim inhibitor with no off target effects. We find that the triple KO cells do not grow well but the addition to these cells of Pim 3 to these cells stimulated their growth similar to normal. In contrast Pim-2 stimulated intermediate growth and Pim-1 alone was not capable of stimulating the growth of these cells at all.

These results are of importance to the prostate cancer field because immunohistochemistry of human prostate cancers compared to normal paired samples from the same patient showed that Pim-3 was over expressed in prostate tumors.

These TKO cells evidenced lower levels of ATP and higher amounts of AMP. The increased AMP is shown to stimulate the AMP-dependent protein kinase (AMPK) in these cells (Fig. 3b). Interestingly the over expression of Pim-3 is shown to reverse the levels of AMP:ATP, and to inhibit AMPK. Additionally, Pim-3 is shown to elevate the levels of c-Myc, both from MEFs derived from Pim-3 only mice and TKO MEFs that express Pim-3 after transduction. To examine how Pim-3 elevated the levels of c-Myc we first did cycloheximide treatment and release. Results demonstrate that TKO/Pim-3 cells synthesize more c-Myc at earlier time points. When a polysome protocol was carried out c-Myc mRNA was found to associate with the polysomes in TKO/Pim-3 and WT MEFs, but in TKO MEFs the c-Myc mRNA was found to be associated with free ribosomes, suggesting that 5' initiated translation was blocked in the absence of the Pims.

We also demonstrate that Pim-3 is capable of elevating the levels of the PGC-1a. Even though both c-Myc and Pim-3 increase the growth of TKO MEFs only Pim-3 is able markedly increase the level of PGC-1α protein. Transduction of PGC-1α into TKO MEFs raised the levels of ATP and lowered the level of phosphorylated AMPK, suggesting that the ability of Pim-3 to control this enzyme is essential for its mechanism of action.

We therefore propose a model by which Pim-3 regulate PGC-1α, lowering the levels of AMP, stimulating mTORC1 activity and increasing the synthesis of c-Myc stimulating the growth of these fibroblasts. We are in the process of validating this model in prostate cancer cells but initial results suggest that there is a significant degree of overlap. First, we find that the levels of Pim-3 are elevated in human prostate cancer cells by IHC. Second, PC-3 and LNCaP cells transfected with Pim-3 grow much better in serum or serum free conditions, suggesting that Pim-3 may be controlling cellular ATP levels.

Task 3 to be completed in year 3. (Reportable outcome: Cancer Research, 2012 Jan 1:72(1):294-303) This task asked us to evaluate the activity of specific Pim inhibitors. We have carried out a study of the Pim inhibitor SMI-4a and published this in Cancer Research in 2012. This work is summarized as follows. Because overexpression of Bcl-2 family members is implicated in chemotherapeutic resistance in prostate cancer, we investigated the cooperative effects of Pim kinase inhibition with ABT-737, a small molecule antagonist of Bcl-2 family members. Strikingly, the addition of ABT-737 to Pim inhibitors triggered a robust apoptosis of prostate cancer cells in vitro and in vivo. Pim inhibitors decreased levels of the Bcl-2 family member Mcl-1, both by blocking 5'-cap dependent translation and decreasing protein half life. In addition, Pim inhibition transcriptionally increased levels of the BH3 protein Noxa by activating the unfolded protein response (UPR), lead to eIF-2α phosphorylation and increased expression of CHOP. Increased levels of Noxa also inactivated the remaining levels of Mcl-1 protein activity. Notably, these specific protein changes were essential to the apoptotic process because ABT-737 did not inhibit Mcl-1 protein activity and Mcl-1 overexpression blocked the apoptotic activity of ABT-737. Our results therefore suggest that this combination treatment could be developed as a potential therapy for human prostate cancer where overexpression of Pim kinases and anti-apoptotic Bcl-2 family members drives tumor cell resistance to current anticancer therapies.

(Reportable outcome: Journal of Experimental Medicine submitted) Another approach to treating prostate cancer is targeting prostate cancer treatment is to block the AKT signaling pathway. Through mutation of PTEN, PI3 kinase, or AKT itself, this pathway is activated in prostate cancer in 50-70% of patients. For this reason pharmaceutical companies have invested in developing molecules that inhibit these enzymes. Importantly, we find that when AKT inhibitors are used to treat prostate cancer that they cause a feedback stimulation of the levels of cell surface receptor tyrosine kinases (RTKs). This increase in RTKs will then enhance AKT stimulation, blunting the effect of these drugs. We find that the AKT inhibitor, GSK690693, not only increases RTK levels but of importance also elevates the levels of Pim-1, but not Pim-2, or Pim-3. Results demonstrate that the AKT inhibitor (GSK-690693) increases Pim-1 transcriptionally.

Importantly, we have discovered that inhibiting or decreasing the level of Pim-1, blocks the feedback ability of AKT inhibitors to elevate the levels of RTKs. This can be shown either using genetic knockouts, siRNAs or the small molecule Pim-1 inhibitor, SMI-4a. This may suggest that inhibiting only Pim-1 will be sufficient to block the feedback increase in RTKs.

The mechanism by which Pim-1 regulates RTKs is unknown. Inhibitors of the mTORC1 activity do not block this increase suggesting that it is cap-independent .We find that both GSK690693 and Pim-1 are able to stimulate translation from an internal ribosome entry site (IRES). In this case we show that c-Met can be activated. This experiment involved cloning the IRES sequence of c-Met in front of firefly luciferase and then examining whether Pim-1 could regulate this sequence. Decreases in Pim-1 levels decreased firefly luciferase while increasing Pim-1 increases this readout. Based on these results we have combined a Pim-1 and AKT inhibitor and shown that they can synergistically inhibit cell growth on plastic, soft-agar growth of prostate cancer cells, and block the subcutaneous growth of tumors in nude mice. These data suggest that this combination by blocking feedback regulation can inhibit tumor growth and may be a novel drug therapy for prostate cancer.

KEY RESEARCH ACCOMPLISHMENTS

- Increases in Pim-1 kinase decreases Skp-2 levels and thus allows p27 protein to increase.
- The changes in these proteins are inhibited by the small molecule Pim-1 inhibitor we have developed.
- Pim-1 binds to Skp-2 and inhibits its ubiquination and thus degradation.
- Skp-2 is phosphorylated by Pim-1 and our small molecule Pim inhibitors block this effect.
- Threonine 417 in Skp-2 is identified as a new phosphorylation site in Skp-2
- Serines 64 and 72 are mapped as Pim phosphorylation sites.
- Pim-directed phosphorylation controls the half-life and activity of Skp-2.
- Pim regulates the phosphorylation of Cdc27 to bind to the APC/C, and controls the phosphorylation of this protein.
- Pim-1 plus Skp-2 enhances transition through the cell cycle.
- Pim kinase inhibitory compounds block the ability of cells to transverse the cell cycle.
- Pim inhibitor treatment of prostate cancer decreased levels of Bcl-2 family member Mcl-1.
- Incubation with Pim inhibitors raised the levels of the Noxa protein.
- Noxa protein levels were increased by an activation of unfolded protein response that led to eIF-2a phosphorylation and increased expression of CHOP.
- These induced protein changes sensitized prostate cancer cells to the pro-apoptotic action of ABT-737, a small molecule that inhibits the activity of Bcl-2 family members.
- In animal models, ABT-737 and the Pim inhibitor SMI-4a (D5) had synergistic activity in killing prostate cancers implanted subcutaneously.
- Inhibition of AKT in prostate cancer cells elevates the levels of both Pim-1, but not Pim-2 or Pim-3, and cell surface receptor tyrosine kinases (RTKs).
- Inhibition of Pim-1 with inhibitor, SMI-4a, or decreasing the level of Pim-1 protein inhibited the ability of AKT inhibitors to induce RTKs.
- AKT inhibition leads to the transcriptional up regulation of Pim-1.
- Pim-1 or small molecule AKT inhibitors are able to increase the levels of RTKs by a cap-independent mechanism.
- The combination of a Pim-1 and AKT inhibitor is synergistic in killing prostate cancer cells in tissue culture and in an animal model.
- Knocking down Pim-1 or inhibiting it with small molecule Pim inhibitor SMI-4a blocked mTORC1 activity.
- Inhibiting Pim-1 led to increases in AMP kinase activity, a known mTORC1 inhibitor
- Mouse embryo fibroblasts (MEFs) which were knock-out for all three Pims (TKO) grew much more slowly than wild type and had elevated ratios of AMP:ATP
- TKO MEFs had elevated AMPK activity.
- These MEFs had decreased rates of protein synthesis and decreased levels of c-Myc protein.
- Elevating the levels of Pim-3 alone was sufficient to markedly increase growth, stimulate increases in c-Myc protein levels, and elevate the levels of PGC-1α.
- Transduction of PGC-1α was sufficient to elevate ATP and c-Myc protein.

REPORTABLE OUTCOMES

Abstracts

1. Cen B, Zemskova M, Beharry Z, Smith C D, Kraft AS. The Pim-1 protein kinase decreases p27 protein half-life and increases prostate epithelial cell migration. AACR Annual Meeting 2009
2. Beharry Z, Lin Y, Mahajan S, Zemskova M, Xia Z, Smith C, Kraft AS. The Pim protein kinases modulate mTOR activity by regulating the protein and mRNA levels of mTOR pathway components and cellular AMP levels. AACR Special Conference in Cancer Research-Metabolism and Cancer. September 2009, La Jolla, CA
3. Kraft AS, Cen B, Zemskova M, Beharry Z, Smith C. Potent protein kinase inhibitors block Pim kinase mediated increase in prostate epithelial cell migration, regulation of p27 protein half-life and secretion of hepatocyte growth factor. AACR Molecular Targets and Cancer Therapeutics Conference, 2009
4. Kraft AS, Beharry Z, Lin Y, Mahajan S, Zemskova M, Xia Z, Smith C. Treatment with the Pim protein kinase inhibitor SMI-4a enhances AMPK phosphorylation, decreases Raptor levels, and blocks mTORC1 activity. AACR Molecular Targets and Cancer Therapeutics Conference, 2009
5. Song JH, Kraft AS. Mechanisms of Therapy-Induced Senescence with ABT-737. AACR 102nd Annual Meeting, 2011
6. Song JH, Kraft AS. Pim Protein Kinase Induce the Unfolded Protein Response and Sensitize Prostate Cancer Cells to Killing by ABT-737-Mediated Apoptosis. AACR Annual Meeting, Advances in Prostate Cancer Research, 2012
7. Song JH, Kraft AS. Pim Kinase Inhibitors Sensitize Cancer Cells to Apoptosis Triggered by Bcl-2 Family Inhibitor ABT-737. AACR Annual Meeting, Advances in Prostate Cancer Research, 2012
8. Cen B, Sandeep M, Kraft AS. Overcoming Resistance to Inhibitors of the AKT Protein Kinases by Targeting the Pim Protein Kinase Pathway. AACR Annual Meeting, Advances in Prostate Cancer Research, 2012

Papers

1. Cen B, Sandeep M, Zemskova M, Beharry Z, Lin YW, Cramer SD, Lilly M, and Kraft AS. Regulation of SKP2 Levels by the PIM-1 Protein Kinase. J Biol Chem 285 (38): 29128-29137, 2010. PMID 20663873, PMCID: PMC2937943
2. Beharry Z, Mahajan S, Zemskova M, Lin Y-W, Tholanikunnel B, Xia Z, Smith CD, and Kraft AS. The Pim protein kinases regulate energy metabolism and cell growth. Proceedings of the National Academy of Sciences. 108:528-533, 2011, PMID:21187426, PMCID: PMC3021022
3. Song JH, Kraft AS. Pim Kinase Inhibitors Sensitize Prostate Cancer Cells to Apoptosis Triggered by Bcl-2 Family Inhibitor ABT-737. Cancer Research, 2012 Jan 1:72(1):294-303, PMID: 22080570, PMCID: PMC3251634 (available 2013/1/1)
4. Cen B, Mahajan S, Wang W, and Kraft AS. Pim-1 Mediates the Elevation of Receptor Tyrosine Kinases Induced by Small Molecule AKT Inhibitors in Prostate Cancer Cells. Submitted Journal of Experimental Medicine 2012

CONCLUSIONS

We can conclude from this research that Pim remains an important target for treatment of human prostate cancer. The Pim-1 protein kinase clearly plays a role in controlling the levels of p27 and transition through the cell cycle. *This work demonstrates that small molecule inhibitors of this protein kinase, such as SMI-4a, will have activity as a treatment for prostate cancer.*

Human prostate cancer cell lines and tumors have all three Pims, 1, 2 and 3. Further research needs to qualify whether inhibition of one or all three Pims is needed to inhibit cell cycle movement to a greater extent than inhibition of Pim-1 alone. Answering this question will greatly assist in the development of targeted therapies to inhibit prostate cancer growth.

The serine/threonine Pim kinases are overexpressed in prostate cancers and promote cell growth and survival. Here, we find that a novel Pim kinase inhibitor, SMI-4a, or Pim-1 siRNA blocked the rapamycin-sensitive mammalian target of rapamycin (mTORC1) activity by stimulating the phosphorylation and thus activating the mTORC1 negative regulator AMP-dependent protein kinase (AMPK). Mouse embryonic fibro- blasts (MEFs) deficient for all three Pim kinases [triple knockout (TKO) MEFs] demonstrated activated AMPK driven by elevated ratios of AMP:ATP relative to wild-type MEFs. Consistent with these findings, TKO MEFs were found to grow slowly in culture and have decreased rates of protein synthesis secondary to a diminished amount of 5-cap–dependent translation. Pim-3 expression alone in TKO MEFs was sufficient to reverse AMPK activation, increase protein synthesis, and drive MEF growth similar to wild type. Pim-3 expression was found to markedly increase the protein levels of both c-Myc and the peroxisome proliferator-activated receptor gamma coactivator 1α (PGC-1α), enzymes capable of regulating glycolysis and mitochondrial biogenesis, which were diminished in TKO MEFs. Overexpression of PGC-1α in TKO MEFs elevated ATP levels and inhibited the activation of AMPK. These results demonstrate the Pim kinase-mediated control of energy metabolism and thus regulation of AMPK activity. We identify an important role for Pim-3 in modulating c-Myc and PGC-1α protein levels and cell growth. We find by IHC of human samples that Pim-3 is elevated in human prostate cancer, suggesting that these results will impact on human prostate cancer growth.

The serine threonine Pim protein kinases are overexpressed in prostate cancers and promote cell growth and survival. The PI3K/AKT pathway is activated in over 60% of human prostate cancers, suggesting that compounds that inhibit this pathway may be useful for therapy. However, accumulating evidence indicates that feedback regulation in response to inhibition of PI3K/AKT signaling pathway may attenuate antitumor activity of inhibitors by increasing the level of cell surface receptor tyrosine kinases (RTKs). We demonstrate that inhibition of AKT in prostate cancer cell lines not only induces the expression of multiple RTKs, but increases the protein levels of serine threonine protein kinase Pim-1. Pim-1 activity is identified as essential in the feedback regulation of RTK levels by AKT inhibition. Knockdown of Pim-1 expression or inhibition of Pim-1 activity with small molecules abrogates the induction of RTKs and overexpression of Pim-1 increases RTK levels. Experiments using dual luciferase vectors demonstrate that Pim-1 controls expression of c-Met and other RTKs at the translational level by modulating IRES activity in a cap-independent manner. Both tissue culture and animal experiments demonstrate that the combination of AKT and Pim inhibitors provides synergistic

inhibition of tumor growth. Our results demonstrate that Pim-1 is a novel mediator of resistance to AKT inhibition, and that targeting Pim kinases significantly improves the efficacy of AKT inhibitors in anticancer therapy.

So What -

The combination therapy of a Pim and AKT inhibitor could be brought into the clinic. This work might suggest that inhibition of Pim-1 and not Pim-2 or 3 might be sufficient as dual therapy. Alternatively, the observations in mouse embryo fibroblasts suggest that it is important to inhibit all Pim kinases. This work suggests that Skp-2 levels and phosphorylation might act as a biomarker of drug action. Our published work from this grant funding also demonstrates additional possible combinations of Pim inhibitors and agents that block the Bcl-2 pathway.

APPENDIX

Abstracts

1. Cen B, Zemskova M, Beharry Z, Smith C D, Kraft AS. The Pim-1 protein kinase decreases p27 protein half-life and increases prostate epithelial cell migration. AACR Annual Meeting 2009
2. Beharry Z, Lin Y, Mahajan S, Zemskova M, Xia Z, Smith C, Kraft AS. The Pim protein kinases modulate mTOR activity by regulating the protein and mRNA levels of mTOR pathway components and cellular AMP levels. AACR Special Conference in Cancer Research-Metabolism and Cancer. September 2009, La Jolla, CA
3. Kraft AS, Cen B, Zemskova M, Beharry Z, Smith C. Potent protein kinase inhibitors block Pim kinase mediated increase in prostate epithelial cell migration, regulation of p27 protein half-life and secretion of hepatocyte growth factor. AACR Molecular Targets and Cancer Therapeutics Conference, 2009
4. Kraft AS, Beharry Z, Lin Y, Mahajan S, Zemskova M, Xia Z, Smith C. Treatment with the Pim protein kinase inhibitor SMI-4a enhances AMPK phosphorylation, decreases Raptor levels, and blocks mTORC1 activity. AACR Molecular Targets and Cancer Therapeutics Conference, 2009
5. Song JH, Kraft AS. Mechanisms of Therapy-Induced Senescence with ABT-737. AACR 102nd Annual Meeting, 2011
6. Song JH, Kraft AS. Pim Protein Kinase Induce the Unfolded Protein Response and Sensitize Prostate Cancer Cells to Killing by ABT-737-Mediated Apoptosis. AACR Annual Meeting, Advances in Prostate Cancer Research, 2012
7. Song JH, Kraft AS. Pim Kinase Inhibitors Sensitize Cancer Cells to Apoptosis Triggered by Bcl-2 Family Inhibitor ABT-737. AACR Annual Meeting, Advances in Prostate Cancer Research, 2012
8. Cen B, Sandeep M, Kraft AS. Overcoming Resistance to Inhibitors of the AKT Protein Kinases by Targeting the Pim Protein Kinase Pathway. AACR Annual Meeting, Advances in Prostate Cancer Research, 2012

Papers

1. Cen B, Sandeep M, Zemskova M, Beharry Z, Lin YW, Cramer SD, Lilly M, and Kraft AS. Regulation of SKP2 Levels by the PIM-1 Protein Kinase. J Biol Chem 285 (38): 29128-29137, 2010. PMID 20663873, PMCID: PMC2937943
2. Beharry Z, Mahajan S, Zemskova M, Lin Y-W, Tholanikunnel B, Xia Z, Smith CD, and Kraft AS. The Pim protein kinases regulate energy metabolism and cell growth. Proceedings of the National Academy of Sciences. 108:528-533, 2011, PMID:21187426, PMCID: PMC3021022
3. Song JH, Kraft AS. Pim Kinase Inhibitors Sensitize Prostate Cancer Cells to Apoptosis Triggered by Bcl-2 Family Inhibitor ABT-737. Cancer Research, 2012 Jan 1:72(1):294-303, PMID: 22080570, PMCID: PMC3251634 (available 2013/1/1)
4. Cen B, Mahajan S, Wang W, and Kraft AS. Pim-1 Mediates the Elevation of Receptor Tyrosine Kinases Induced by Small Molecule AKT Inhibitors in Prostate Cancer Cells. Submitted Journal of Experimental Medicine 2012

The Pim-1 protein kinase decreases p27 protein half-life and increases prostate epithelial cell migration

Bo Cen, Marina Zemskova, Zanna Beharry, Charles D. Smith, Andrew S. Kraft

Medical University of South Carolina, Charleston, SC

Abstract

Pim-1 proto-oncogene encodes a serine/threonine protein kinase that regulates apoptosis, cell cycle progression, and transcription. The expression of this protein kinase is elevated in both prostate intraepithelial neoplasia (PIN) and prostatic adenocarcinoma, suggesting an important role for this protein kinase in prostate cancer growth and development. However, the mechanism by which Pim-1 promotes cell proliferation and transformation is not fully understood. To examine the role of kinase in regulating prostate cancer cell growth, we have overexpressed Pim in mouse prostate epithelial cells (MPECs), a cell line that demonstrates stem cell characteristics. We find that overexpression of Pim-1 markedly increases hepatocyte growth factor/ scatter factor (HGF/SF) induced migration of MPECs. This increased migration is completely inhibited by two novel small molecule Pim inhibitors 16a and 4a. Additionally we find that HGF/SF induced p27 upregulation in MPECs was strongly inhibited by the overexpression of Pim-1. Further studies showed that, overexpression of Pim-1 did not alter the mRNA level of p27, but enhanced the degradation and thus decreased the half-life of the p27 protein. The p27 degradation induced by Pim-1 was cell cycle dependent. Consistent with this finding ubiquitylation assays examining p27 demonstrate that Pim-1 increases this modification in vivo. We find that the Pim-1-mediated ubiquitinylation is regulated by complex formation between Pim-1 and Skp2. Skp2 levels, as part of the SCF protein complex, regulate the ubiquintylation and degradation of p27. Pim-1 does not affect Skp2's E3 ligase activity, but appears to inhibit the degradation of this protein. Pim-1 directly phosphorylates Skp2 in vitro, suggesting a mechanism for the stabilization of this protein. Together our data demonstrate the complex pathway by which Pim-1 protein kinase regulates p27 levels, and thus controls cell proliferation and possibly transformation.

The Pim protein kinases modulate mTOR activity by regulating the protein and mRNA levels of mTOR pathway components and cellular AMP levels

Zanna Beharry[1], Ying-Wei Lin[2], Sandeep Mahajan[4], Marina Zemskova[3], Zuping Xia[1], Charles Smith[1,4] and Andrew S. Kraft[4]

[1]Departments of Pharmaceutical and Biomedical Sciences, South Carolina College of Pharmacy, [2]Department of Pediatrics, [3]Department of Cell and Molecular Pharmacology, and [4]The Hollings Cancer Center, Medical University of South Carolina, Charleston, SC 29425

Abstract

We have identified a small molecule inhibitor of the Pim protein kinases, SMI-4a, and found that the addition of this compound to cells blocks the phosphorylation of the mTOR regulatory protein PRAS40 and subsequently the activity of the mTOR pathway (*Mol. Cancer. Ther.* (2009) 8: 1473; *Cancer Biol. Ther.* (2009) 8: 846). Now we show that the addition of SMI-4a to malignant cells increases the phosphorylation of AMPKα on Thr 172 in a LKB1-dependent manner, induces the phosphorylation of raptor on Ser792, decreases the levels of Raptor protein, and inhibits mTORC1 activity. Immunoprecipitation of mTOR from SMI-4a treated cells consistently showed lower levels of bound Raptor and *in vitro* mTOR kinase assays showed a decreased ability to phosphorylate 4E-BP1. Addition of proteasome inhibitors to these cells reversed the decrease in Raptor protein levels, suggesting that Pim kinases prevent the ubiquitin-mediated degradation of this protein. Knockdown of *PIM-1* via siRNA in K562 leukemic cells showed increased AMPKα phosphorylation and decreased raptor protein levels, further demonstrating an important role for Pim in regulating AMPK phosphorylation and Raptor levels. Additionally, mouse embryo fibroblasts (MEFs) deficient for Pim-1, Pim-2 and Pim-3 kinase (TKO MEFs) showed a significantly increased level of AMPKα phosphorylation compared to wild type MEFs. This was attributed to an increase in the cellular level of AMP in TKO MEFs as measured by HPLC. Furthermore, the correlation between increased AMPKα phosphorylation and a lower level of raptor protein observed with SMI-4a treatment or siRNA knockdown of Pim-1 in leukemic cells was also observed in TKO MEFs, along with a decrease in mTOR protein level. Transfection of individual Pim kinases into these TKO MEFs was able to reverse these effects, decreasing AMPKα phosphorylation, and increasing raptor and mTOR protein levels. The cellular activity of mTORC1 was difficult to assess in TKO MEFs as we found substantially lower protein levels of the mTORC1 substrates 4E-BP1 and p70S6K. However, mTORC2 activity was unaffected by Pim kinase knockout as Akt was readily phosphorylated upon serum stimulation of TKO MEFs. QT-PCR analysis of TKO MEFs demonstrated that the decrease in protein levels of 4E-BP1 correlated with a decrease in the mRNA encoding this protein. Our data demonstrate an important role for the Pim family of protein kinases in regulating the mTOR pathway by affecting the level of the pathway components through transcriptional and post-transcriptional mechanisms, as well as regulation of cellular AMP levels.

Potent protein kinase inhibitors block Pim kinase-mediated increase in prostate epithelial cell migration, regulation of p27 protein half-life, and secretion of hepatocyte growth factor

Andrew S. Kraft, Bo Cen, Marina Zemskova, Zanna Beharry and Charles D. Smith

Medical University of SC Hollings Cancer Center, Charleston, SC.

Abstract

Pim-1 proto-oncogene encodes a serine/threonine protein kinasethat regulates apoptosis, cell cycle progression, and transcription.The expression of this protein kinase is elevated in both prostateintraepithelial neoplasia (PIN) and prostatic adenocarcinoma,suggesting an important role for Pim-1 kinase in prostate cancerdevelopment and growth. To investigate the role of Pim-1 incontrolling tumor growth we have synthesized novel benzylidene-thiazolidine2,4-dione (J. Med. Chem. (2009) 52:74) inhibitors of this kinase.The most potent members of this chemotype have IC50s of 13 nMfor Pim-1. To examine the activity of these agents in prostatecancer we have first set out to define the biochemical activityof Pim-1 in epithelial cells. We have expressed Pim-1 in a mouseprostate epithelial cell (MPECs) line that demonstrates stemcell characteristics. We find that Pim-1 expressing cells produceand secrete markedly increased levels of hepatocyte growth factor/scatterfactor (HGF/SF), and this protein kinase stimulates increasesin HGF/SF mRNA. Additionally, expression of Pim-1 markedly increasesHGF/SF induced migration of MPECs. The contribution of Pim-1kinase to this biochemical pathway is confirmed in murine embryonicfibroblasts (MEFs) that are deficient for all three Pim proteinkinases (TKO) and evidence reduced level of HGF mRNA in TKOversus wild type MEFs. The Pim-1-stimulated migration of MPECsis inhibited by two benzylidene-thiazolidine-2, 4-diones, SMI-4aand 16a, as well as known inhibitors of the HGF receptor, c-Met.HGF treatment of MPECs induced p27 upregulation that could beinhibited by the expression of Pim-1, thus allowing cell cycleprogression. Further studies showed that expression of Pim-1did not alter the mRNA level of p27, but enhanced the cell cycle-dependentdegradation and thus decreased the half-life of the p27 protein.Consistent with this finding, p27 ubiquitination assays showedthat Pim-1 increases this modification in vivo. We found thatthe Pim-1-mediated ubiquitination is regulated by complex formationbetween Pim-1 and Skp2, a protein component of the SCF complex,which is known to regulate the ubiquitination and degradationof p27. Pim-1 does not affect Skp2's E3 ligase activity, butappears to inhibit the degradation of Skp2 through phosphorylation.Incubation of these cells with the Pim protein kinase inhibitor,SMI-4a, decreased Skp2 expression and increased p27 and cyclinE expression. Together our data demonstrates the complex pathwayby which Pim-1 protein kinase regulates HGF/SF and p27 levels,thus controlling cell migration, proliferation, and potentiallytransformation. Potent Pim kinase inhibitors block these twosignaling pathways thus inhibiting prostate epithelial cellmigration and growth.

Treatment with the Pim protein kinase inhibitor SMI-4a enhances AMPK phosphorylation, decreases Raptor levels, and blocks mTORC1 activity

Andrew S. Kraft1, Zanna Beharry1, Ying-Wei Lin1, Sandeep Mahajan1, Marina Zemskova1, Zuping Xia2 and Charles Smith1

1 Medical University of SC Hollings Cancer Center, Charleston, SC; 2 Medical University of SC College of Pharmacy, Charleston, SC.

Abstract

We have identified a class of small molecule inhibitors of the Pim protein kinases, benzylidene thiazolidine-2-4 diones (J.Med. Chem. (2009) 52:74) with the most potent members havingIC50s of 13 nM for Pim-1 and 2.3 µM for Pim-2. Compounds in this chemotype demonstrated selectivity of more than 2500-foldand 400-fold for Pim-1 or Pim-2 respectively while other congenershad equivalent potency towards both isozymes. In vivo, these molecules inhibited Pim kinase autophosphorylation and in amurine model inhibited the growth of subcutaneously implanted murine adenocarcinoma JC cells. One of the members of this chemotype,SMI-4a, has been shown to block the phosphorylation of the mTORregulatory protein PRAS40 and subsequently the activity of themTOR pathway (Mol. Cancer. Ther. (2009) 8: 1473; Cancer Biol.Ther. (2009) 8: 846). Now we show that the addition of SMI-4ato malignant cells increases the phosphorylation of AMPK onThr 172 in a LKB1-dependent manner, induces the phosphorylationo f Raptor on Ser792, decreases the levels of Raptor protein,and inhibits mTORC1 activity. Immunoprecipitation of mTOR fromSMI-4a treated cells consistently showed lower levels of bound Raptor and in vitro mTOR kinase assays from treated cells demonstrated a decreased ability to phosphorylate 4E-BP1. Knockdown of PIM-1via siRNA in K562 leukemic cells showed increased AMPK phosphorylation and decreased Raptor protein levels, further demonstrating an important role for Pim kinase in regulating AMPK phosphorylationand Raptor levels. Additionally, mouse embryo fibroblasts (MEFs)deficient for Pim-1, Pim-2 and Pim-3 kinase (TKO MEFs) showed a significantly increased level of AMPK phosphorylation compared to wild type MEFs, which correlated with decreased mTORC1 activity and increased binding of 4E-BP1 with eIF-4E. The TKO MEFs grew significantly more slowly than wild type. The decreased mTORC1activity correlated with an increase in the cellular level of AMP in TKO MEFs. Furthermore, the correlation between increased AMPK phosphorylation and a lower level of Raptor protein observed with SMI-4a treatment was also observed in TKO MEFs. Infectionof TKO MEFs with lentiviruses expressing Pim 1 or Pim2 was able to reverse these effects, decreasing AMPK phosphorylation, and increasing Raptor protein levels. The cellular activity of mTORC1was difficult to assess in TKO MEFs as we found substantially lower protein levels of the mTORC1 substrates 4E-BP1 and p70S6K.Akt was readily phosphorylated upon serum stimulation of TKOMEFs and mTORC2 activity was unchanged. Given the role of Pim kinase in regulating mTORC1 activity, we have combined SMI-4aand the mTOR inhibitor rapamycin inducing synergistic blockade of this pathway.

AACR American Association for Cancer Research 102nd ANNUAL MEETING
April 2-6, 2011 • Orange County Convention Center, Orlando, Florida

Presentation Abstract

Abstract Number:	2636
Presentation Title:	Mechanisms of therapy-induced senescence with ABT-737
Presentation Time:	Monday, Apr 04, 2011, 1:00 PM - 5:00 PM
Location:	Exhibit Hall A4-C, Poster Section 30
Poster Section:	30
Poster Board Number:	2
Author Block:	Jin H. Song, Andrew S. Kraft. Medical Univ. of South Carolina, Charleston, SC

Abstract Body:

Aberrant expression of the antiapoptotic Bcl-2 family of proteins in human cancer is correlated with poor outcomes after standard chemotherapy. ABT-737 is a cell permeable Bcl-2 family antagonist that is capable of binding to Bcl-2, Bcl-x_L, and Bcl-w. ABT-737 functions by displacing BH3 proteins, such as Bim, from these proteins activating Bax and Bak to induce apoptotic cell death. Resistance to ABT-737 appears to be mediated by the elevated expression of Mcl-1 or Bfl-1/A1 which are not capable of binding this compound. Since renal, prostate and lung carcinomas, exhibit elevated levels of endogenous Mcl-1 many of these tumor cell lines are resistant to killing by this agent.

Gene chip analysis in order to understand anticancer action of ABT-737 in human cancer cells reveals an intrigue data that ABT-737 regulates key genes involving cytokines and chemokines associated with senescence phenotype. Because senescence is considered to be a key mechanism that protects against cancer development, we investigated the mechanism of action for ABT-737 in human cancer cells where this compound is incapable of inducing apoptotic cell death, inhibit growth of tumor cells by the induction of cell senescence. Here, we identify a novel pathway involving the induction of DNA damage response by caspase-3 cleavage that normally induces apoptosis, which instead leads to promotion of cellular senescence.

Treatment of renal, lung and prostate cancer cell lines with ABT-737, but not an inactive enantiomer, caused the induction of senescence-associated β-galactosidase, and additional changes associated with the senescence phenotype including increases in specific gene transcription, secretion of IL-6 and IL-8, and stimulation of the activity of C/EBPβ. ABT-737 treatment of these cell lines induced activation of the DNA damage response pathway as demonstrated by increases in γ-H2AX and phosphorylation of both the ATM and Chk2 protein kinases. Decreasing ATM levels with shRNA blocked the senescent phenotype suggesting that this pathway was critical for the induction of ABT-737-mediated senescence. DNA damage induced by ABT-737 treatment was caused by low level activation of the caspase cascade, which was blocked by decreasing caspase-3 levels with shRNA. ABT-737-induced senescence appeared to be p53-dependent, since the overexpression of dominant-negative p53 inhibited the ABT-737-induced increases in p21 protein levels, β-galactosidase, and IL-6 transcription.

These findings suggest that in multiple cancer cell types where ABT-737 is incapable of inducing sufficient DNA damage to activate apoptosis, it instead inhibits cancer cell growth by inducing senescence, a phenotype that is associated with major changes in gene transcription and protein secretion.

American Association for Cancer Research
615 Chestnut St. 17th Floor
Philadelphia, PA 19106

Print this Page

AACR ANNUAL MEETING
March 31- April 4, 2012 • Chicago, IL

Presentation Abstract

Abstract Number:	LB-487
Presentation Title:	Pim protein kinase inhibitors induce the unfolded protein response and sensitize prostate cancer cells to killing by ABT-737-mediated apoptosis.
Presentation Time:	Wednesday, Apr 04, 2012, 8:00 AM - 12:00 PM
Location:	McCormick Place West (Hall F), Poster Section 37
Author Block:	*Jin H. Song*, *Andrew S. Kraft*. Medical University of South Carolina, Charleston, SC
Abstract Body:	Pim serine/threonine kinases contribute to prostate tumorigenesis and therapeutic resistance, yet anticancer efficacy of Pim kinase inhibitors on prostate cancer is unknown. We demonstrate for the first time that a genetically engineered decrease in Pim kinase levels or the addition of Pim kinase small molecule inhibitors (e.g. SMI-4a) to human prostate cancer cells, including LNCaP and PC-3, causes ER stress and activates the unfolded protein response (UPR) stimulating increases in eIF-2α phosphorylation, ATF-4, CHOP proteins, and cleavage of XBP-1. Because (1) Bcl-2 family proteins reside on the ER lumen and play an important role in regulation of XBP-1 splicing, (2) Bcl-2 family members are over expressed in prostate cancer to enhance Pim kinase anti-cancer activity, and (3) Pim kinase inhibitors decrease Mcl-1 and increase Noxa protein, we treated prostate cancer cell lines with SMI-4a plus the Bcl-2 family antagonist ABT-737, a small molecule antagonist of Bcl-2 family members. Strikingly, the addition of ABT-737 to Pim inhibitors triggered a robust apoptosis of prostate cancer cells in vitro and in vivo. Pim inhibitors decreased levels of the Bcl-2 family member Mcl-1, both by blocking 5'-cap dependent translation and decreasing protein half life. Additionally, Pim inhibition transcriptionally increased levels of the BH3 protein Noxa by activating the UPR, lead to eIF2α phosphorylation and increased expression of CHOP. Increased levels of Noxa also inactivated the remaining levels of Mcl-1 protein activity. Notably, these specific protein changes were essential to the apoptotic process because ABT-737 did not inhibit Mcl-1 protein activity and Mcl-1 overexpression blocked the apoptotic activity of ABT-737. We find that the Pim kinase inhibitors and ABT-737 are highly synergistic in killing prostate cancer both in vitro and when used together in a subcutaneous animal model of prostate cancer therapy. Our results therefore suggest that this combination treatment could be developed as a potential therapy for human prostate cancer where overexpression of Pim kinases and antiapoptotic Bcl-2 family members drives tumor cell resistance to current anticancer therapies.

American Association for Cancer Research
615 Chestnut St. 17th Floor
Philadelphia, PA 19106

Pim kinase inhibitors sensitize prostate cancer cells to apoptosis triggered by Bcl-2 family inhibitor ABT-737

Song JH, Kraft AS.

Department of Biochemistry and Molecular Biology, Hollings Cancer Center, Medical University of South Carolina, Charleston, South Carolina 29425, USA. songjin@musc.edu

Abstract

Pim serine/threonine kinases contribute to prostate tumorigenesis and therapeutic resistance, yet Pim kinase inhibitors seem to have only limited effects on prostate cancer cell survival. Because overexpression of Bcl-2 family members are implicated in chemotherapeutic resistance in prostate cancer, we investigated the cooperative effects of Pim kinase inhibition with ABT-737, a small molecule antagonist of Bcl-2 family members. Strikingly, the addition of ABT-737 to Pim inhibitors triggered a robust apoptosis of prostate cancer cells in vitro and in vivo. Pim inhibitors decreased levels of the Bcl-2 family member Mcl-1, both by blocking 5'-cap dependent translation and decreasing protein half-life. In addition, Pim inhibition transcriptionally increased levels of the BH3 protein Noxa by activating the unfolded protein response (UPR), lead to eIF-2α phosphorylation and increased expression of CHOP. Increased levels of Noxa also inactivated the remaining levels of Mcl-1 protein activity. Notably, these specific protein changes were essential to the apoptotic process because ABT-737 did not inhibit Mcl-1 protein activity and Mcl-1 overexpression blocked the apoptotic activity of ABT-737. Our results therefore suggest that this combination treatment could be developed as a potential therapy for human prostate cancer where overexpression of Pim kinases and antiapoptotic Bcl-2 family members drives tumor cell resistance to current anticancer therapies.

Overcoming Resistance to Inhibitors of the AKT Protein Kinases by Targeting the Pim Protein Kinase Pathway

Bo Cen, Sandeep Mahajan, and Andrew S. Kraft, The Hollings Cancer Center at the Medical University of South Carolina, Charleston, South Carolina 29425

Abstract

The AKT protein kinases are an important signal transduction target for the inhibition of prostate cancer growth. AKT is activated in 50-80% of cancers secondary to deletions, mutations and loss of heterozygosity of the PTEN phosphatase. Resistance to small molecule chemical inhibitors of protein kinases in human patients involves the induction of alternative signal transduction pathways. We demonstrate that the addition of the pan-AKT inhibitor GSK690693 to prostate cancer cell lines, Du145, PC3 and PC3-LN4 induced marked up-regulation of multiple receptor tyrosine kinases, including c-Met, Her3, IGF-IR, INSR and EphA2. Increases in these receptors have the potential to block the growth inhibitory action of this AKT kinase inhibitor. In addition to changes in these RTKs, GSK690693 also markedly increased the levels of the Pim-1 protein kinase. Importantly, down regulation of Pim-1 either through using cells derived from genetically engineered knock-out mice, knocking down the levels of Pim-1 with siRNAs or treating cells with Pim-1 inhibitory small molecules, blocked the ability of GSK690693 treatment to induce increases in RTKs. In comparison, knockdown of wild type levels of Pim-1 was sufficient to lead to decreased expression of endogenous RTKs. The addition of GSK690693 and the Pim-1 inhibitor SMI-4a to PC3-LN4 cells caused a highly synergistic inhibition of growth both in tissue culture and in soft agar assay. When these agents were administered to immune-compromised mice that had been previously injected subcutaneously with PC3-LN4 cells, the combination markedly inhibited tumor growth where each agent given alone had only a partial inhibitory effect. Based on these results we suggest that the Pim-1 protein kinase plays a critical role in the induction of RTKs by AKT inhibitors. Thus combination therapy of prostate cancer with a Pim and AKT inhibitor is likely to be a novel effective therapeutic strategy to overcome potential resistance mechanisms to AKT kinase inhibitors.

Supplemental Material can be found at:
http://www.jbc.org/content/suppl/2010/07/27/M110.137240.DC1.html

THE JOURNAL OF BIOLOGICAL CHEMISTRY VOL. 285, NO. 38, pp. 29128–29137, September 17, 2010
© 2010 by The American Society for Biochemistry and Molecular Biology, Inc. Printed in the U.S.A.

Regulation of Skp2 Levels by the Pim-1 Protein Kinase*[S]

Received for publication, April 22, 2010, and in revised form, July 22, 2010 Published, JBC Papers in Press, July 27, 2010, DOI 10.1074/jbc.M110.137240

Bo Cen[‡], Sandeep Mahajan[§], Marina Zemskova[¶], Zanna Beharry[‖], Ying-Wei Lin[**], Scott D. Cramer[‡‡], Michael B. Lilly[§§], and Andrew S. Kraft[‡§1]

*From the [‡]Department of Medicine, [§]Hollings Cancer Center, and the Departments of [¶]Cell and Molecular Pharmacology, [‖]Pharmaceutical and Biomedical Sciences, and **Pediatrics, Medical University of South Carolina, Charleston, South Carolina 29425, the [‡‡]Department of Cancer Biology and Comprehensive Cancer Center, Wake Forest University School of Medicine, Winston-Salem, North Carolina 27157, and the [§§]Division of Hematology/Oncology, Department of Medicine, University of California, Irvine, California 92868*

The Pim-1 protein kinase plays an important role in regulating both cell growth and survival and enhancing transformation by multiple oncogenes. The ability of Pim-1 to regulate cell growth is mediated, in part, by the capacity of this protein kinase to control the levels of the p27, a protein that is a critical regulator of cyclin-dependent kinases that mediate cell cycle progression. To understand how Pim-1 is capable of regulating p27 protein levels, we focused our attention on the SCF^{Skp2} ubiquitin ligase complex that controls the rate of degradation of this protein. We found that expression of Pim-1 increases the level of Skp2 through direct binding and phosphorylation of multiple sites on this protein. Along with known Skp2 phosphorylation sites including Ser^{64} and Ser^{72}, we have identified Thr^{417} as a unique Pim-1 phosphorylation target. Phosphorylation of Thr^{417} controls the stability of Skp2 and its ability to degrade p27. Additionally, we found that Pim-1 regulates the anaphase-promoting complex or cyclosome (APC/C complex) that mediates the ubiquitination of Skp2. Pim-1 phosphorylates Cdh1 and impairs binding of this protein to another APC/C complex member, CDC27. These modifications inhibit Skp2 from degradation. Marked increases in Skp2 caused by these mechanisms lower cellular p27 levels. Consistent with these observations, we show that Pim-1 is able to cooperate with Skp2 to signal S phase entry. Our data reveal a novel Pim-1 kinase-dependent signaling pathway that plays a crucial role in cell cycle regulation.

The Pim family of serine/threonine kinases regulates the growth and survival of cells and plays a role in enhancing the transformed phenotype driven by oncogenes, including Myc and Akt (1–3). As the Pim kinases are elevated in human tumors, including prostate, leukemia, and pancreatic cancer, and appear to be useful in distinguishing benign from malignant tumors (4), it has been suggested that they play a role in the growth or progression of these malignancies (5, 6). In prostate cancer, decreased Pim-1 expression correlated significantly with measures of poor outcome and was found to be associated with a higher cumulative rate of prostate-specific antigen failure and a strong predictor of prostate-specific antigen recurrence (4). Based on crystal structural analysis (7–11), the Pim family of kinases appears to be constitutively active and not regulated by a kinase cascade. To explain the ability of the Pim protein kinases to regulate growth and survival, research has initially focused on the ability of these protein kinases to regulate CDC25A and CDC25C, $p21^{Waf1}$, and the C-TAK1[2] protein kinase (12–14). Recently, Pim-1 has been shown to increase the cyclin-dependent kinase-2 activity, by decreasing the levels of $p27^{Kip1}$ (p27) protein (15). Similarly, we have demonstrated that small molecule inhibitors of Pim-1 both translocate the p27 protein to the nucleus and markedly increase its levels (16, 17), suggesting that inhibiting Pim-1 activity may regulate the cell cycle by controlling p27 levels and localization.

The SCF^{Skp2} ubiquitin ligase (Skp1/cullin/F-box protein) targets cell cycle negative regulators p27, $p21^{Waf1}$, and p130 (18) to the proteasome for degradation and controls progression through the cell cycle. A key protein in this complex Skp2 binds phosphorylated p27 and is responsible for its destruction. The fact that increased Skp2 expression is frequently found in many cancers (19, 20) and Skp2 overexpression can drive cell transformation suggests the importance of the levels of this protein in regulating cell growth (19, 21, 22). The amount of the Skp2 protein in cells is tightly regulated by multiple pathways, including phosphorylation and proteasome degradation. The anaphase-promoting complex or cyclosome (APC/C) is active from mitosis to late G_1 (23, 24) and functions as the E3 ligase for this protein when activated by Cdh1 (25, 26). Phosphorylation of Skp2 by CDK2 (27) and Akt1 (28, 29) on Ser^{64} and Ser^{72} protects it from degradation by the APC/C^{Cdh1} complex and elevates the levels of this protein. However, the role of Skp2 Ser^{72} phosphorylation is under debate as contradictory findings have been reported (30, 31). Further studies are required to elucidate fully the mechanisms by which cells regulate Skp2 levels.

Here, we demonstrate that Pim-1 kinase activity stabilizes and increases the levels of Skp2 protein, thus decreasing p27 levels and promoting cell cycle progression. Pim-1 both binds Skp2 and phosphorylates it on Ser^{64} and Ser^{72}, but also on a novel site, Thr^{417}. Furthermore, Pim-1 phosphorylates Cdh1,

* This work was supported by Department of Defense Grants W8IXWH-08 and W81XWH-10-1-0249. The flow cytometry core received support from 1P30-CA138313.

[S] The on-line version of this article (available at http://www.jbc.org) contains supplemental Figs. S1–S5 and additional references.

[1] To whom correspondence should be addressed: 86 Jonathan Lucas St., Charleston, SC 29425. Fax: 843-792-9456; E-mail: kraft@musc.edu.

[2] The abbreviations used are: C-TAK1, Cdc25C-associated kinase 1; APC/C, anaphase-promoting complex or cyclosome; HGF, hepatocyte growth factor; SCF, Skp1/cullin/F-box protein.

Downloaded from www.jbc.org at MUSC Library, on May 22, 2012

impairing its association with CDC27 and inhibiting APC/C activity, thus protecting Skp2 from degradation.

EXPERIMENTAL PROCEDURES

Antibodies, Drugs, and Reagents—Anti-Pim-1 (19F7) antibody was produced and purified in this laboratory. Anti-cyclin E (HE12), anti-Met (25H2), anti-phospho-Met (D26), Myc tag (71D10), anti-AKT, anti-phospho-AKT (S473), and anti-polo-like kinase-1 antibodies were purchased from Cell Signaling Technology. Anti-p27 (C19), anti-CDC27 (AF3.1), and anti-cyclin B1 (H-433) were from Santa Cruz Biotechnology. Anti-β-actin (AC-15), anti-FLAG M2, anti-HA (HA-7), and anti-β-tubulin (TUB 2.1) antibodies were from Sigma. Anti-Skp2 and anti-Cks1 antibodies were from Invitrogen/Zymed Laboratories Inc.. Anti-His tag antibody was from Qiagen. Anti-Cdh1(DH01) antibody was from Abcam. Anti-lamin B antibody was from Calbiochem.

Roscovitine and reagents for *in vitro* ubiquitination assay were from Biomol. Cycloheximide, MG132, LY294002, wortmannin, nocodazole, and thymidine were from Sigma. GSK690693 was provided by Glaxo Smith Kline.

Recombinant human HGF was from Antigenix America. Active GST-tagged Pim-1 was from SignalChem. Active His-tagged human Pim-1 was purified from *Escherichia coli* using a Calbiochem nickel-nitrilotriacetic acid column. GST and GST-Skp2 proteins were purified from *E. coli* using glutathione-Sepharose 4B resin (GE Healthcare).

Plasmids—A Pim-1 siRNA plasmid and the control plasmid were described previously (32). pGIPZ Pim-1 shRNA constructs were from Open Biosystems.

pCMV-Skp2 plasmid expressing FLAG-tagged Skp2 was kindly provided by Dr. Liang Zhu (33). Site-directed mutants were prepared using PCR based on this plasmid. HA-Cdh1 and HA-Cdc20 plasmids were described elsewhere (34). The Ubc3 and ubiquitin plasmids have been previously described (35). The HA-Pim-1 and FLAG-Pim-1 constructs were generated by subcloning murine Pim-1 cDNA into pcDNA3 vector, and the K67M (HA-tagged) mutant was constructed using PCR. An N-terminally truncated mutant (NT81) of Pim-1 was described previously (36). Lentiviral expression constructs pLEX-Pim-1 and pLEX-Skp2 was obtained by subcloning human Pim-1 and Skp2 cDNAs into pLEX vector (Open Biosystems). A human Pim-1 construct, pcDNA3-Pim-1, was described elsewhere (32).

Cell Culture, Transfections, Transductions, and Cell Synchronization—Cell lines were grown in RPMI 1640 medium (PC3) or DMEM (HeLa, HEK293T, Rat1, and mouse embryonic fibroblasts). The triple knock-out mouse of the Pim-1, -2, -3 genes used to isolate mouse embryonic fibroblasts were described previously (17). Mouse prostate epithelial cells were isolated as described (37). HEK293T cells were transfected by the calcium phosphate method, and HeLa cells were transfected with Lipofectamine 2000 reagent. Lentiviruses were produced and transduced into Rat1 cells using kits from Open Biosystems.

For synchronization experiments, HeLa cells were treated with 2 mM thymidine for 18 h, washed, and released into fresh medium for 9 h. Then, a second thymidine treatment was applied to yield cells at the G_1/S transition. Mitotic HeLa cells were obtained by treating HeLa cells with 2 mM thymidine for 24 h, washing, and releasing into fresh medium for 3 h. The cells were then treated with 100 ng/ml nocodazole for 12 h.

Ubiquitination Assays—In vitro p27 ubiquitination assays were performed essentially as described (38). In brief, the SCF^{Skp2} complex was expressed and purified from insect cells (39) and mixed with *in vitro*-translated ^{35}S-labeled p27 that had previously been incubated with cyclin E/Cdk2 along with methylated ubiquitin and ubiquitin aldehyde for 60 min at 30 °C. The reaction was stopped with 2× SDS sample buffer and run on polyacrylamide gels. *In vivo* ubiquitination assays were performed as described (40). HEK293T cells were transfected with the indicated plasmids for 24 h, treated with 10 μM MG132 for 6 h, and lysed in denaturing buffer (6 M guanidine-HCl, 0.1 M Na_2HPO_4/NaH_2PO_4, 10 mM imidazole). The cell extracts were then incubated with nickel beads for 3 h, washed, and subjected to immunoblot analysis.

In Vitro and in Vivo Phosphorylation Assay—FLAG-Skp2 or its mutants were immunoprecipitated with anti-FLAG antibody from HEK293T cells. Immune complexes were washed three times in radioimmune precipitation assay lysis buffer (150 mM NaCl, 10 mM Tris-HCl, pH 7.5, 1% Nonidet P-40, 0.5% deoxycholate, 0.1% SDS), then washed twice in 1× kinase buffer (25 mM Tris-HCl, pH 7.5, 5 mM β-glycerophosphate, 2 mM dithiothreitol, 0.1 mM Na_3VO_4, 10 mM $MgCl_2$, 2 μM unlabeled ATP) and incubated with 0.5 μg of recombinant active Pim-1 kinase and 2 μCi of [γ-^{32}P]ATP in 3 μl of total reaction buffer for 30 min at 30 °C. Phosphorylation of Cdh1 or Cdc20 was detected using *in vitro* translated proteins produced by TNT Coupled Reticulcyte Lysate System (Promega). Reactions were stopped by washing twice in kinase buffer and boiling in 2× SDS loading buffer. Proteins were resolved by 9% SDS-PAGE, and ^{32}P incorporation was detected by autoradiography. For *in vivo* labeling experiments, HeLa cells were transfected with the indicated plasmids for 24 h, and the medium was changed to phosphate-free DMEM with 0.5% dialyzed FBS containing 200 $\mu Ci\ ml^{-1}$ ortho-$^{32}PO_4$ for 4 h. Cells were lysed by radioimmune precipitation assay buffer for immunoprecipitation, and the immune complexes were subjected to 9% SDS-PAGE followed by autoradiography analysis.

Flow Cytometry—Cell cycle distribution was monitored by FACS analysis of ethanol-fixed, propidium iodide-stained cells on a Becton Dickinson FACSCalibur Analytical Flow Cytometer.

BrdU Incorporation Assay—Rat1 cells were seeded in 96-well plates (3000 cells/well) and maintained as described in the figure legends. An ELISA BrdU kit (Roche Applied Science) was used to assay the cell cycle. Absorbance at 370 nm (reference wavelength 492 nm) was measured using a Molecular Devices microplate reader.

Densitometry Analysis—Densitometry was determined with ImageJ version 1.42q software (National Institutes of Health) with normalization to the corresponding controls (β-actin or input).

Statistical Analysis—All assays were repeated at least three times. The results of quantitative studies are reported as mean ± S.D. Differences were analyzed by Student's *t* test. $p <$

Downloaded from www.jbc.org at MUSC Library, on May 22, 2012

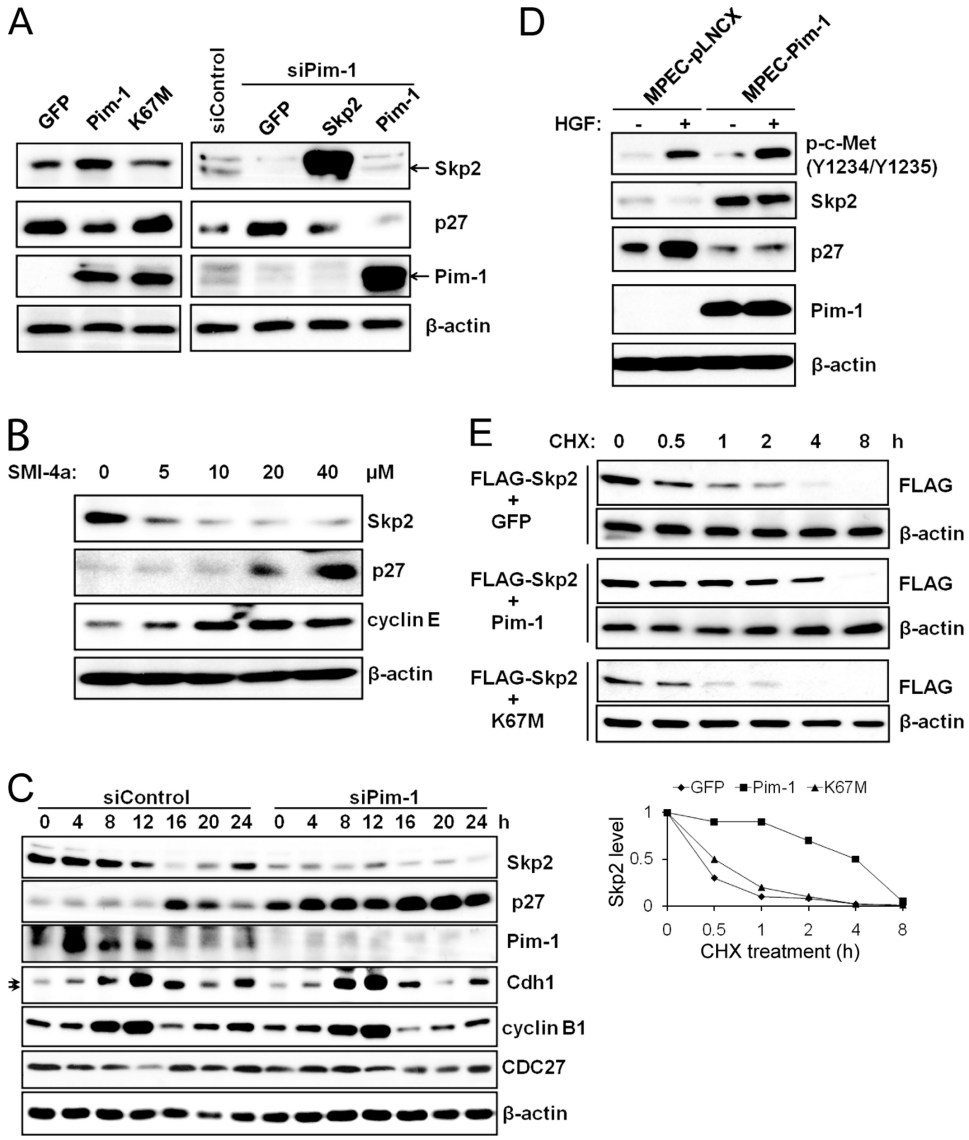

FIGURE 1. **Regulation of Skp2 protein levels by Pim-1.** *A*, HeLa cells were transiently transfected with cDNAs encoding green fluorescent protein (*GFP*), Pim-1, kinase-dead Pim-1 (K67M), or a siRNA to Pim-1 together with GFP, or Skp2, or Pim-1, or a scrambled sequence. Forty-eight h after transfection, extracts of these cells were probed on Western blots with the listed antibodies. *B*, HeLa cells were treated with various concentrations of Pim kinase inhibitor SMI-4a for 16 h, extracts were prepared, and immunoblotting was carried out with the identified antibodies. *C*, HeLa cells were transfected with the indicated siRNA plasmids followed by a double-thymidine block treatment (see "Experimental Procedures"). Lysates were prepared at the indicated time points after release from the thymidine block and subjected to immunoblot analysis. *Arrows* indicate phosphorylated and unphosphorylated forms of Cdh1. *D*, mouse prostate epithelial cells (*MPECs*) stably transfected with a control vector (pLNCX) or a human Pim-1-expressing plasmid were treated with HGF (50 ng/ml) for 24 h followed by immunoblot analysis. *E*, 24 h after transfection with expression plasmids (time 0), HEK293T cells were incubated for the indicated times with cycloheximide (*CHX*, 100 μg/ml) followed by immunoblot analysis with FLAG or β-actin antibodies. Densitometric analysis was performed using ImageJ software to quantify the expression of Skp2. Skp2 band intensity was normalized to β-actin, then normalized to the $t = 0$ controls.

0.05 was regarded as significant, and such differences are indicated in the figures.

RESULTS

Pim-1 Stabilizes Skp2 Protein—Overexpression in HeLa cells of wild type Pim-1 but not a kinase-dead mutant, K67M, leads to a decrease in the level of the p27 protein (Fig. 1*A*) without any change in the mRNA level of this protein (supplemental Fig. S2*D*). To evaluate the mechanism by which Pim-1 functions, we focused attention on the E3 ligase SCF complex that targets p27 for proteasomal degradation and in particular the Skp2 protein which is known to directly bind p27. Western blots demonstrate that transfection of the Pim-1 kinase increases the levels of Skp2 protein (Fig. 1*A*), while conversely siRNA or shRNA (supplemental Fig. S1*A*) knockdown of endogenous Pim-1 expression reduces Skp2 levels. The interplay between these two proteins is further demonstrated by the observation that transfection of murine Pim-1 into HeLa cells in which endogenous enzyme has been knocked down again elevates the level of Skp2 (Fig. 1*A*). Using two small molecule Pim kinase inhibitors, SMI-4a, which has demonstrated excellent selectivity (16, 17, 41), and a structurally unrelated Pim kinase inhibitor, K00135 (27), treatment of both HeLa cells (Fig. 1*B*) and PC3 prostate cancer cells (supplemental Fig. S1, *B* and *C*) causes a dose-dependent reduction of Skp2 protein expression and a concomitant rise in p27. We and others have shown that Pim-1 facilitates cell cycle progression as overexpression of Pim-1 promotes G_1-S transition (15) whereas Pim kinase inhibitor caused cell cycle arrest at G_1 (16). Because the Akt protein kinase family is thought to control the level of Skp2 (28, 29), we evaluated whether the PI3K inhibitor, wortmannin or a pan-Akt inhibitor, GSK690693, had similar affects on Skp2 levels. However, no significant changes in the levels of Skp2 were seen after treatment with these reagents until the highest concentrations tested (supplemental Fig. S1, *D* and *E*). Interestingly, LY294002, which is both a PI3K and Pim-1 inhibitor (9), reduced Skp2 expression (supplemental Fig. S1*E*).

To test whether the effects of Pim-1 knockdown were cell cycle-specific, we transfected HeLa cells with Pim-1 siRNA, blocked them in the G_1/S boundary, and then released them into the cell cycle and measured the Skp2 and p27 levels. We found that the siRNA knockdown of Pim-1 regulated these two proteins throughout the cell cycle (Fig. 1*C*).

To test the activity of Pim-1 in a different cellular system we examined the role of Pim-1 overexpression in mouse prostate epithelial cells. These cells respond to hepatocyte growth factor

Downloaded from www.jbc.org at MUSC Library, on May 22, 2012

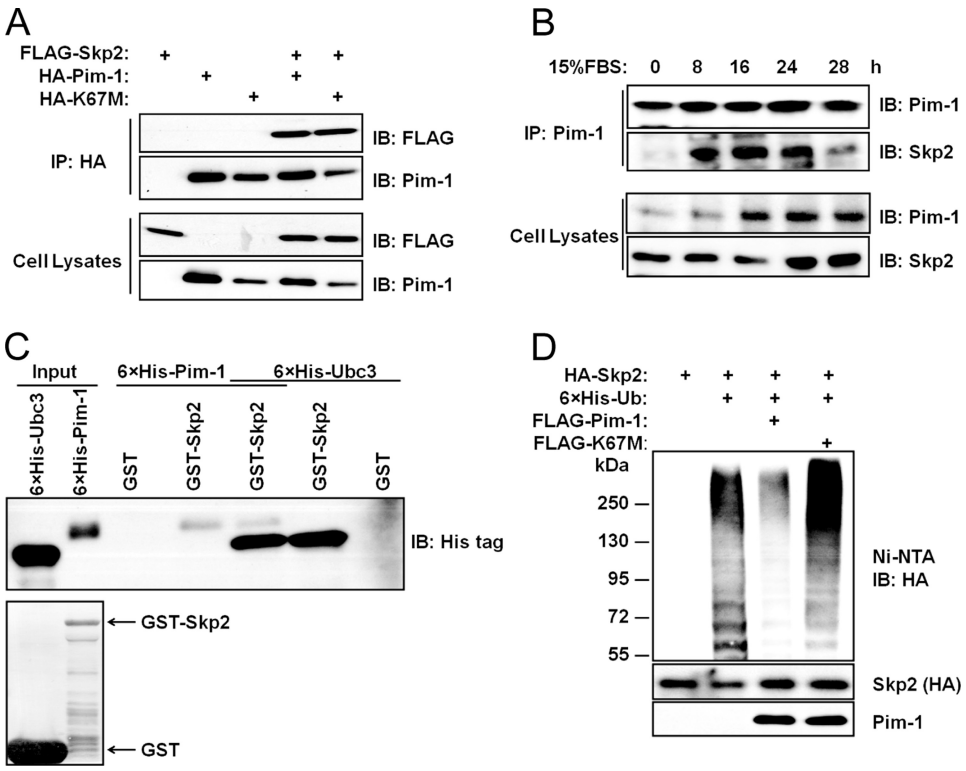

FIGURE 2. **Pim-1 binds to Skp2.** *A*, HEK293T cells were transfected with the indicated plasmids, protein immunoprecipitated (*IP*) with HA antibody and immunoblotted with FLAG or Pim-1 antibody. Lysates of cells used for this assay are probed with identical antibodies. *B*, HEK293T cells were serum-starved (0.2%) for 48 h prior to the addition of 15% FBS at 0 time. Cells were then harvested at the indicated time points, and coimmunprecipitation (*co-IP*) was performed. *C*, GST-Skp2 proteins were incubated overnight with His-tagged Pim-1 or Ubc3 proteins purified from *E. coli* at 4 °C, washed with PBS, and subjected to immunoblot analysis (*upper panel*). GST and GST-Skp2 were stained with Coomassie Brilliant Blue (*lower panel*). *D*, HEK293T cells were transfected with the indicated plasmids, treated with 10 μM MG132 for 6 h, and ubiquitination as measured by binding to nickel-nitrilotriacetic acid (*Ni-NTA*) beads (see "Experimental Procedures") followed by an immunoblot with anti-HA antibody. Immunoblot (*IB*) analysis was performed on total cell lysates from these HEK293T cells (*two lower panels*).

(HGF), a powerful mitogen and morphogen for epithelial and endothelial cells, through binding to its receptor the Met tyrosine kinase (42, 43). The growth inhibitory activity of HGF on cancer cells is associated with up-regulation of p27 expression (44), mediated by down-regulation of Skp2 expression (45). We found that the HGF-induced p27 up-regulation is inhibited by Pim-1 in mouse prostate epithelial cells (Fig. 1*D*). Similar results were also obtained in Pim-overexpressing HeLa cells when they were treated with HGF (supplemental Fig. S1*F*).

Finally, in HEK293T cells the coexpression of Pim-1, but not kinase-dead Pim-1, K67M, or GFP, was able to induce a longer Skp2 half-life (Fig. 1*E*). Taken together, these experiments suggest that Pim-1 controls the levels of Skp2 and consequently regulates the amounts of p27 protein in cells.

Pim-1 Binds Directly to Skp2 and Reduces Skp2 Ubiquitination—We cotransfected HEK293 cells with FLAG-Skp2 and either HA-Pim-1 or kinase-dead Pim-1 (HA-K67M) expression constructs. When cell lysates were subjected to immunoprecipitation with HA antibody, we found that Pim-1 and Skp2 are able to interact physically in cells irrespective of the Pim-1 kinase activity (Fig. 2*A*). In HEK293T cells that are transfected then serum-starved and finally released into 15% serum, this interaction between Pim-1 and Skp2 occurs maximally between hours 8 and 24 (Fig. 2*B*). We did not perform a cell cycle analysis on these cells. However, knockdown of endogenous Pim-1 in HeLa cells appears to reduce Skp2 expression throughout a full cell cycle (Fig. 1*C*). These observations suggest that Pim-1 may regulate other molecule(s) controlling Skp2 levels *in vivo*. This binding is also seen *in vitro* in glutathione *S*-transferase (GST) pull-down experiments. Recombinant His-tagged Pim-1 protein binds to Skp2; the binding of Pim-1 did not interfere with the interaction between Skp2 and Ubc3, an E2 ubiquitin enzyme that is known to interact with the Skp2 protein (Fig. 2*C*). Furthermore, Pim-1 did not interfere with the formation of the SCF^{Skp2} complex, from Skp2, Ubc3, and Rbx1 proteins (supplemental Fig. S2*A*).

Like p27, Skp2 levels are regulated by ubiquitination and proteasome degradation (25, 26), suggesting that Pim-1 could decrease the levels of Skp2 ubiquitination. Using protein extracts from HEK293T cells transfected with Pim-1 and Skp2, we found that the presence of active but not kinase-dead Pim-1 is sufficient to repress the ubiquitination of the Skp2 protein markedly (Fig. 2*D*). Using this same approach, consistent with the effect on Skp2, Pim-1 transfection was found to also increase p27 ubiquitination (supplemental Fig. S2*C*). This suggests that an increase in Skp2 levels is needed to mediate increased ubiquitination of p27 by Pim-1. Indeed, in an *in vitro* assay, the presence of Pim-1 did not directly influence p27 ubiquitination (supplemental Fig. S2*B*).

Pim-1 Phosphorylates Skp2 on Multiple Sites—To determine whether Skp2 was a substrate for Pim-1, purified His-tagged protein kinase was incubated with immunoprecipitated FLAG-Skp2 in the presence of [γ-^{32}P]ATP. In this assay, Skp2 was clearly phosphorylated, and this phosphorylation was decreased by the addition of a small molecule Pim-1 inhibitor, SMI-4a (Fig. 3*A*). Pim-1 is known to phosphorylate the sequence R-*X*-R-L-S/T (46). Scanning the Skp2 sequence, we identified a potential Pim-1 consensus site at the C terminus of Skp2, Thr^{417}, which is conserved from frog to humans (Fig. 3*B*). Mutation of this residue from threonine to alanine (T417A) led to reduced Skp2 phosphorylation by Pim-1 *in vitro*, but did not completely abolish this modification (Fig. 3*C*). Previous studies (8–10) have demonstrated that Ser^{64} and Ser^{72} in Skp2 are CDK2 phosphorylation sites (27), and Ser^{72} can also be phosphorylated by Akt1 (28, 29). Using GST-Pim-1 as a kinase, mutation of either Ser^{64} or Ser^{72} to Ala markedly decreased Skp2 phosphorylation by Pim-1 with both of these changes hav-

Downloaded from www.jbc.org at MUSC Library, on May 22, 2012

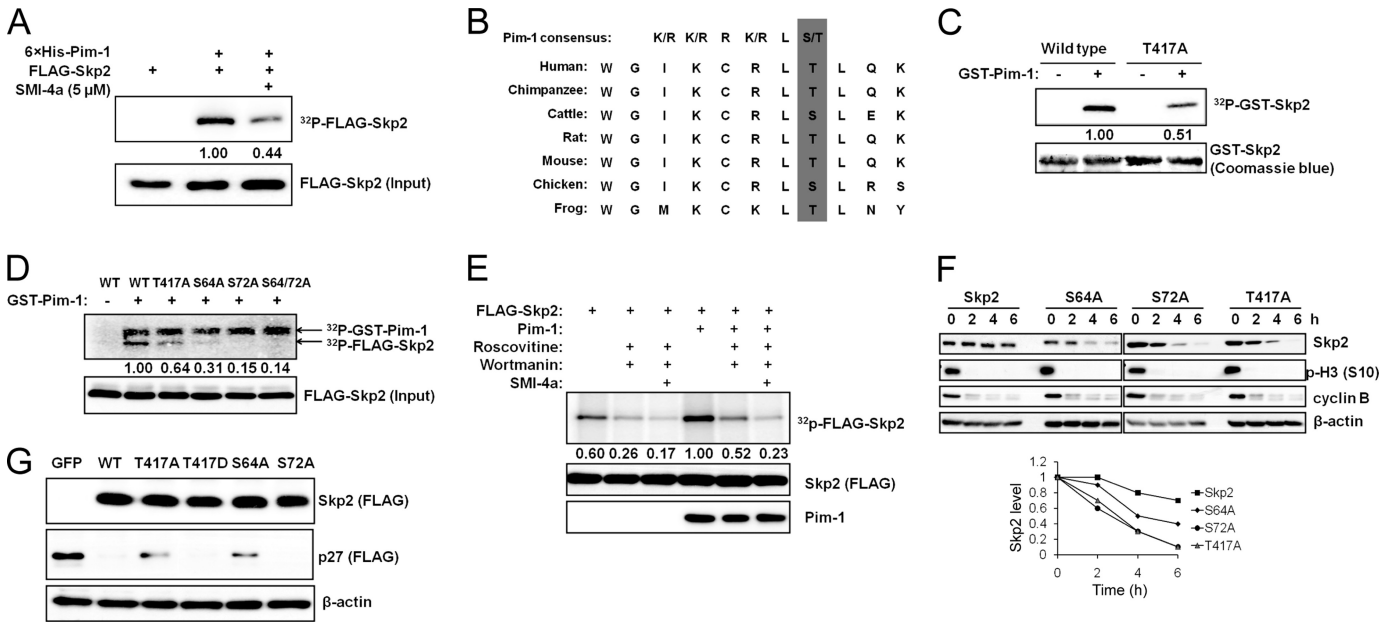

FIGURE 3. **Pim-1 phosphorylates Skp2.** *A*, FLAG-Skp2 was immunoprecipitated from HEK293T cells, incubated with recombinant His-tagged Pim-1 for 30 min with or without SMI-4a for an *in vitro* kinase assay ("Experimental Procedures") followed by SDS-PAGE autoradiography (*upper panel*) and immunoblot analyses (*lower panel*). The phosphorylation of FLAG-Skp2 was quantified by densitometry from three independent experiments after normalization to input. *B*, C-terminal sequence of Skp2 contains a Pim-1 consensus site. *C*, GST-tagged Skp2 proteins or a T417A mutant was incubated with recombinant GST-Pim-1 and [γ-^{32}P]ATP for 30 min, and subjected to SDS-PAGE followed by autoradiography. The phosphorylation of GST-Skp2 was quantified by densitometry from three independent experiments with normalization to Coomassie Blue staining. *D*, wild type (*WT*) FLAG-Skp2 and its mutants T417A, S64A, S72A, and S64A/S72A were immunoprecipitated from HEK293T cells, incubated with recombinant GST-tagged Pim-1 and [γ-^{32}P]ATP for 30 min, followed by SDS-PAGE autoradiography (*upper panel*) and immunoblot analysis (*lower panel*). The phosphorylation of FLAG-Skp2 was quantified by densitometry from three independent experiments following normalization to the level of protein input. *E*, HeLa cells were pretreated with roscovitine (20 μM), wortmannin (1 μM), or SMI-4a (10 μM) for 1 h, transfected with human Pim-1 and Skp2, and labeled with $^{32}P_i$ followed by FLAG immunoprecipitation, autoradiography (*upper panel*), and FLAG/Pim-1 immunoblots (*two lower panels*). The phosphorylation of FLAG-Skp2 was quantified by densitometry from three independent experiments along with normalization to Skp2 expression. *F*, HeLa cells were transfected with the indicated Skp2 constructs and synchronized in M phase by mitotic shake-off of cells obtained after release from a thymidine-nocodazole block. The cells were then replated and allowed to progress through the cell cycle in the presence of cycloheximide (100 μg/ml). Immunoblot analysis was performed at specific time points using antibodies to cyclin B and phosphohistone H3 Ser^{10} (*p-H3* (*S10*)) as controls. Densitometric analysis was performed using ImageJ software to quantify the expression of Skp2. Skp2 band intensity was normalized to β-actin and then normalized to the $t = 0$ controls. *G*, HEK293T cells were transfected with a FLAG-tagged p27 Skp2 construct or a GFP control. Expression of exogenous p27 and Skp2 is measured by immunoblotting.

ing a somewhat greater effect than the T417A mutation (Fig. 3*D*), suggesting that each of these sites might also be a Pim-1 target. It appears that phosphorylation of Ser^{64} and/or Ser^{72} may be required for Thr^{417} phosphorylation to take place because mutation of either Ser^{64} or Ser^{72} almost completely abolished Skp2 phosphorylation in this experiment. However, a complete understanding of the relationship between these sites requires further studies.

To test whether Pim-1 has a role in regulating Skp2 phosphorylation *in vivo*, HeLa cells were transfected with Pim-1 and Skp2, metabolically labeled with orthophosphate, and then treated with kinase inhibitors such as roscovitine (pan-CDK inhibitor), wortmannin (PI3K inhibitor), and SMI-4a (Pim-1 inhibitor). Treatment with roscovitine and wortmannin reduced Skp2 phosphorylation *in vivo*. Overexpression of Pim-1 markedly increased Skp2 phosphorylation, and this phosphorylation was inhibited by all three agents (Fig. 3*E*), suggesting that multiple kinases can play a role in regulating phosphorylation of this protein.

Skp2 is a degraded by the APC/C^{Cdh1} (25, 26) which is known to have its highest activity from late mitosis to the G_1 phase of the cell cycle (47). To test the impact of phosphorylation of Skp2 on protein stability, we used HeLa cells that were released from a thymidine-nocodazole block in the G_1 phase of the cell cycle into media containing cycloheximide. Exit from mitosis was monitored by the loss of histone H3 phospho-Ser^{10} immunoreactivity and the degradation of cyclin B1 on Western blots (Fig. 3*F*). Using this technique, we found that all three individual Skp2 phosphorylation mutants were more efficiently degraded than the wild type Skp2 protein (Fig. 3*F*), suggesting that phosphorylation by protein kinases, including Pim-1, controls the rate of degradation of Skp2.

We next examined the biological activity of wild type and Skp2 phosphorylation mutants by transfecting them along with p27 into HeLa cells and then examining p27 levels by Western blotting. We found that both the Skp2 T417A and S64A mutants decreased the ability of Skp2 to stimulate the degradation of p27, but T417A retained some degrading activity (Fig. 3*G*). In contrast, an aspartate mutation, T417D, that mimics phosphorylation at this site was more efficient than the T417A at degrading p27. Surprisingly, S72A mutation did not cause any detectable effect on p27 degradation (Fig. 3*G*).

Pim-1 Impairs Cdh1 and CDC27 Interaction and Phosphorylates Cdh1—Because Pim-1 regulates Skp2 ubiquitination, we examined whether this enzyme might interact with components of the APC/C complex that are responsible for Skp2 degradation. In coimmunoprecipitation experiments done in transfected HEK293T cells, Pim-1 was found to complex with

Downloaded from www.jbc.org at MUSC Library, on May 22, 2012

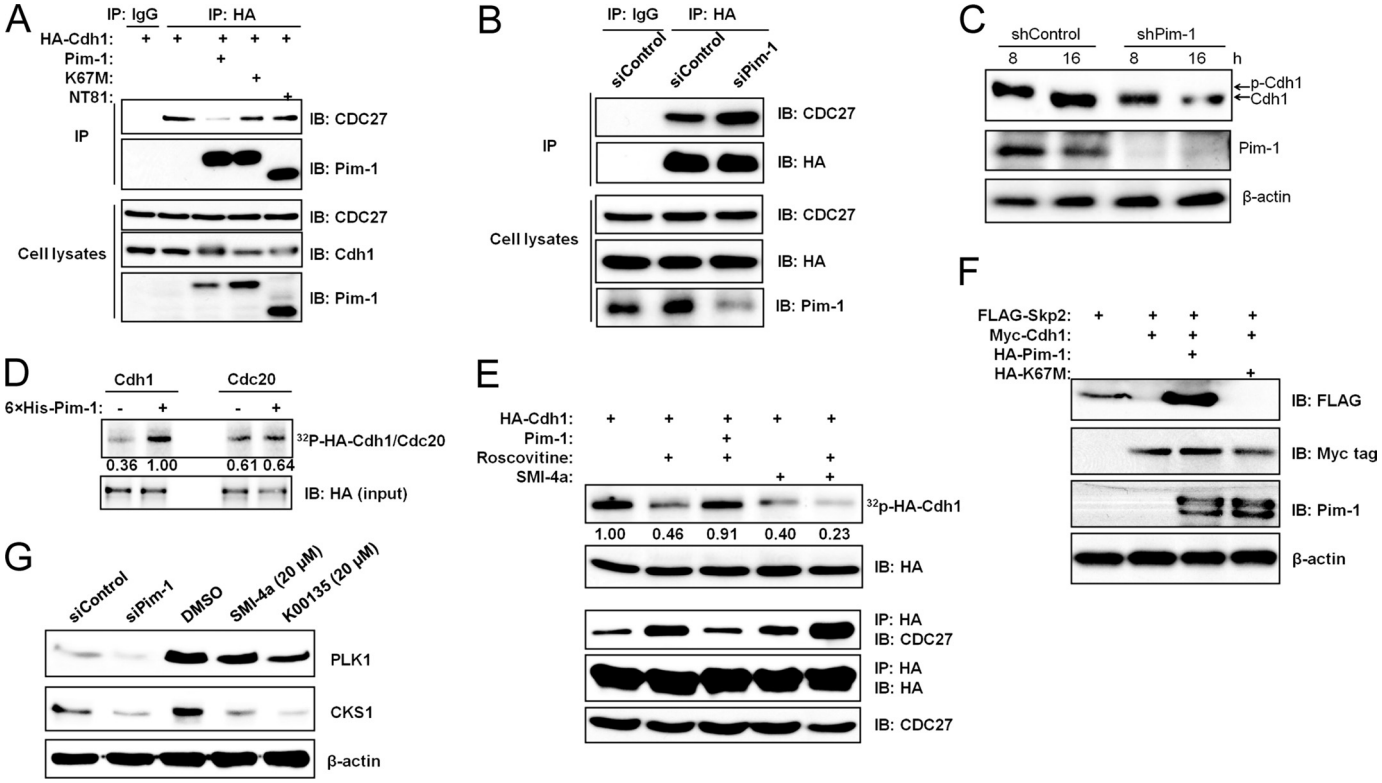

FIGURE 4. **Pim-1 kinase phosphorylates Cdh1 and impairs its binding to CDC27.** *A*, HEK293T cells were transfected with HA-Cdh-1, Pim-1, or kinase-dead Pim-1 K67M or NT81, immunoprecipitated (*IP*) with HA antibody followed by Western blotting with antibodies to CDC27 and Pim-1. Lysates from these cells were immunoblotted (*IB*) with antibody as shown. *B*, HeLa cells were cotransfected with HA-Cdh1 and Pim-1 or scrambled siRNA plasmids before harvesting for coimmunoprecipitation analysis. Levels of transfected proteins in lysates were monitored by immunoblotting. *C*, HeLa cells were transfected with the indicated shRNA plasmids followed by a double-thymidine block. After release from the block cell, lysates were prepared at 8 and 16 h and subjected to immunoblot analysis. The *arrows* indicate phosphorylated and unphosphorylated Cdh-1. *D*, *in vitro* translated HA-tagged Cdh1 or Cdc20 was incubated with recombinant Pim-1 and [γ-^{32}P]ATP in an *in vitro* kinase assay. Autoradiography (*upper panel*) and immunoblot (*lower panel*) analyses were performed. The phosphorylation of Cdh1 or Cdc20 was quantified by densitometry from three independent experiments after normalization to the loaded protein. *E*, HeLa cells were transfected with HA-Cdh1 and human Pim-1, and the kinase inhibitors roscovitine (20 μM) and SMI-4a (10 μM) were added 1 h before labeling with $^{32}P_i$. HA-Cdh-1 was immunoprecipitated, and autoradiography (*top panel*) and immunoblot analysis were performed (*second panel*). The phosphorylation of Cdh1 was quantified by densitometry from three independent experiments with normalization to Cdh1 expression (HA). A coimmunoprecipitation experiment was performed to monitor Cdh1 and CDC27 interaction under the same experimental conditions (*lower three panels*). *F*, HEK293T cells were transfected with FLAG-Skp2, myc-Cdh-1, and HA-tagged WT and kinase-dead (K67M) Pim kinase, and the extracts were immunoblotted with the specified antibodies. *G*, HeLa cells were transiently transfected with a siRNA to Pim-1 or a scrambled sequence. Forty-eight h after transfection, extracts of these cells were probed on Western blots with the listed antibodies (*left two lanes*). HeLa cells were treated with 20 μM Pim kinase inhibitor SMI-4a or K00135 for 16 h, extracts were prepared, and immunoblotting was carried out with the identified antibodies (*right three lanes*).

either Cdh1 or CDC20, two well known activators of APC/C (supplemental Fig. S3*A*). However, Pim-1 did not physically impair the interaction between Cdh1 or CDC20 and Skp2 (supplemental Fig. S3*B*). Using the same methodology, in contrast, we found that Pim-1 could impair the interaction between Cdh1 and CDC27, another APC/C component, in a phosphorylation-dependent manner (Fig. 4*A*). The two kinase-dead Pim-1 mutants, K67M and NT81 (36), are also able to form a complex with Cdh1, but only wild type Pim-1 was capable of reducing the interaction between Cdh1 and CDC27 (Fig. 4*A*). Additionally, incubation with the Pim-1 inhibitor, SMI-4a (supplemental Fig. S4*C*) or treatment with siRNA to knock down endogenous Pim-1 expression (Fig. 4*B*) increased the Cdh1/CDC27 interaction.

Our results are consistent with previous findings that demonstrate that phosphorylation of Cdh1 dissociates this protein from the APC/C complex (48, 49). Cdh1 is hyperphosphorylated *in vivo* during S, G_2, and M phases, and this phosphorylation causes an electrophoretic mobility shift on SDS-polyacrylamide gels (Fig. 5*A*) (48, 50, 51). To explore the role of Pim-1 in phosphorylation of Cdh1 further, we first reprobed the same membrane used in Fig. 1*C* with antibodies against Cdh1 and CDC27. In cells treated with Pim-1 siRNA, Cdh1 displayed higher mobility at 0, 4, 8, and 12 h compared with those in control cells (Fig. 1*C*), suggesting that phosphorylation was reduced. To confirm this finding, we knocked down endogenous Pim-1 expression in HeLa cells using shRNA and then subjected these cells to a double-thymidine block. The cells were then released from the block (for cell cycle analysis, see Fig. 5*A*), and immunoblotting was performed to examine Cdh1 phosphorylation. Phosphorylation of endogenous Cdh1 at 8 h after release from a double-thymidine block was dramatically reduced in Pim-1 knockdown cells as judged by the protein mobility shift (Fig. 4*C*).

Additionally, we found that recombinant Pim-1 was capable of phosphorylating *in vitro* translated Cdh1 but not CDC20 (Fig. 4*D*). Cdh1 is heavily phosphorylated by CDKs *in vivo*. To examine whether Pim-1 can also phosphorylate Cdh1 *in vivo*, we first treated HeLa cells with the CDK inhibitor roscovitine or Pim inhibitor SMI-4a and then labeled them with $^{32}P_i$.

Downloaded from www.jbc.org at MUSC Library, on May 22, 2012

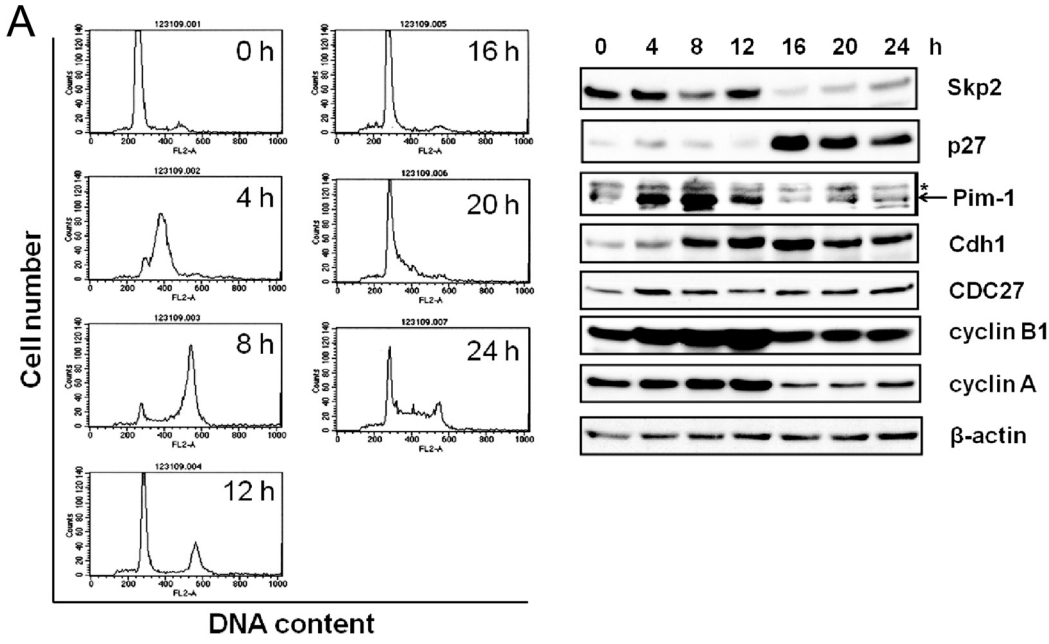

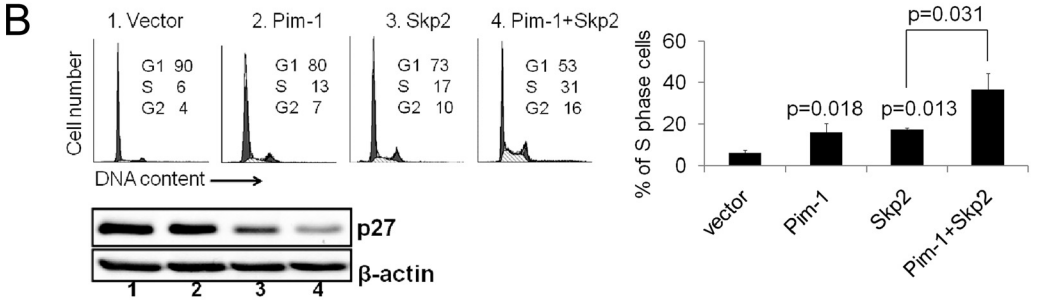

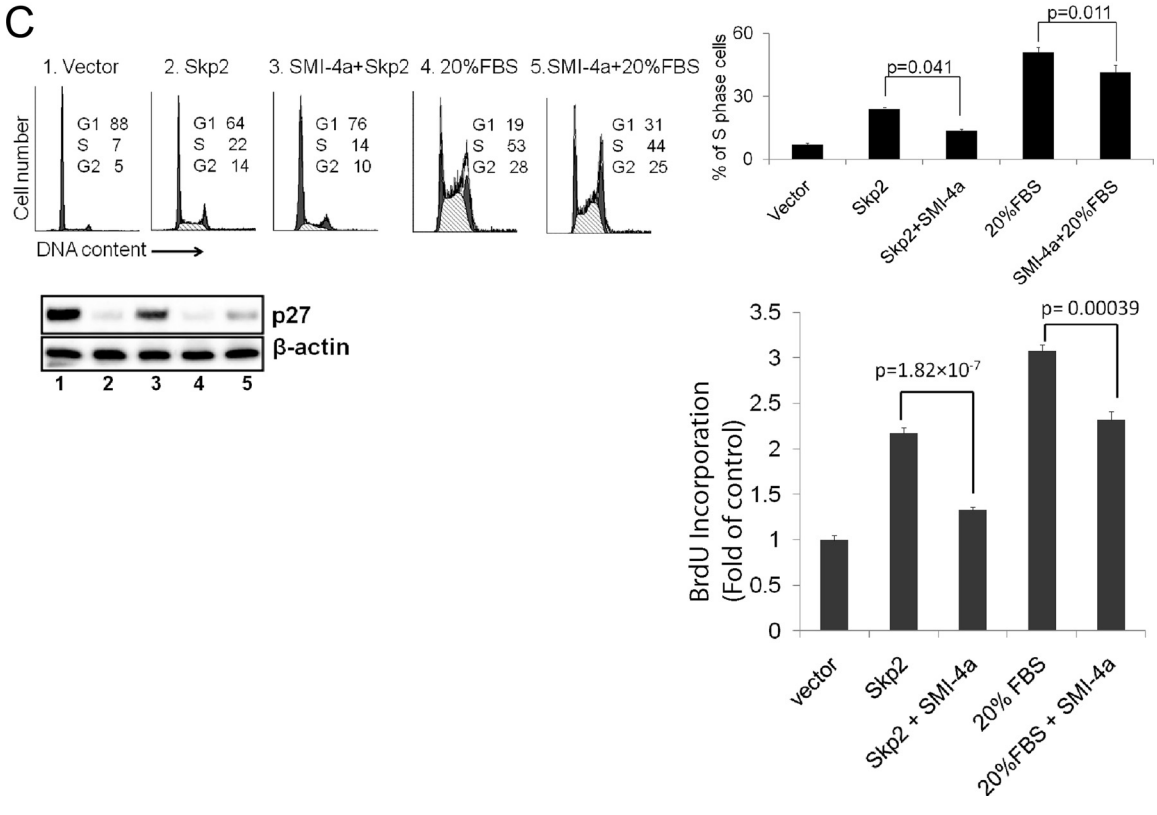

Downloaded from www.jbc.org at MUSC Library, on May 22, 2012

Roscovitine or SMI-4a treatment reduced Cdh1 phosphorylation, and overexpression of Pim-1 in the presence of roscovitine reversed the roscovitine effect, although the combination of roscovitine and SMI-4a treatment further decreased Cdh1 phosphorylation (Fig. 4*E*). We performed coimmunoprecipitation experiments to monitor the Cdh1/CDC27 interactions under these conditions. Consistently, roscovitine treatment increased the Cdh1/CDC27 interaction whereas overexpression of Pim-1 in the presence of roscovitine suppressed this effect. Combined treatment with roscovitine and SMI-4a further increased the Cdh1/CDC27 interaction compared with roscovitine or SMI-4a alone (Fig. 4*E*).

Because the APC/C activity to degrade Skp2 can be activated by Cdh1 overexpression (25, 26), we tested the ability of Pim-1 to reverse this effect. We found that coexpression of wild-type Pim-1, but not its mutant, K67M, is capable of blocking Cdh1-mediated degradation of Skp2 (Fig. 4*F*). However, data in Fig. 4*F* cannot distinguish whether Pim-1 blocks degradation of Skp2 by acting on Cdh1 or Skp2 or both.

Because Pim-1 expression impairs APC/C^{Cdh1} activity, we examined whether other known APC/C^{Cdh1} substrates are regulated by Pim-1 expression. Knockdown of endogenous Pim-1 expression or suppression of Pim-1 kinase activity with Pim kinase inhibitors SMI-4a or K00135 in HeLa cells led to reduced protein expression of both polo-like kinase-1 and CDK subunit 1 (Cks1), two proteins known to be regulated by APC/C^{Cdh1} (Fig. 4*G*). This finding further demonstrates that Pim-1 is a negative regulator of APC/C^{Cdh1} activity.

Pim-1 Is Required for Skp2 to Signal Cell Cycle S Phase Entry—Based on the activities of Pim-1, we have attempted to correlate the levels of this enzyme with other cell cycle regulatory components. HeLa cells were released from a double-thymidine block, cell cycle progression was monitored by FACS analysis (Fig. 5*A*), and the expression patterns of Skp2, p27, Cdh1, CDC27, cyclin B1, and cyclin A were measured by Western blotting (Fig. 5*B*). We found that Pim-1 levels were very high at S (4 h) and G_2/M phases (8 h) of the cell cycle. Lower Pim-1 expression was seen at G_1 and the G_1/S boundary (0, 16, 20, and 24 h; Figs. 5*A* and 1*C*). Because Pim-1 is a constitutively active kinase (7–11), this expression pattern of Pim-1 should represent its activity profile during cell cycle progression. Interestingly, but not surprisingly, Pim-1 activity coincides with Skp2 expression (Fig. 5*A*) and inversely correlates with Cdh1 activity (47, 52) during the cell cycle (Fig. 5*A*). Because Skp2 is known to have the ability to induce S phase in quiescent fibroblasts (40, 53), we determined whether the Skp2/Pim-1 interaction is important for S phase progression. Investigation of this question was carried out using Rat1 cells because they were able to undergo complete cell cycle blockade at G_0/G_1 upon serum starvation. As judged by FACS analysis, we found that in the absence of serum addition, overexpressed Skp2 or Pim-1 each stimulates S phase entry (Fig. 5*B*), and coexpression of Skp2 and Pim-1 further enhances the S phase entry of these cells (Fig. 5*B*). Conversely, as revealed by both FACS analysis and BrdU incorporation, treatment with a small molecule Pim inhibitor, SMI-4a, reduced Skp2-induced S phase progression (Fig. 5*C*) and impaired serum-induced S phase entry (Fig. 5*C*). Another structurally unrelated small molecule Pim inhibitor, K00135 (54), displayed a similar effect (supplemental Fig. S5*A*). These observations suggest that Pim kinases are required along with Skp2 to allow cells to exit from quiescence.

DISCUSSION

The data presented suggest the novel observation that the Pim-1 protein kinase through a dual mechanism can regulate the levels and hence the activity of Skp2. Pim-1 is capable of binding and phosphorylating Skp2 and stabilizing protein levels, but does not affect the interaction of Skp2 with the E2 ligase Ubc3. Conversely, both siRNA and small molecule Pim-1 inhibitors decrease Skp2 levels and phosphorylation. Skp2 is phosphorylated by CDK2 at Ser^{64} and Ser^{72} (27) and by Akt1 at Ser^{72} to stabilize this protein (28, 29). Pim-1 appears capable of phosphorylating Skp2 at these two sites (Fig. 3), as well as a unique site in the C terminus, Thr^{417}, that is highly conserved throughout the animal kingdom, including humans and mice. Phosphorylation of this site is required for maximal Skp2 activity and stabilization of Skp2 protein levels *in vivo* (Fig. 3). In the prostate cancer cell line PC3 that contains an activated Akt, a small molecule Pim inhibitor SMI-4a but not wortmannin or the Akt inhibitor GSK690693 decreased the levels of Skp2. LY294002, which inhibits both Akt and Pim, displayed an effect similar to that of SMI-4a, suggesting that in this cell line the Pims are essential for the regulation of Skp2 levels. Unlike Akt (28, 29), Pim-1 kinase did not appear to regulate Skp2 subcellular localization (supplemental Fig. S4). The Pim kinases share multiple similarities with AKT (1, 55, 56). It is possible that the relative abundance of each of these Skp2-phosphorylating kinases may decide which is essential to the control of Skp2 levels. It is quite surprising that our Skp2 S72A mutant did not lose p27 degradation activity compared with the wild type Skp2 (Fig. 3*G*) because two previous studies demonstrated that this very same Skp2 mutant completely lost ubiquitin ligase activity (28, 29). However, another two recent reports confirmed our finding (30, 31). The half-life of this mutant was indeed shorter than that of wild-type Skp2 (Fig. 3*F*), consistent with previous reports (27–29).

The degradation of Skp2 is regulated by APC/C^{Cdh1} complex (25, 26) which preferentially associates with non-phospho-Ser^{64} form of Skp2 (27). Pim-1 kinase activity does not affect the binding of Cdh1 to total Skp2 (supplemental Fig. S3*B*), but does impair the interaction between Cdh1 and CDC27 (Fig. 4*A*), Interaction with CDC27/APC3 protein allows Cdh1 to activate the APC/C (57). Although Cdh1 is inhibited by both the Emi-1 protein and multiple phosphorylations initiated in part by

FIGURE 5. **Pim-1 is required for Skp2 to signal cell cycle S phase entry.** *A*, HeLa cells were treated with a double-thymidine block and released into fresh medium. Cells were then harvested at the indicated time points and subjected to FACS (*left panel*) and immunoblot analysis (*right panel*). The *arrow* denotes the Pim-1 signal. * indicates a nonspecific signal. *B*, Rat1 cells were transduced with a lentivirus carrying the indicated cDNAs. Cells were maintained in low serum conditions (0.2%) for 48 h before harvested for FACS (*upper panel*) and immunoblot (*lower panel*) analyses. Percent of S phase cells was compared with vector control, except where indicated by a *bracket*. *C*, the experiment was performed as in *B* except that SMI-4a (5 μM) was added 3 h before a 20% FBS stimulation (16 h). S phase induction was also determined by BrdU incorporation assay. *Brackets* indicate comparison of with and without SMI-4a treatment.

Downloaded from www.jbc.org at MUSC Library, on May 22, 2012

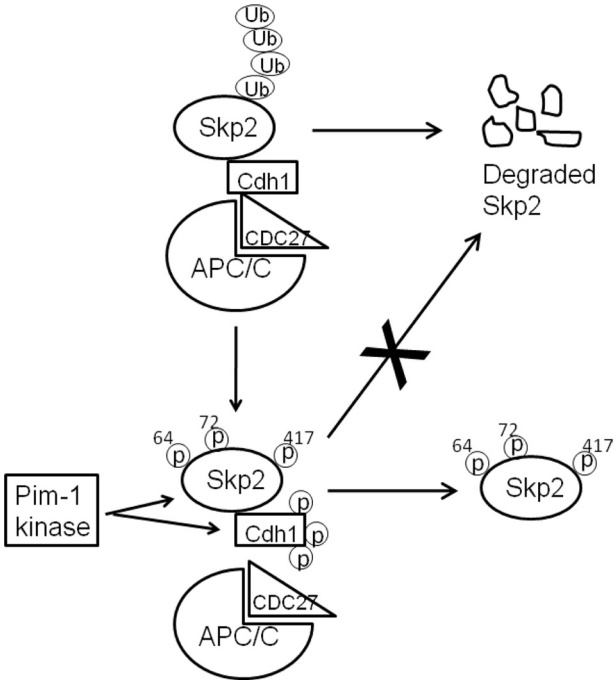

FIGURE 6. **Model of Pim-1 regulation on Skp2 degradation.** Nonphosphorylated Skp2 binds to E3 ligase APC/C^{Cdh1} and gets ubiquitinated (*Ub*) followed by proteasome-mediated degradation. Pim-1 kinase phosphorylates Skp2 on multiple sites: Ser^{64}, Ser^{72}, and Thr^{417}. Furthermore, the phosphorylation of Cdh1 by Pim-1 reduces Cdh1 and APC/C interaction. Both Pim-1 actions result in decreased Skp2 ubiquitination and consequently increased Skp2 stability.

cyclin A-CDK2 and cyclin B1-CDK1 (47, 52), it has been proposed that an additional kinase may play a role (58). Here, we demonstrate that Cdh1 is a phosphorylation target of Pim-1 (Fig. 4, *D* and *E*) and the knockdown of Pim-1 with siRNA reduces Cdh1 phosphorylation during S, G_2, and M phases (Figs. 1*C* and 4*C*), demonstrating the critical involvement of Pim-1 in tightly controlled Cdh1 phosphorylation during the cell cycle. It remains unknown whether Pim-1 and CDKs share some phosphorylation sites on Cdh1. Further studies are required to determine the precise Pim-1 sites and how these two different types of kinases cooperate to control Cdh1 activity. Interestingly, the levels of Pim-1 protein are correlated with Cdh1 phosphorylation during cell cycle progression as high Pim-1 expression and high Cdh1 phosphorylation were seen during S, G_2, and M phases, and the opposite occurred during the G_1 phase (Fig. 5*A*). Given the role of Cdh1 in regulating mitosis, this may explain why Pim-1 is not only required for Skp2 to signal S phase entry (Fig. 5), but also plays a critical role in G_2/M phase regulation. Consistent with this hypothesis, mouse embryo fibroblasts that are knocked out for all three Pim kinase isoforms display increased number of cells in the G_2/M phase of the cell cycle (supplemental Fig. S5). These observations are in concert with previous discoveries suggesting that Pim-1 functions in mitosis (59–61). Therefore, the Pim-1 kinase regulates Skp2 levels through the Pim-1 kinase activity, reduces APC/C^{Cdh1} E3 ligase activity, and thus protects Skp2 from degradation (Fig. 4*F*).

The Pim-1 protein kinase is abnormally elevated in human cancers, regulated by growth factors, and collaborates with other oncogenes to induce cell transformation (1, 2, 5, 6). The ability of this enzyme to modulate the activity of both the SCF^{Skp2} and APC/C^{Cdh1} (Fig. 6) and thus control p27 levels is likely to be essential to the biological activities of this protein kinase.

Acknowledgments—We thank Dr. Liang Zhu (Albert Einstein College of Medicine, Yeshiva University) for providing the Skp2 expression construct and Dr. Xuedong Liu (University of Colorado-Boulder) for providing the active Skp2 complex for the in vitro ubiquitination assay.

REFERENCES

1. Hammerman, P. S., Fox, C. J., Birnbaum, M. J., and Thompson, C. B. (2005) *Blood* **105,** 4477–4483
2. Ellwood-Yen, K., Graeber, T. G., Wongvipat, J., Iruela-Arispe, M. L., Zhang, J., Matusik, R., Thomas, G. V., and Sawyers, C. L. (2003) *Cancer Cell* **4,** 223–238
3. Zippo, A., De Robertis, A., Serafini, R., and Oliviero, S. (2007) *Nat. Cell Biol.* **9,** 932–944
4. Dhanasekaran, S. M., Barrette, T. R., Ghosh, D., Shah, R., Varambally, S., Kurachi, K., Pienta, K. J., Rubin, M. A., and Chinnaiyan, A. M. (2001) *Nature* **412,** 822–826
5. Shah, N., Pang, B., Yeoh, K. G., Thorn, S., Chen, C. S., Lilly, M. B., and Salto-Tellez, M. (2008) *Eur. J. Cancer* **44,** 2144–2151
6. Speers, C., Tsimelzon, A., Sexton, K., Herrick, A. M., Gutierrez, C., Culhane, A., Quackenbush, J., Hilsenbeck, S., Chang, J., and Brown, P. (2009) *Clin. Cancer Res.* **15,** 6327–6340
7. Bullock, A. N., Debreczeni, J., Amos, A. L., Knapp, S., and Turk, B. E. (2005) *J. Biol. Chem.* **280,** 41675–41682
8. Kumar, A., Mandiyan, V., Suzuki, Y., Zhang, C., Rice, J., Tsai, J., Artis, D. R., Ibrahim, P., and Bremer, R. (2005) *J. Mol. Biol.* **348,** 183–193
9. Jacobs, M. D., Black, J., Futer, O., Swenson, L., Hare, B., Fleming, M., and Saxena, K. (2005) *J. Biol. Chem.* **280,** 13728–13734
10. Qian, K. C., Wang, L., Hickey, E. R., Studts, J., Barringer, K., Peng, C., Kronkaitis, A., Li, J., White, A., Mische, S., and Farmer, B. (2005) *J. Biol. Chem.* **280,** 6130–6137
11. Bullock, A. N., Russo, S., Amos, A., Pagano, N., Bregman, H., Debreczeni, J. E., Lee, W. H., von Delft, F., Meggers, E., and Knapp, S. (2009) *PLoS One* **4,** e7112
12. Mochizuki, T., Kitanaka, C., Noguchi, K., Muramatsu, T., Asai, A., and Kuchino, Y. (1999) *J. Biol. Chem.* **274,** 18659–18666
13. Bachmann, M., Hennemann, H., Xing, P. X., Hoffmann, I., and Möröy, T. (2004) *J. Biol. Chem.* **279,** 48319–48328
14. Wang, Z., Bhattacharya, N., Mixter, P. F., Wei, W., Sedivy, J., and Magnuson, N. S. (2002) *Biochim. Biophys. Acta* **1593,** 45–55
15. Morishita, D., Katayama, R., Sekimizu, K., Tsuruo, T., and Fujita, N. (2008) *Cancer Res.* **68,** 5076–5085
16. Beharry, Z., Zemskova, M., Mahajan, S., Zhang, F., Ma, J., Xia, Z., Lilly, M., Smith, C. D., and Kraft, A. S. (2009) *Mol. Cancer Ther.* **8,** 1473–1483
17. Lin, Y. W., Beharry, Z. M., Hill, E. G., Song, J. H., Wang, W., Xia, Z., Zhang, Z., Aplan, P. D., Aster, J. C., Smith, C. D., and Kraft, A. S. (2009) *Blood* **115,** 824–833
18. Cardozo, T., and Pagano, M. (2004) *Nat. Rev. Mol. Cell Biol.* **5,** 739–751
19. Gstaiger, M., Jordan, R., Lim, M., Catzavelos, C., Mestan, J., Slingerland, J., and Krek, W. (2001) *Proc. Natl. Acad. Sci. U.S.A.* **98,** 5043–5048
20. Signoretti, S., Di Marcotullio, L., Richardson, A., Ramaswamy, S., Isaac, B., Rue, M., Monti, F., Loda, M., and Pagano, M. (2002) *J. Clin. Invest.* **110,** 633–641
21. Latres, E., Chiarle, R., Schulman, B. A., Pavletich, N. P., Pellicer, A., Inghirami, G., and Pagano, M. (2001) *Proc. Natl. Acad. Sci. U.S.A.* **98,** 2515–2520
22. Shim, E. H., Johnson, L., Noh, H. L., Kim, Y. J., Sun, H., Zeiss, C., and Zhang, H. (2003) *Cancer Res.* **63,** 1583–1588
23. Reed, S. I. (2003) *Nat. Rev. Mol. Cell Biol.* **4,** 855–864
24. Nakayama, K. I., and Nakayama, K. (2006) *Nat. Rev. Cancer* **6,** 369–381

Downloaded from www.jbc.org at MUSC Library, on May 22, 2012

25. Bashir, T., Dorrello, N. V., Amador, V., Guardavaccaro, D., and Pagano, M. (2004) *Nature* **428,** 190–193
26. Wei, W., Ayad, N. G., Wan, Y., Zhang, G. J., Kirschner, M. W., and Kaelin, W. G., Jr. (2004) *Nature* **428,** 194–198
27. Rodier, G., Coulombe, P., Tanguay, P. L., Boutonnet, C., and Meloche, S. (2008) *EMBO J.* **27,** 679–691
28. Gao, D., Inuzuka, H., Tseng, A., Chin, R. Y., Toker, A., and Wei, W. (2009) *Nat. Cell Biol.* **11,** 397–408
29. Lin, H. K., Wang, G., Chen, Z., Teruya-Feldstein, J., Liu, Y., Chan, C. H., Yang, W. L., Erdjument-Bromage, H., Nakayama, K. I., Nimer, S., Tempst, P., and Pandolfi, P. P. (2009) *Nat. Cell Biol.* **11,** 420–432
30. Bashir, T., Pagan, J. K., Busino, L., and Pagano, M. (2010) *Cell Cycle* **9,** 971–974
31. Boutonnet, C., Tanguay, P. L., Julien, C., Rodier, G., Coulombe, P., and Meloche, S. (2010) *Cell Cycle* **9,** 975–979
32. Zemskova, M., Sahakian, E., Bashkirova, S., and Lilly, M. (2008) *J. Biol. Chem.* **283,** 20635–20644
33. Ji, P., Jiang, H., Rekhtman, K., Bloom, J., Ichetovkin, M., Pagano, M., and Zhu, L. (2004) *Mol. Cell* **16,** 47–58
34. Biggs, J. R., Peterson, L. F., Zhang, Y., Kraft, A. S., and Zhang, D. E. (2006) *Mol. Cell. Biol.* **26,** 7420–7429
35. Cen, B., Li, H., and Weinstein, I. B. (2009) *J. Biol. Chem.* **284,** 5265–5276
36. Aho, T. L., Sandholm, J., Peltola, K. J., Mankonen, H. P., Lilly, M., and Koskinen, P. J. (2004) *FEBS Lett.* **571,** 43–49
37. Barclay, W. W., and Cramer, S. D. (2005) *Prostate* **63,** 291–298
38. Carrano, A. C., Eytan, E., Hershko, A., and Pagano, M. (1999) *Nat. Cell Biol.* **1,** 193–199
39. Wang, W., Ungermannova, D., Chen, L., and Liu, X. (2003) *J. Biol. Chem.* **278,** 32390–32396
40. Kim, S. Y., Herbst, A., Tworkowski, K. A., Salghetti, S. E., and Tansey, W. P. (2003) *Mol. Cell* **11,** 1177–1188
41. Xia, Z., Knaak, C., Ma, J., Beharry, Z. M., McInnes, C., Wang, W., Kraft, A. S., and Smith, C. D. (2009) *J. Med. Chem.* **52,** 74–86
42. Balkovetz, D. F., and Lipschutz, J. H. (1999) *Int. Rev. Cytol.* **186,** 225–260
43. Bottaro, D. P., Rubin, J. S., Faletto, D. L., Chan, A. M., Kmiecik, T. E., Vande Woude, G. F., and Aaronson, S. A. (1991) *Science* **251,** 802–804
44. Nagahara, H., Vocero-Akbani, A. M., Snyder, E. L., Ho, A., Latham, D. G., Lissy, N. A., Becker-Hapak, M., Ezhevsky, S. A., and Dowdy, S. F. (1998) *Nat. Med.* **4,** 1449–1452
45. Zhang, H., Ozaki, I., Mizuta, T., Yoshimura, T., Matsuhashi, S., Hisatomi, A., Tadano, J., Sakai, T., and Yamamoto, K. (2003) *Hepatology* **38,** 305–313
46. Bachmann, M., and Möröy, T. (2005) *Int. J. Biochem. Cell Biol.* **37,** 726–730
47. Peters, J. M. (2006) *Nat. Rev. Mol. Cell Biol.* **7,** 644–656
48. Jaspersen, S. L., Charles, J. F., and Morgan, D. O. (1999) *Curr. Biol.* **9,** 227–236
49. Visintin, R., Craig, K., Hwang, E. S., Prinz, S., Tyers, M., and Amon, A. (1998) *Mol. Cell* **2,** 709–718
50. Zachariae, W., Schwab, M., Nasmyth, K., and Seufert, W. (1998) *Science* **282,** 1721–1724
51. Kramer, E. R., Scheuringer, N., Podtelejnikov, A. V., Mann, M., and Peters, J. M. (2000) *Mol. Biol. Cell* **11,** 1555–1569
52. van Leuken, R., Clijsters, L., and Wolthuis, R. (2008) *Biochim. Biophys. Acta* **1786,** 49–59
53. Sutterlüty, H., Chatelain, E., Marti, A., Wirbelauer, C., Senften, M., Müller, U., and Krek, W. (1999) *Nat. Cell Biol.* **1,** 207–214
54. Pogacic, V., Bullock, A. N., Fedorov, O., Filippakopoulos, P., Gasser, C., Biondi, A., Meyer-Monard, S., Knapp, S., and Schwaller, J. (2007) *Cancer Res.* **67,** 6916–6924
55. Choudhary, C., Olsen, J. V., Brandts, C., Cox, J., Reddy, P. N., Böhmer, F. D., Gerke, V., Schmidt-Arras, D. E., Berdel, W. E., Müller-Tidow, C., Mann, M., and Serve, H. (2009) *Mol. Cell* **36,** 326–339
56. Amaravadi, R., and Thompson, C. B. (2005) *J. Clin. Invest.* **115,** 2618–2624
57. Kraft, C., Vodermaier, H. C., Maurer-Stroh, S., Eisenhaber, F., and Peters, J. M. (2005) *Mol. Cell* **18,** 543–553
58. Hall, M. C., Warren, E. N., and Borchers, C. H. (2004) *Cell Cycle* **3,** 1278–1284
59. Bhattacharya, N., Wang, Z., Davitt, C., McKenzie, I. F., Xing, P. X., and Magnuson, N. S. (2002) *Chromosoma* **111,** 80–95
60. Roh, M., Gary, B., Song, C., Said-Al-Naief, N., Tousson, A., Kraft, A., Eltoum, I. E., and Abdulkadir, S. A. (2003) *Cancer Res.* **63,** 8079–8084
61. Roh, M., Song, C., Kim, J., and Abdulkadir, S. A. (2005) *J. Biol. Chem.* **280,** 40568–40577

Downloaded from www.jbc.org at MUSC Library, on May 22, 2012

The Pim protein kinases regulate energy metabolism and cell growth

Zanna Beharry[a], Sandeep Mahajan[b], Marina Zemskova[c], Ying-Wei Lin[d], Baby G. Tholanikunnel[b], Zuping Xia[a], Charles D. Smith[a,b], and Andrew S. Kraft[b,1]

[a]Department of Pharmaceutical and Biomedical Sciences, South Carolina College of Pharmacy, [b]Hollings Cancer Center, [c]Department of Cell and Molecular Pharmacology, and [d]Department of Pediatrics, Medical University of South Carolina, Charleston, SC 29425

Edited by Peter K. Vogt, The Scripps Research Institute, La Jolla, CA, and approved November 19, 2010 (received for review September 3, 2010)

The serine/threonine Pim kinases are overexpressed in solid cancers and hematologic malignancies and promote cell growth and survival. Here, we find that a novel Pim kinase inhibitor, SMI-4a, or Pim-1 siRNA blocked the rapamycin-sensitive mammalian target of rapamycin (mTORC1) activity by stimulating the phosphorylation and thus activating the mTORC1 negative regulator AMP-dependent protein kinase (AMPK). Mouse embryonic fibroblasts (MEFs) deficient for all three Pim kinases [triple knockout (TKO) MEFs] demonstrated activated AMPK driven by elevated ratios of AMP:ATP relative to wild-type MEFs. Consistent with these findings, TKO MEFs were found to grow slowly in culture and have decreased rates of protein synthesis secondary to a diminished amount of 5′-cap–dependent translation. Pim-3 expression alone in TKO MEFs was sufficient to reverse AMPK activation, increase protein synthesis, and drive MEF growth similar to wild type. Pim-3 expression was found to markedly increase the protein levels of both c-Myc and the peroxisome proliferator-activated receptor gamma coactivator 1α (PGC-1α), enzymes capable of regulating glycolysis and mitochondrial biogenesis, which were diminished in TKO MEFs. Overexpression of PGC-1α in TKO MEFs elevated ATP levels and inhibited the activation of AMPK. These results demonstrate the Pim kinase-mediated control of energy metabolism and thus regulation of AMPK activity. We identify an important role for Pim-3 in modulating c-Myc and PGC-1α protein levels and cell growth.

LKB1 | mitochondria | mTOR | 4EBP1

The Pim serine/threonine kinases include three isoforms, Pim-1, Pim-2, and Pim-3, that are implicated in the growth and progression of hematological malignancies, prostate cancer, and, in the case of Pim-3, in precancerous and cancerous lesions of the pancreas, liver, colon, and stomach (1–5). Pim-1 and Pim-2 have been shown to cooperate with c-Myc in inducing lymphoma (6), and prostate cancer (7), and in the absence of Pim-1 and Pim-2, Pim-3 is activated in c-Myc-induced lymphomas (8). The mechanisms suggested to explain this Pim–Myc synergism include Pim-mediated stabilization of c-Myc protein (9) and regulation of gene transcription via Pim-1 phosphorylation of histone H3 at active sites of c-Myc transcription (10). Other Pim kinase substrates that suggest these enzymes play a role in cell cycle progression and antiapoptosis include BAD, Bcl-2, Bcl-xL (11, 12), $p27^{Kip1}$ (13), and Cdc25A (14).

Recently, Pim kinases have been suggested to promote the activity of the rapamycin-sensitive mammalian target of rapamycin (mTORC1) (15–17). mTORC1 is a serine/threonine kinase that regulates cell growth and metabolism (18). The mTORC1 complex, composed of mTOR, raptor, GβL, and PRAS40, promotes protein synthesis by phosphorylating 4EBP1, thus stimulating its dissociation from the translational regulator eukaryotic initiation factor 4E (eIF4E) (17) allowing for cap-dependent translation. mTORC1 activity is regulated by a cascade of enzymes including LKB1, AMP-dependent protein kinase (AMPK), and TSC1 and 2 (19). AMPK senses the cellular energy status and is activated via LKB1-mediated phosphorylation when there is a decline in ATP levels and concomitant rise in AMP levels; i.e., high AMP:ATP ratio (20). Activated AMPK down-regulates the energetically demanding process of protein synthesis by inhibiting mTORC1 activity through phosphorylating TSC2 and raptor (20). The mechanisms by which Pim kinase stimulates mTORC1 appear complex and include 4EBP1, eIF4E (16, 21–23), and PRAS40 phosphorylation (15).

Because of the importance of the Pim kinase signal transduction pathway in the progression of various cancers, multiple groups have developed small-molecule inhibitors of this kinase family (24–28). We have identified unique benzylidene-thiazolidine-2-4-diones (23, 29) that inhibit Pim kinase activity in vitro at nanomolar concentrations, and in culture induce apoptosis of human leukemic cells (30) and synerigize with rapamycin to downregulate 4EBP1 phosphorylation and inhibit cell growth (29). Taking advantage of these inhibitors, siRNA, and genetically engineered Pim-deficient cells, we have discovered a unique role for Pim-3 in regulating mTORC1 activity through modulation of ATP levels by the induction of c-Myc and the transcriptional coactivator and master regulator of mitochondrial biogenesis peroxisome proliferator-activated receptor gamma coactivator 1α (PGC-1α).

Results

Pim Kinase Negatively Regulates AMPK. To examine the mechanisms by which Pim kinase can regulate the mTORC1 pathway, the human erythroleukemia cell line K562 was incubated with the thiazolidinedione Pim kinase inhibitor SMI-4a (23), and the phosphorylation of AMPK was studied. AMPK activation results in the phosphorylation of raptor and TSC2 and thus inhibits mTORC1 activity (20, 31). Pim kinase inhibition with SMI-4a induced the activation of AMPK as determined by phosphorylation of AMPKα at Thr172, and the AMPK targets acetyl-CoA carboxylase (ACC) at Ser79 and raptor at Ser792 and inhibition of mTORC1 activity as determined by decreased phosphorylation of the mTORC1 targets S6K and 4EBP1 (Fig. 1 *A* and *B*). Additionally, knockdown of Pim-1 levels with a targeted siRNA increased AMPK phosphorylation (Fig. 1*C*), suggesting that Pim-1 negatively regulates the phosphorylation of this enzyme. Because the LKB1 kinase is known to activate AMPK via phosphorylation at Thr172 (32) and loss of LKB1 activity is frequently associated with the transformed phenotype (32), we examined the ability of SMI-4a and SMI-16a, another Pim kinase inhibitor, (29) to regulate AMPK phosphorylation in a panel of LKB1-containing (H358, H661) and deficient (H23, H460, A549) lung cancer cell

Author contributions: Z.B. and A.S.K. designed research; Z.B., S.M., M.Z., Y.-W.L., and B.G.T. performed research; Z.B., S.M., M.Z., Y.-W.L., B.G.T., Z.X., and C.D.S. contributed new reagents/analytic tools; Z.B., S.M., M.Z., B.G.T., and A.S.K. analyzed data; and Z.B. and A.S.K. wrote the paper.

The authors declare no conflict of interest.

This article is a PNAS Direct Submission.

[1]To whom correspondence should be addressed. E-mail: kraft@musc.edu.

This article contains supporting information online at www.pnas.org/lookup/suppl/doi:10.1073/pnas.1013214108/-/DCSupplemental.

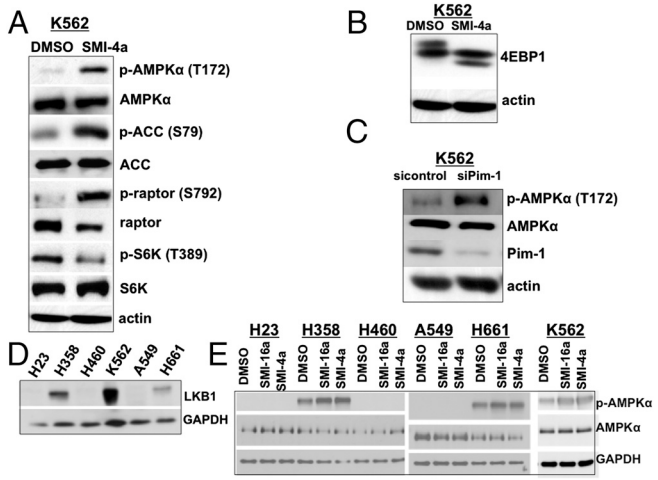

Fig. 1. Pim kinase inhibition activates AMPK. (*A* and *B*) K562 cells were treated with DMSO or SMI-4a (5 μM) for 1 h in the absence of serum, and lysates were probed for the indicated proteins by Western blotting. (*C*) K562 cells were transfected with scrambled siRNA (sicontrol) or Pim-1 siRNA (siPim-1), and 48 h later lysates were probed for the indicated proteins by Western blotting. (*D*) Western blot for LKB1 levels in lung cancer cell lines and the leukemia cell line K562. (*E*) Lung and leukemia cells were treated with DMSO, SMI-4a, or SMI-16a (5 μM) for 1 h in the absence of serum, and lysates were probed for the indicated proteins by Western blotting.

lines along with the LKB1-positive K562 cell line (Fig. 1*D*). These results demonstrate that the Pim kinase inhibitors SMI-4a and SMI-16a required LKB1 to stimulate AMPK activity (Fig. 1*E*).

To further confirm that Pim kinase regulates the activation of AMPK, we generated mouse embryonic fibroblasts (MEFs) deficient for Pim-1, -2, and -3 [triple knockout (TKO)] (33), and wild-type (WT) littermate control MEFs. Consistent with both the siRNA and small-molecule inhibition of Pim kinase activity, TKO MEFs had significantly higher AMPK phosphorylation compared to WT MEFs (Fig. 2*A*). To determine the contribution of each Pim isoform to AMPK activation, TKO MEFs were transduced with Pim-1, -2, or -3 lentiviruses. Although each Pim isoform reduced p-AMPK levels, Pim-3 showed the greatest effect (Fig. S1*A*) leading us to focus on elucidating the unique role of Pim-3. To confirm this result, we generated MEFs deficient in Pim-1 and Pim-2 (Pim-$1^{-/-}$, -$2^{-/-}$, -$3^{+/+}$) but expressing Pim-3, and demonstrated that these cells showed less activated AMPK than TKO MEFs (Fig. 2*A*). As AMPK activation is regulated by increased AMP, we measured the levels of AMP and ATP and found that AMPK phosphorylation correlates with the cellular AMP:ATP ratio in these knockout MEFs (Fig. 2*B*). Growth curves of these MEFs demonstrated a further correlation between proliferation, AMP:ATP ratio, and AMPK phosphorylation status (Fig. 2*C*) with the TKO MEFs showing the slowest growth rate. Similar results were obtained with immortalized WT or TKO MEFs transduced with empty vector or a lentivirus expressing Pim-3 (Fig. S1*B*).

Because activation of AMPK leads to inhibition of mTORC1 activity (31), we measured the level of protein synthesis in each of the MEFs. Labeling of MEFs with ^{35}S-methionine and measuring newly synthesized protein demonstrated, as predicted, that TKO MEFs when compared to WT have lower rates of protein synthesis (approximately 58% relative to WT). Expression of Pim-3 in the TKO cells increased protein synthesis from 58% (TKO) to 83% relative to WT (Fig. 2*D*). Consistent with this result, we found that in TKO MEFs the cap-dependent but not internal ribosome entry site (IRES)-dependent translational activity is reduced (Fig. 2*E*). Cap-dependent translation depends on the mTORC1-mediated release of 4EBP1 from eIF4E and the for-

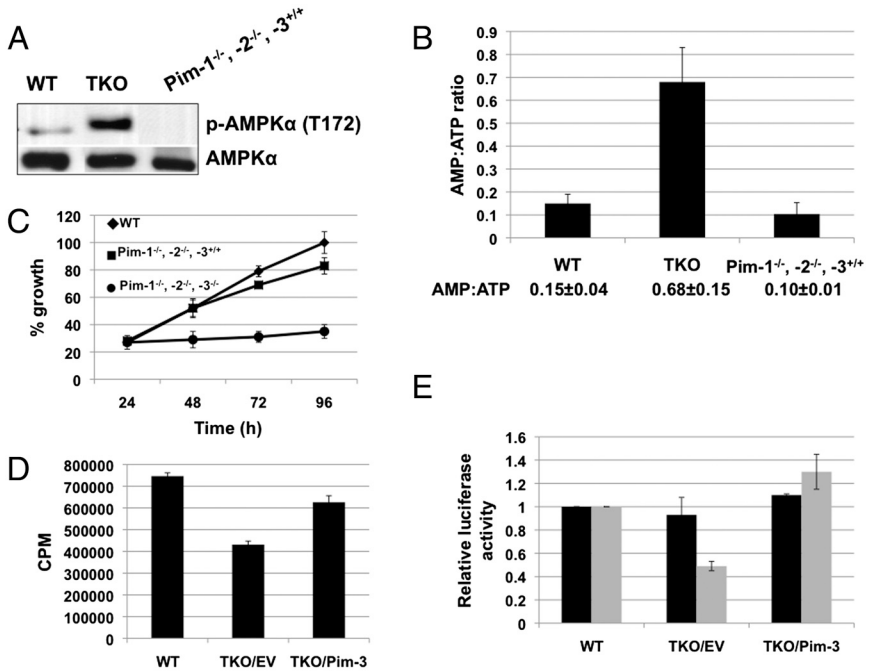

Fig. 2. Knockout of Pim kinase isoforms inhibits protein synthesis and cell growth. (*A*) Lysates were prepared from the different MEF cell lines and probed for the indicated proteins by Western blotting. (*B*) AMP:ATP ratios were determined by HPLC as described in *Materials and Methods*. Values are the average of three independent experiments, and the standard deviation from the mean is shown. (*C*) Growth curve of MEFs as determined by MTT assay. Percentage values are relative to the growth of WT MEFs at the 96 h time point (100%). The data points are the average of three independent measurements, and the standard deviation from the mean is shown. (*D*) ^{35}S-methionine incorporation into WT and TKO MEFs expressing empty vector (TKO/EV) or Pim-3 (TKO/Pim-3). Values (cpm/mg protein) are the average of three independent measurements, and the standard deviation for the mean is shown. (*E*) Cap-dependent (gray bars) and IRES-dependent (black bars) translation in MEFs as measured by Renilla and Firefly luciferase activities, respectively. As described in *Materials and Methods*, MEFs were infected with a virus expressing cap- and IRES-driven luciferase constructs. Values are the ratio of luciferase activity relative to WT and are the average of three independent measurements with the standard deviation from the mean shown.

mation of the eIF4F complex. Using m^7-GTP beads in a pull-down assay (34), we found that in TKO MEFs eIF4E is highly bound to 4EBP1, whereas eIF4G binding is lost and thus the ability of eIF4E to promote translation is inhibited (Fig. S1*C*). These results demonstrate that reduced Pim kinase activity correlates with increased AMP:ATP ratio, activation of AMPK, inhibition of mTORC1 activity, and reduced overall protein synthesis.

Pim-3 Regulates c-Myc Levels. In comparison to TKO MEFs, Pim-3–expressing cells demonstrated increased 5′-cap-dependent protein synthesis and growth similar to WT MEFs. Because the levels of the c-Myc protein are controlled by 5′-cap-dependent transcription, and c-Myc is important in the regulation of both cell growth and overall cellular metabolism, we examined the levels of c-Myc in MEFs from each genotype. Western blots demonstrate that the expression of Pim-3 either in primary MEFs (Fig. 3*A*) or after transduction into TKO MEFs (Fig. 3*B*) markedly increased c-Myc protein. Similar to p-AMPK (Fig. S1*A*), neither Pim-1 nor Pim-2 was able to induce the significant levels of c-Myc protein observed with Pim-3 overexpression in TKO MEFs (Fig. 3*B*). Furthermore, expression of Pim-1 or Pim-2 in Pim-3–only MEFs led to a decrease in c-Myc protein levels (Fig. S1*D*), suggesting the possibility that the Pim kinases could compete for substrates or interact directly. Because of the marked difference in c-Myc protein levels in MEFs containing Pim-3 only, we tested two additional MEF cell lines generated from different embryos of the same genotype and again observed increased c-Myc protein levels (Fig. S2*B*). To determine whether the increased c-Myc level in Pim-3–expressing cells is unique to MEFs in culture, we measured the c-Myc levels in spleen lysates of 4-mo-old WT, TKO, and Pim-$1^{-/-}$, -$2^{-/-}$, -$3^{+/+}$ mice and again found the highest level of c-Myc protein in the Pim-3–only genotype (Fig. S2*C*). Because deletion of one Pim might grossly elevate the level of another, in this case Pim-3, we measured the level of Pim-3 mRNA in the different MEF genotypes but did not find a significant difference (Fig. S2*A*). These results suggested that Pim-3 might modulate c-Myc translation.

To determine the effect of Pim-3 on c-Myc translation, we treated MEFs with cycloheximide until c-Myc protein was completely degraded, washed out the cycloheximide, and then monitored by Western blotting the rate of increase in c-Myc protein over time. To make this comparison possible, 2.5 times more protein from TKO MEFs was loaded on these SDS gels. TKO MEFs showed a delay in protein synthesis with only 53 and 43% as much c-Myc protein synthesis in the first 15 min when compared to WT and TKO/Pim-3 MEFS, respectively (Fig. 3*C*). This result is consistent with the reduced protein synthesis in the TKO MEFs (Fig. 2*D*). Because the overall translational efficiency in cells is reflected by changes in the polysome/monosome ratio, we determined the polysome profile using cytosolic extracts of WT, TKO, and TKO/Pim-3 cells. TKO cells showed a significant reduction in heavy polysomes and a corresponding increase in free ribosome subunits (Fig. 3*D Upper*). However, expression of Pim-3 in TKO cells resulted in a significant increase in heavy polysomes. c-Myc mRNA showed redistribution from heavy toward lighter polysomes and monosomes and free subunits in TKO cells relative to WT (Fig. 3*D Lower*). This shift was reversed by Pim-3 expression, suggesting that Pim-3 is capable of controlling the translation of c-Myc mRNA (Fig. 3*D Lower*). Because Pim-1 and -2 have been shown to increase the stability of c-Myc (9), we examined changes in c-Myc protein stability in TKO and TKO/Pim-3 MEFs after cycloheximide treatment but found no significant difference in c-Myc half-life in the Pim-3–containing cells (Fig. S2*D*). Finally, we found that the expression of c-Myc in TKO MEFs led to a decrease in AMPK activation (Fig. S2*E*) consistent with the ability of c-Myc to stimulate cell growth.

Pim-3 and c-Myc Regulate PGC-1α Levels. The differences in the growth rate between the TKO and Pim-3 only MEFs could possibly be explained by the Pim-3–mediated increased c-Myc because the latter is known to control multiple factors that regulate cell growth and metabolism (35, 36). Therefore, we compared the growth rate of TKO MEFs stably expressing empty vector, Pim-3, or c-Myc to WT MEFs. The TKO/c-Myc MEFs were able to

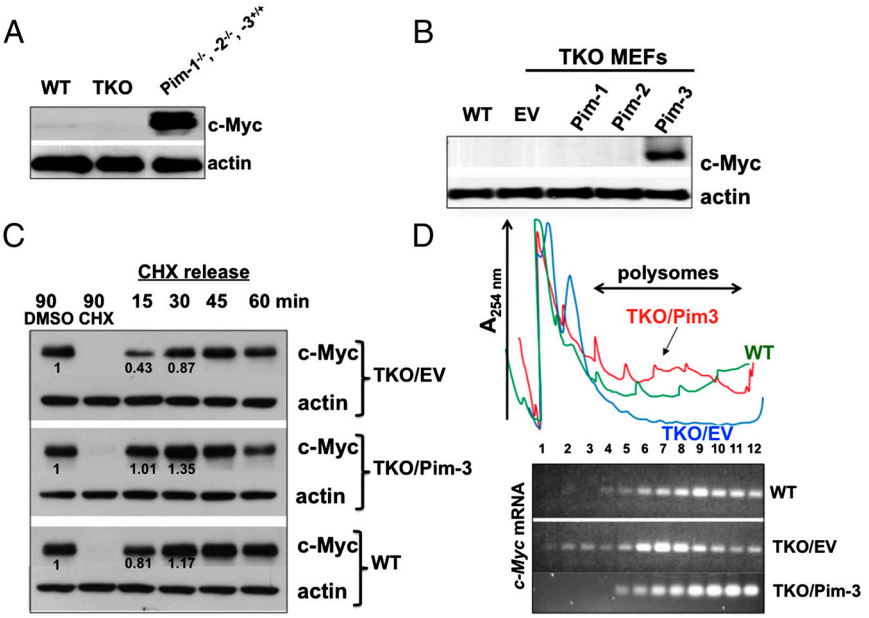

Fig. 3. Pim-3 elevates c-Myc levels. (*A*) c-Myc protein levels in each MEF genotype as determined by Western blotting. (*B*) TKO MEFs were infected with empty vector (EV), Pim-1, -2, or -3 lentiviruses, and 48 h later lysates were probed for c-Myc levels and compared to WT MEFs. (*C*) TKO MEFs expressing EV or Pim-3 were treated for 90 min with cycloheximide (CHX, 10 μM), the media replaced, and lysates probed for c-Myc levels by Western blotting. Densitometry analysis was performed, and the values at the 15 min time point relative to DMSO are shown. To obtain a relatively equal amount of c-Myc protein at the 90 min time point with DMSO, ~2.5-fold more TKO/EV protein lysate was loaded relative to TKO/Pim-3. (*D*) Ribosome fractions of WT and TKO MEFs expressing EV or Pim-3 were prepared by sucrose gradient (see *Materials and Methods*), and the level of c-Myc mRNA associated with each fraction was determined by PCR.

grow in the absence of Pim kinases but did not reach the same density in 96 h (Fig. 4*A*). The shRNA-mediated knockdown of c-Myc in TKO/Pim-3 MEFs did not completely inhibit cell proliferation (Fig. 4*B*). Together, these results suggest that Pim-3 and c-Myc do not have completely overlapping biologic activities. To understand how Pim-3 decreases the AMP:ATP ratio and inhibits AMPK phosphorylation, we measured the levels of PGC-1α. PGC-1α activates a wide variety of transcription factors that result in increased mitochondrial biogenesis and oxidative phosphorylation (37). Increased expression of PGC-1α can lead to elevations in ATP levels (38), whereas PGC-1α knockout leads to reduced ATP levels in murine hearts (39). PGC-1α expression and PGC-1α–dependent gene expression are induced by chemical activation of AMPK, and AMPK directly phosphorylates PGC-1α, leading to increased transcriptional activity (40–42). We found that the levels of PGC-1α mRNA and protein were greatly reduced in TKO MEFs, highest in Pim-3–only MEFs, and intermediate in WT cells (Fig. 4*C* and *D*). To examine the contributions of Pim-3 and c-Myc in regulating PGC-1α levels, we infected TKO MEFs with lentiviruses expressing c-Myc or Pim-3 and found that Pim-3 induced marked increases in PGC-1α mRNA (12-fold) and protein; the effect of c-Myc alone was a 4-fold increase in mRNA, and the increase in protein was quantitated at only 10% that of Pim-3 (Fig. 4*D*, *E*).

The above results suggest that the increased AMP:ATP ratio in TKO MEFs may be attributed to low ATP levels due to decreased PGC-1α protein, thus leading to AMPK activation. To examine whether overexpression of PGC-1α in TKO MEFs was sufficient to reduce p-AMPK by increasing the level of cellular ATP, we transduced TKO MEFs with a lentivirus expressing PGC-1α. Western blots and biochemical analysis demonstrate that PGC-1α expression in TKO MEFs decreased the level of p-AMPK (Fig. 5*A*) and increased the levels of ATP (Fig. 5*B*), leading to decreased 4EBP1 binding to eIF4E while increasing eIF4G association with the eIF4E protein (Fig. S3). In contrast, PGC-1α expression in TKO MEFs showed little effect on c-Myc levels (Fig. 5*A*). Thus, Pim-3, by controlling the levels of both c-Myc and PGC-1α, is able to impact on AMPK phosphorylation, mTORC1 activity, 5′-cap-dependent translation, and ultimately cell growth (Fig. 5*C*).

Discussion

The combined approach of genetic knockout, RNAi, and small-molecule inhibition implicate the Pim kinases in regulating the AMP:ATP ratio and energy metabolism. These effects lead to the modulation of the mTORC1 pathway by AMPK and the control of cell growth. In leukemic cells, the pan-Pim kinase inhibitor SMI-4a stimulated the phosphorylation and activation of AMPK, whereas in TKO MEFs the ratio of AMP:ATP was markedly increased and AMPK was activated. Because AMPK is a negative regulator of mTORC1, we found in leukemic cells treated with SMI-4a and in TKO MEFs that mTORC1 activity is inhibited and cap-dependent translation is significantly decreased. In MEFs, the expression of Pim-3 alone could reverse these processes, lowering the AMP:ATP ratio, decreasing the activation of AMPK, and increasing cap-dependent translation, all resulting in cellular growth rates comparable to WT MEFs. The differences between the TKO and Pim-3–only MEFs could be explained in part by the Pim-3–mediated increased c-Myc because the latter controls multiple transcription factors that regulate cell growth and metabolism (35, 36). Infection of TKO MEFS with a lentivirus expressing c-Myc increased the growth of these cells but did not duplicate the growth curve of Pim-3–expressing MEFs.

In muscle and fat tissue, the ability of activated AMPK to maintain an energy balance is achieved in part by stimulating PGC-1α (41). The ability of PGC-1α to coactivate multiple transcription factors makes this protein a master regulator of mitochondrial biogenesis (43). Considering this link between

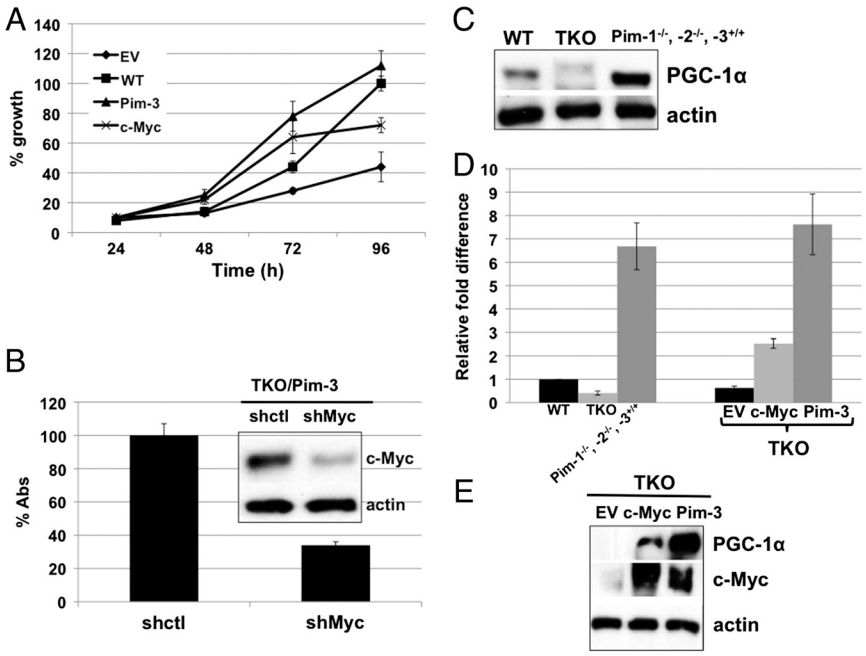

Fig. 4. Pim-3 and c-Myc affect PGC-1α levels. (*A*) Growth curve of TKO MEFs expressing empty vector (EV), c-Myc, or Pim-3 as determined by an MTT assay. Percentage values are relative to the value of WT MEFs at the 96 h time point (100%). The data points are the average of three independent measurements, and the standard deviation from the mean is shown. (*B*) TKO/Pim-3 MEFs were infected with nontargeting shRNA (shctl) or c-Myc targeting shRNA (shMyc) lentiviruses. Equal numbers of shctl and shMyc cells were plated 48 h postinfection, and after an additional 72 h viability was determined by an MTT assay and represented as a percent absorbance (%Abs) with shctl set at 100%. The data points are the average of three independent measurements, and the standard deviation from the mean is shown. (*Inset*) Lysates were prepared at 120 h postinfection and probed for the indicated proteins by Western blotting. (*C*) PGC-1α protein levels in MEFs as determined by Western blotting. (*D*) PGC-1α mRNA levels in primary MEFs (WT, TKO, Pim-1$^{-/-}$, -2$^{-/-}$, -3$^{+/+}$) or TKO MEFs infected with EV, c-Myc, or Pim-3 lentiviruses as determined by QT-PCR 48 h after infection. Values are the average of three independent measurements, and the standard deviation from the mean is shown. (*E*) PGC-1α protein levels as determined by Western blotting in TKO MEFs 48 h postinfection with EV, c-Myc, or Pim-3.

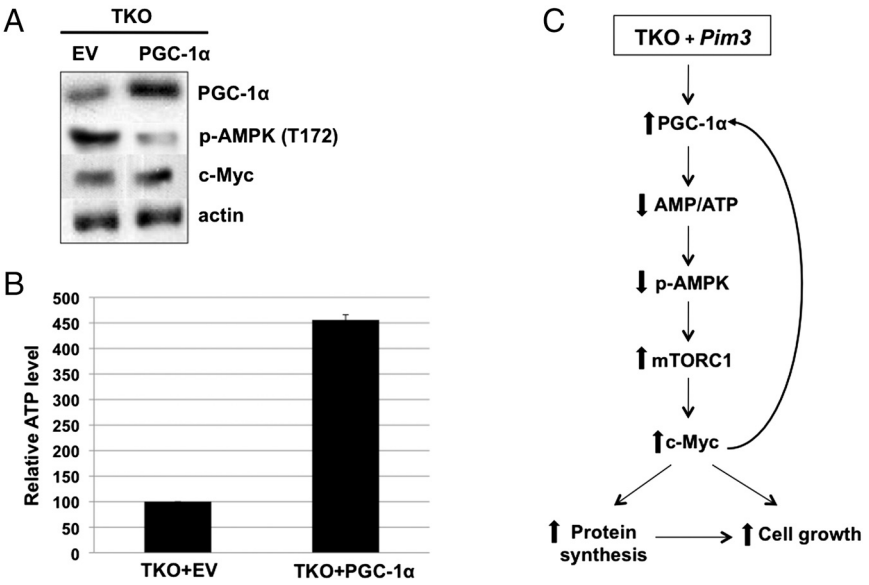

Fig. 5. Expression of PGC-1α restores the AMP:ATP ratio in TKO MEFs. (*A*) PGC-1α overexpression in TKO MEFs reduces AMPK activation. Lysates were prepared from TKO MEFs 48 h after transduction with empty vector (EV) or PGC-1α lentiviruses, and protein levels compared by Western blotting. (*B*) ATP levels determined in lysates from Fig. 5*A* as described in *Materials and Methods*. Values are the average of three independent measurements, and the standard deviation from the mean is shown. (*C*) Schematic summary of biologic changes observed in TKO MEFs expressing Pim-3.

AMPK and PGC-1α in the sensing and regulation of the cell's energy status, the levels of PGC-1α were investigated and found to be significantly lower in TKO MEFs. In comparison, Pim-3–containing MEFs showed increased levels of PGC-1α relative to WT. Therefore, in the case of the TKO MEFs, chronic AMPK activation coupled with drastically reduced levels of PGC-1α protein resulted in an elevated AMP:ATP ratio. Accordingly, infection of TKO MEFs with a lentivirus expressing PGC-1α was shown to increase ATP levels and decrease AMPK activation. The increased PGC-1α levels in Pim-3–only MEFs cannot be attributed solely to increased c-Myc because TKO/c-Myc MEFs showed lower levels of PGC-1α mRNA and protein relative to TKO/Pim-3 MEFs. This suggests the possibility that Pim-3 and c-Myc could cooperate in regulating PGC-1α levels in MEFs. This cooperation may extend beyond transcription/translation because PGC-1α levels and activity are regulated by multiple posttranslational mechanisms (37).

Pim-3 is the least-studied kinase of the Pim family; however, it has been linked to the development and progression of colon and pancreatic cancers (2–4, 44). Despite the high sequence identity and overlapping substrate specificity of the Pim kinases, Pim-3 expression alone is shown to overcome at least some of the defects found in the loss of both Pim-1 and Pim-2, including growth rate. Additionally, the knockout of Pim-1 and -2 and the expression of Pim-3 only led to a marked increase in c-Myc protein relative to WT MEFs. The observation that the transduction of Pim-1 or -2 into MEFs containing Pim-3 suppressed c-Myc levels suggested the possibility that individual Pim isoforms may regulate each other either directly or through substrate competition. This poses the question of whether Pim isoforms either individually or acting in concert regulate different biological processes and under what cellular circumstances. The question of the activity of Pim isoforms is of importance to the design of small-molecule inhibitors targeting these kinases and their use in the treatment of diseases, including cancer. Both Pim-1 and -2 are known to enhance c-Myc–induced transformation (6, 12) and phosphorylate and stabilize c-Myc protein, leading to increased transcriptional activity (9). In the MEFs used in this study, Pim-3 expression alone enhanced cap-dependent translation, increased c-Myc levels without changing the protein's stability, and increased the cell growth rate. Because elevated levels of both Pim-3 and c-Myc are found in gastrointestinal cancers, our results suggest the possibility that Pim-3 might enhance the growth of these tumor cells in part by regulating c-Myc levels, thus highlighting the potential utility of Pim-3 targeted inhibitors.

Materials and Methods

Cell Culture. MEFs were derived from 14.5-d-old embryos and were genotyped as described (45). For stable cell lines, TKO MEFs were transduced with lentiviruses encoding empty vector, PIM-1, Pim-2, Pim-3, or c-Myc and selected with puromycin (4 μg/mL).

Construction of Lentiviral Vectors. The open reading frames of PIM-1 (human, 33 kDa isoform), PIM-2 (mouse), Pim-3 (mouse), c-Myc (mouse), and PGC-1α (human, a gift from Young-In Chi, Department of Molecular and Cellular Biochemistry, University of Kentucky, Lexington, KY) were amplified by PCR from full-length cDNA clones and subcloned into the *AgeI-MluI* sites of pLex-MCS lentiviral vector (Open Biosystems). Methods for preparation of lentiviral stocks are detailed in *SI Materials and Methods*.

Quantitative RT-PCR (QT-PCR). Total RNA was isolated from MEFs using the RNeasy kit (Qiagen) according to the manufacturer's protocol. The first-strand cDNA was synthesized using Superscript first-strand synthesis kit and Oligo (dT) primer (Invitrogen).

Biochemical Analysis. K562 cells were transfected with scrambled siRNA or siPim-1 (ON-TARGETplus SMARTpool, Thermo Scientific) using Lipofectamine™2000 (Invitrogen) according to the manufacturer's protocol, and 48 h posttransfection lysates were prepared. Cell growth was measured using the 3-(4,5-dimethylthiazol-2-yl)-2,5-diphenyl tetrazolium bromide (MTT) assay. ATP, ADP, and AMP were measured by HPLC as described previously (46), and ATP was also measured using the ATP Bioluminescence Assay Kit HS II (Roche) with 10^5 cells. eIF4E was captured on m^7-GTP sepharose (GE Lifesciences) from WT and TKO MEFs lysate and bound 4EBP1 and eIF4G determined by Western blotting.

^{35}S-Methionine Incorporation. Cells were serum starved for 1 h in methionine-free medium (Invitrogen), followed by labeling with 100 mCi of ^{35}S-methionine/mL. Lysates and labeled proteins were precipitated with trichloroacetic acid on glass microfiber filters (Whatman) using vacuum filtration, and ^{35}S-incorporation was counted.

Cap- vs. IRES-Dependent Translation. A bicistronic retroviral vector, pMSCV/rLuc-pol IRES-fLuc (a gift from Peter B. Bitterman, Department of Medicine, University of Minnesota, Minneapolis, MN), was used to produce viral particles for infecting WT, TKO and TKO/Pim-3 MEFs. Cells were collected

48 hr postinfection and Renilla/Firefly luciferase activities were quantified using the dual-luciferase reporter assay system (Promega) and a luminometer according to the manufacturer's instructions.

Polysome Profile Analysis. Sucrose density gradient centrifugation was employed to separate the ribosome fractions as described previously (47). c-Myc mRNA level in each fraction was measured by PCR.

ACKNOWLEDGMENTS. We thank Yefim Manevich and Robin Muise-Helmericks (Medical University of South Carolina) for technical assistance. We are grateful to Anton Berns (Netherlands Cancer Institute) and Paul B. Rothman (University of Iowa Medical Center) for the generous gift of Pim TKO mice. We also thank Vortex Biotechnology for providing the Pim kinase inhibitors used in this study. This work was supported in part by Department of Defense Grant W81XWH-08-PCRP-IDA, and the shared resources are supported by the Hollings Cancer Center.

1. Shah N, et al. (2008) Potential roles for the PIM1 kinase in human cancer—A molecular and therapeutic appraisal. *Eur J Cancer* 44:2144–2151.
2. Fujii C, et al. (2005) Aberrant expression of serine/threonine kinase Pim-3 in hepatocellular carcinoma development and its role in the proliferation of human hepatoma cell lines. *Int J Cancer* 114:209–218.
3. Li YY, et al. (2006) Pim-3, a proto-oncogene with serine/threonine kinase activity, is aberrantly expressed in human pancreatic cancer and phosphorylates bad to block bad-mediated apoptosis in human pancreatic cancer cell lines. *Cancer Res* 66:6741–6747.
4. Popivanova BK, et al. (2007) Proto-oncogene, Pim-3 with serine/threonine kinase activity, is aberrantly expressed in human colon cancer cells and can prevent Bad-mediated apoptosis. *Cancer Sci* 98:321–328.
5. White E (2003) The pims and outs of survival signaling: Role for the Pim-2 protein kinase in the suppression of apoptosis by cytokines. *Genes Dev* 17:1813–1816.
6. Allen JD, Verhoeven E, Domen J, van der Valk M, Berns A (1997) Pim-2 transgene induces lymphoid tumors, exhibiting potent synergy with c-myc. *Oncogene* 15:1133–1141.
7. Wang J, et al. (2010) Pim1 kinase synergizes with c-MYC to induce advanced prostate carcinoma. *Oncogene* 29:2477–2487.
8. Mikkers H, et al. (2002) High-throughput retroviral tagging to identify components of specific signaling pathways in cancer. *Nat Genet* 32:153–159.
9. Zhang Y, Wang Z, Li X, Magnuson NS (2008) Pim kinase-dependent inhibition of c-Myc degradation. *Oncogene* 27:4809–4819.
10. Zippo A, De Robertis A, Serafini R, Oliviero S (2007) PIM1-dependent phosphorylation of histone H3 at serine 10 is required for MYC-dependent transcriptional activation and oncogenic transformation. *Nat Cell Biol* 9:932–944.
11. Macdonald A, et al. (2006) Pim kinases phosphorylate multiple sites on Bad and promote 14-3-3 binding and dissociation from Bcl-XL. *BMC Cell Biol* 7:1.
12. Shirogane T, et al. (1999) Synergistic roles for Pim-1 and c-Myc in STAT3-mediated cell cycle progression and antiapoptosis. *Immunity* 11:709–719.
13. Morishita D, Katayama R, Sekimizu K, Tsuruo T, Fujita N (2008) Pim kinases promote cell cycle progression by phosphorylating and down-regulating p27Kip1 at the transcriptional and posttranscriptional levels. *Cancer Res* 68:5076–5085.
14. Bachmann M, et al. (2006) The oncogenic serine/threonine kinase Pim-1 directly phosphorylates and activates the G2/M specific phosphatase Cdc25C. *Int J Biochem Cell Biol* 38:430–443.
15. Zhang F, et al. (2009) PIM1 protein kinase regulates PRAS40 phosphorylation and mTOR activity in FDCP1 cells. *Cancer Biol Ther* 8:846–853.
16. Hammerman PS, Fox CJ, Birnbaum MJ, Thompson CB (2005) Pim and Akt oncogenes are independent regulators of hematopoietic cell growth and survival. *Blood* 105:4477–4483.
17. Laplante M, Sabatini DM (2009) mTOR signaling at a glance. *J Cell Sci* 122:3589–3594.
18. Gibbons JJ, Abraham RT, Yu K (2009) Mammalian target of rapamycin: Discovery of rapamycin reveals a signaling pathway important for normal and cancer cell growth. *Semin Oncol* 36:S3–S17.
19. Bai X, Jiang Y (2010) Key factors in mTOR regulation. *Cell Mol Life Sci* 67:239–253.
20. Shaw RJ (2009) LKB1 and AMP-activated protein kinase control of mTOR signalling and growth. *Acta Physiol* 196:65–80.
21. Chen WW, Chan DC, Donald C, Lilly MB, Kraft AS (2005) Pim family kinases enhance tumor growth of prostate cancer cells. *Mol Cancer Res* 3:443–451.
22. Lilly M, Kraft A (1997) Enforced expression of the Mr 33,000 Pim-1 kinase enhances factor-independent survival and inhibits apoptosis in murine myeloid cells. *Cancer Res* 57:5348–5355.
23. Xia Z, et al. (2009) Synthesis and evaluation of novel inhibitors of Pim-1 and Pim-2 protein kinases. *J Med Chem* 52:74–86.
24. Pogacic V, et al. (2007) Structural analysis identifies imidazo[1,2-b]pyridazines as PIM kinase inhibitors with in vitro antileukemic activity. *Cancer Res* 67:6916–6924.
25. Akue-Gedu R, et al. (2009) Synthesis, kinase inhibitory potencies, and in vitro antiproliferative evaluation of new Pim kinase inhibitors. *J Med Chem* 52:6369–6381.
26. Chen LS, Redkar S, Bearss D, Wierda WG, Gandhi V (2009) Pim kinase inhibitor, SGI-1776, induces apoptosis in CLL lymphocytes. *Blood* 114:4150–4157.
27. Grey R, et al. (2009) Structure-based design of 3-aryl-6-amino-triazolo[4,3-b]pyridazine inhibitors of Pim-1 kinase. *Bioorg Med Chem Lett* 19:3019–3022.
28. Tong Y, et al. (2008) Isoxazolo[3,4-b]quinoline-3,4(1H,9H)-diones as unique, potent and selective inhibitors for Pim-1 and Pim-2 kinases: Chemistry, biological activities, and molecular modeling. *Bioorg Med Chem Lett* 18:5206–5208.
29. Beharry Z, et al. (2009) Novel benzylidene-thiazolidine-2,4-diones inhibit Pim protein kinase activity and induce cell cycle arrest in leukemia and prostate cancer cells. *Mol Cancer Ther* 8:1473–1483.
30. Lin Y, et al. (2009) A small molecule inhibitor of Pim protein kinases blocks the growth of precursor T-cell lymphoblastic leukemia/lymphoma. *Blood* 115:824–833.
31. Gwinn DM, et al. (2008) AMPK phosphorylation of raptor mediates a metabolic checkpoint. *Mol Cell* 30:214–226.
32. Hezel AF, Bardeesy N (2008) LKB1; linking cell structure and tumor suppression. *Oncogene* 27:6908–6919.
33. Mikkers H, et al. (2004) Mice deficient for all PIM kinases display reduced body size and impaired responses to hematopoietic growth factors. *Mol Cell Biol* 24:6104–6115.
34. Connolly E, Braunstein S, Formenti S, Schneider RJ (2006) Hypoxia inhibits protein synthesis through a 4E-BP1 and elongation factor 2 kinase pathway controlled by mTOR and uncoupled in breast cancer cells. *Mol Cell Biol* 26:3955–3965.
35. Liu YC, et al. (2008) Global regulation of nucleotide biosynthetic genes by c-Myc. *PLoS One* 3–e2722.
36. Li F, et al. (2005) Myc stimulates nuclearly encoded mitochondrial genes and mitochondrial biogenesis. *Mol Cell Biol* 25:6225–6234.
37. Canto C, Auwerx J (2009) PGC-1alpha, SIRT1 and AMPK, an energy sensing network that controls energy expenditure. *Curr Opin Lipidol* 20:98–105.
38. Liang H, Bai Y, Li Y, Richardson A, Ward WF (2007) PGC-1alpha-induced mitochondrial alterations in 3T3 fibroblast cells. *Ann NY Acad Sci* 1100:264–279.
39. Arany Z, et al. (2005) Transcriptional coactivator PGC-1 alpha controls the energy state and contractile function of cardiac muscle. *Cell Metab* 1:259–271.
40. Suwa M, Nakano H, Kumagai S (2003) Effects of chronic AICAR treatment on fiber composition, enzyme activity, UCP3, and PGC-1 in rat muscles. *J Appl Physiol* 95:960–968.
41. Jäger S, Handschin C, St.-Pierre J, Spiegelman BM (2007) AMP-activated protein kinase (AMPK) action in skeletal muscle via direct phosphorylation of PGC-1α. *Proc Natl Acad Sci USA* 104:12017–12022.
42. Irrcher I, Ljubicic V, Kirwan AF, Hood DA (2008) AMP-activated protein kinase-regulated activation of the PGC-1alpha promoter in skeletal muscle cells. *PLoS One* 3:e3614.
43. Finley LW, Haigis MC (2009) The coordination of nuclear and mitochondrial communication during aging and calorie restriction. *Ageing Res Rev* 8:173–188.
44. Li YY, Wu Y, Tsuneyama K, Baba T, Mukaida N (2009) Essential contribution of Ets-1 to constitutive Pim-3 expression in human pancreatic cancer cells. *Cancer Sci* 100:396–404.
45. Xu J (2005) Preparation, culture, and immortalization of mouse embryonic fibroblasts. *Curr Protoc Mol Biol* Chap 28: Unit 28.1.
46. Hahn-Windgassen A, et al. (2005) Akt activates the mammalian target of rapamycin by regulating cellular ATP level and AMPK activity. *J Biol Chem* 280:32081–32089.
47. Ishimaru D, et al. (2009) Regulation of Bcl-2 expression by HuR in HL60 leukemia cells and A431 carcinoma cells. *Mol Cancer Res* 7:1354–1366.

Published OnlineFirst November 11, 2011; DOI:10.1158/0008-5472.CAN-11-3240

Pim Kinase Inhibitors Sensitize Prostate Cancer Cells to Apoptosis Triggered by Bcl-2 Family Inhibitor ABT-737

Jin H. Song[1,3] and Andrew S. Kraft[2,3]

Abstract

Pim serine/threonine kinases contribute to prostate tumorigenesis and therapeutic resistance, yet Pim kinase inhibitors seem to have only limited effects on prostate cancer cell survival. Because overexpression of Bcl-2 family members are implicated in chemotherapeutic resistance in prostate cancer, we investigated the cooperative effects of Pim kinase inhibition with ABT-737, a small molecule antagonist of Bcl-2 family members. Strikingly, the addition of ABT-737 to Pim inhibitors triggered a robust apoptosis of prostate cancer cells *in vitro* and *in vivo*. Pim inhibitors decreased levels of the Bcl-2 family member Mcl-1, both by blocking 5′-cap dependent translation and decreasing protein half life. In addition, Pim inhibition transcriptionally increased levels of the BH3 protein Noxa by activating the unfolded protein response (UPR), lead to eIF-2α phosphorylation and increased expression of CHOP. Increased levels of Noxa also inactivated the remaining levels of Mcl-1 protein activity. Notably, these specific protein changes were essential to the apoptotic process because ABT-737 did not inhibit Mcl-1 protein activity and Mcl-1 overexpression blocked the apoptotic activity of ABT-737. Our results therefore suggest that this combination treatment could be developed as a potential therapy for human prostate cancer where overexpression of Pim kinases and antiapoptotic Bcl-2 family members drives tumor cell resistance to current anticancer therapies. *Cancer Res; 72(1); 294–303. ©2011 AACR.*

Introduction

The Pim family of serine threonine protein kinases plays a critical but unexplicated role in the growth and progression of human prostate cancer (1). This enzyme family is overexpressed in human prostate cancer compared with benign biopsies (2) and enhanced levels of nuclear Pim-2 in tumor cells have been associated with a higher risk of prostate-specific antigen (PSA) recurrence and with perineural invasion of the prostate gland (3). Moderate to strong cytoplasmic staining of Pim-1 was seen in tumors of 68% of patients with a Gleason score of 7 or higher (4). Pim-1 is overexpressed in high grade prostate intraepithelial neoplasia, and Pim staining may be helpful in differentiating benign glands from intraepithelial neoplasia (2). We have previously reported that the expression of Pim-1 in prostate cancer cells confers a growth advantage on these tumor cells (5). Patients with high levels of Pim-1 expression in the prostate are at significantly greater risk for developing metastatic cancer (6). In animals, overexpression of the c-Myc protein in the prostate induces neoplasia and is associated with increased Pim protein kinase levels (7). In a subrenal capsular assay for prostate regeneration, expression of Pim-1 kinase promotes c-Myc-driven prostate carcinogenesis (8). These studies suggest that the Pim protein kinases may be a target to inhibit prostate cancer growth.

Through chemical library screening (9), we have identified the chemotype of benzylidene-thiazolidine-2,4-diones as a specific Pim protein kinase inhibitor and focused on SMI-4a, a pan isotype inhibitor, as a potential lead compound. SMI-4a induces both apoptosis and cell-cycle arrest in a wide variety of leukemic cell lines (10). In addition, oral administration of SMI-4a to mice is well tolerated and causes moderate inhibition of leukemic growth when cells are grown as tumor xenografts (11). When administered to prostate cancer cells, Pim inhibitors induce a cell-cycle block but are only moderately inhibitory to growth (10). Although the mechanism of action of this agent has not been fully evaluated, we have shown that application of SMI-4a to both leukemia and prostate cells inhibits mammalian target of rapamycin complex 1 (mTORC1) activity and 4E-BP1 phosphorylation (10, 12), possibly by activating the AMP-dependent protein kinase (AMPK). Application of Pim inhibitors stimulates a fall in ATP levels and increases the concentration of AMP (12). Activated AMPK phosphorylates raptor and TSC2 to block mTORC1 activity (13). AMPK activation by Pim inhibition requires phosphorylation of Thr-172 by LKB (12), suggesting that control of energy supplies by SMI-4a could be an essential part of its activity.

Authors' Affiliations: Departments of [1]Biochemistry and Molecular Biology, and [2]Medicine, and [3]the Hollings Cancer Center, the Medical University of South Carolina, Charleston, South Carolina

Note: Supplementary data for this article are available at Cancer Research Online (http://cancerres.aacrjournals.org/).

Corresponding Authors: Jin H. Song, Department of Biochemistry and Molecular Biology, Medical University of South Carolina, 86 Jonathan Lucas Street, Charleston, SC 29425. Phone: 843-792-9366; Fax: 843-792-3200; E-mail: songjin@musc.edu; and Andrew S. Kraft, Department of Medicine, Medical University of South Carolina, 86 Jonathan Lucas Street, Charleston, SC 29425. Phone: 843-792-8284; Fax: 843-792-3200; E-mail: kraft@musc.edu

doi: 10.1158/0008-5472.CAN-11-3240

©2011 American Association for Cancer Research.

Downloaded from cancerres.aacrjournals.org on May 22, 2012
Copyright © 2012 American Association for Cancer Research

Published OnlineFirst November 11, 2011; DOI:10.1158/0008-5472.CAN-11-3240

The resistance of prostate cancers to undergo apoptosis when challenged with various chemotherapeutic agents could be due to the overexpression of antiapoptotic members of the Bcl-2 protein family. Studies have shown that metastatic prostate cancer and castration-refractory tumors are positively associated with Bcl-2 overexpression (14), so the moderate sensitivity of prostate cancer cells to Pim kinase inhibitors could be due to deregulated expression of pro- and antiapoptotic Bcl-2 proteins. ABT-737, a small molecule BH3 mimetic that interacts tightly with Bcl-2/Bcl-xL/Bcl-w and inhibits their activity, has the potential to overcome this resistance (15). However, this agent does not bind to Mcl-1 and Bfl-1 proteins. Research by us and others shows that Mcl-1 can constrain the proapoptotic activity of ABT-737 (16). Recent reports showed that that ABT-737 acquires intrinsic resistance to apoptosis by increasing Mcl-1 binding with Bim (17), and ABT-737 resistance is associated with reduced levels of Bcl-2:Bim heterodimers (18) and high Mcl-1 expression (16, 19). Although ABT-737 has generated anticancer activity in small cell lung cancer, leukemia, and multiple myeloma, prostate cancer cells *in vitro* exhibit a poor response to the proapoptotic action of ABT-737 because the Mcl-1 protein is widely expressed at high levels in prostate cancer cell lines and inhibits the proapoptotic function of ABT-737. We have shown that ABT-737 as a single agent has little proapoptotic activity in prostate cancer cells (20, 21). However, the combination of ABT-737 and a Pim inhibitor is highly synergistic in inducing apoptotic cell death. We investigated the ABT-737/Pim inhibitor synergy, with particular focus on the mechanism by which Pim inhibitors regulate apoptotic pathways. Thus, we suggest a rationale for this novel combination therapy.

Materials and Methods

Cell lines, cell culture, and chemicals

Prostate cancer cell lines LNCaP, PC-3, DU-145, and 22Rv1 were purchased from the ATCC. Cells were grown in DMEM or RPMI1640 supplemented with 10% FBS, 2 mmol/L Glutamax and 1% antibiotics (Invitrogen) as previously described (21). Subconfluent cells were treated with Pim inhibitors or vehicle in the absence of FBS. (Z)-5-(3-Trifluoromethylbenzylidene) thiazolidine-2,4-dione (referred to as SMI-4a) and [Z,E]-5-[4-ethylbenzylidine]-2-thioxothiazolidin-4-one (referred to as 10058-F4) were from Calbiochem. For animal experiment, SMI-4a was prepared as we reported previously (9). K00135 was purchased from BioFocus. 8-(4-Hydroxylphenyl)-2-[(dimethlamino)methyl][1]benzothieno-[3,2-d]pyrimidin-4 (3H)-one (referred to as Pimi-14j; ref. 22) and ABT-737 were a gift of Abbott Laboratories. Other chemicals of analytic grade were purchased from EMD Chemicals and Sigma-Aldrich.

Short hairpin RNAs and plasmids

The Arrest-In Lentiviral expression system (Open Biosystems was used to establish a LNCaP cell line harboring small hairpin microRNAs (shRNA) as described previously (12, 20). Lentiviruses pGIPZ shRNAmir against human Pim-1 (RHS4531-NM_002648), Pim-2 (RHS4531-NM_006875), and Pim-3 (RHS4531-NM_001001852), and a nonsilencing control (RHS4348) were purchased from Open Biosystems. PC-3 cells were transfected with pcDNA3.1-HA-Bcl-2 (23) and pcDNA3-Bcl-2 (AddGene) by LipofectAMINE2000 (Invitrogen) and then transfectants were selected and grown in 1 mg/mL of G418 (Sigma-Aldrich).

Tumor growth *in vivo*

Xenografts bearing prostate tumors were generated by injection of LNCaP cells (5×10^6) in the flanks of the male NU/NU nude mice (Charles River). After tumors were grown to at least 100 mm^3 (~1 week after implantation), 36 mice were randomly divided into 4 different treatment groups: Group 1 (6 mice), vehicle only (30% propylene glycol, 5% Tween-80, 65% of 5% dextrose in water, pH 4–5); Group 2 (12 mice), 60 mg/kg SMI-4a twice daily treatments (BID); Group 3 (6 mice), 50 mg/kg ABT-737 once a day (QD); and Group 4 (12 mice), combination treatment with SMI-4a (BID) and ABT-737 (QD). Mice received oral gavages for SMI-4a or/and intraperitoneal injection for ABT-737. Treatment was begun on day 8 and administered 5 of 7 days each week for 3 weeks. The growth of the subcutaneous tumors was measured twice each week, and mouse body weight was determined on days 0 and 21. Tumor size was calculated using the equation $(L \times W^2)/2$. The Institutional Animal Care and Use Committee at the Medical University of South Carolina approved these animal experiments. For the immunohistochmistry of xenograft tumor tissues, tissue slices were processed to generate 5 μm tissue slides. Sections were stained with H&E, mouse monoclonal antibody to human Mcl-1 (Santa Cruz Biotechnology), and rabbit antibody to cleaved caspase-3 (Cell Signaling Technology) according to the manufacturer's protocol for these products.

Quantitative real time PCR, immunoblotting, and biochemical analysis

Quantitative real time PCR (qT-PCR) and immunoblot analyses were carried out as previously reported (20) with slight modification as described in the Supplementary Methods. Methods for the 7-Methyl-GTP cap binding assay and ^{35}S-methinone incorporation were reported previously (12) and are further described in the Supplementary Methods.

Results

Inhibition of Bcl-2 like proteins with ABT-737 synergizes with SMI-4a to induce apoptosis

SMI-4a, a small molecule Pim kinase inhibitor, has preclinical efficacy in lymphoid and myeloid leukemia (11) but the human prostate cancer cell lines LNCaP, PC-3, and 22Rv1 only respond modestly to SMI-4a treatment (Supplementary Fig. S1A). To show whether the response to Pim inhibitors was Pim specific, we knocked down the expression of all 3 Pims, 1, 2, and 3, using shRNAs. The knockdown of each of these individual Pim kinases in LNCaP cells, as shown by qT-PCR, decreased the growth of these human prostate cancer cells (Supplementary Fig. S2). Because Bcl-2 protein family expression is associated with resistance of prostate cancer to standard chemotherapy, and a higher frequency of Bcl-2 expression is seen in recurrent

Downloaded from cancerres.aacrjournals.org on May 22, 2012
Copyright © 2012 American Association for Cancer Research

Published OnlineFirst November 11, 2011; DOI:10.1158/0008-5472.CAN-11-3240

tumors after castration (24, 25), we examined whether combination therapy with a small molecule BH3 mimetic ABT-737 and a Pim inhibitor would provide an enhanced apoptotic response. ABT-737 binds and induces apoptosis by inhibiting the activity of Bcl-2, Bcl-x_L, and Bcl-w. However, this compound is incapable of binding to Bcl-2 like the protein Mcl-1, and increased expression of this protein in numerous cancer cell types was sufficient to inhibit the activity of ABT-737 (21). ABT-737 treatment of LNCaP cells alone induced only a small percentage of cell death, but when combined with SMI-4a, a high degree of synergy in inducing cell death occurred (Fig. 1A). ABT-737 treatment alone induced slight cleavage of PARP-1 (Fig. 1B), a marker of apoptosis, but when combined with SMI-4a marked cleavage of this protein was seen. Similar synergistic results were obtained with another structurally different Pim inhibitor Pimi-14j (22), which blocks Pim activity *in vitro* in the low nanomolar range (Fig. 1A). Combination therapy with this Pim kinase inhibitor and ABT-737 induced enhanced caspase-3 and PARP-1 cleavage (Fig. 1B). A robust induction of cell death by these 2 agents was also seen in PC-3 cells, another human prostate cancer cell line (Supplementary Fig. S3). A third Pim kinase inhibitor K00135 was also synergistic with ABT-737 (Supplementary Fig. S3). Moreover, this combination overcame resistance to cell death in human prostate cancer cells overexpressing Bcl-2 (Fig. 1C).

Pim kinase inhibitors downregulate Mcl-1 protein expression by lowering global protein synthesis

To determine a potential mechanism by which Pim inhibitors synergize with ABT-737 to kill prostate cancer cells, we examined the ability of SMI-4a to regulate the levels of BH3 and Bcl-2 family member proteins important in controlling apoptotic cell death. Western blot results (Fig. 2A) show that either inhibition of Pim kinases with SMI-4a or knockdown of Pim kinases with shRNAs induced a marked decrease in Mcl-1 and an increase in Noxa protein. These results are significant because Noxa is capable of binding and inhibiting the anti-apoptotic activity of Mcl-1 and thereby overcomes ABT-737 resistance. In LNCaP cells, the levels of Mcl-1 expression were reduced by SMI-4a treatment in a time- and dose-dependent manner (Fig. 2B). In addition, in the PC-3 cell line a decrease in the Mcl-1 protein levels was induced by SMI-4a treatment (Supplementary Fig. S4A) and 2 additional small molecule Pim kinase inhibitors, K00135 and Pimi-14j (Supplementary Fig. S4B). No significant change in the levels of *MCL-1* mRNA occurred after the treatment with the Pim inhibitor SMI-4a (Supplementary Fig. S4C). A further suggestion that Pim kinase plays a role in regulating Mcl-1 protein levels comes from the evaluation of mouse embryo fibroblasts (MEF) derived from mice that were genetically engineered to knock out all 3 Pim proteins (TKO; ref. 12). After ^{35}S-methionine labeling, these MEFs showed a lower level of the Mcl-1 protein (Supplementary Fig. S4D; ref. 12). Given that *MCL-1* mRNA levels were unaffected by Pim inhibitors, we next labeled LNCaP cells with ^{35}S-methionine followed by immunoprecipitation and examined the Mcl-1 synthesis. Our results show that SMI-4a inhibits the translation of this protein (Fig. 2C). In addition, ^{35}S methionine-labeled whole cell extracts showed that this drug treatment suppressed total protein synthesis in LNCaP cells (Fig. 2D). These results are identical to those previously

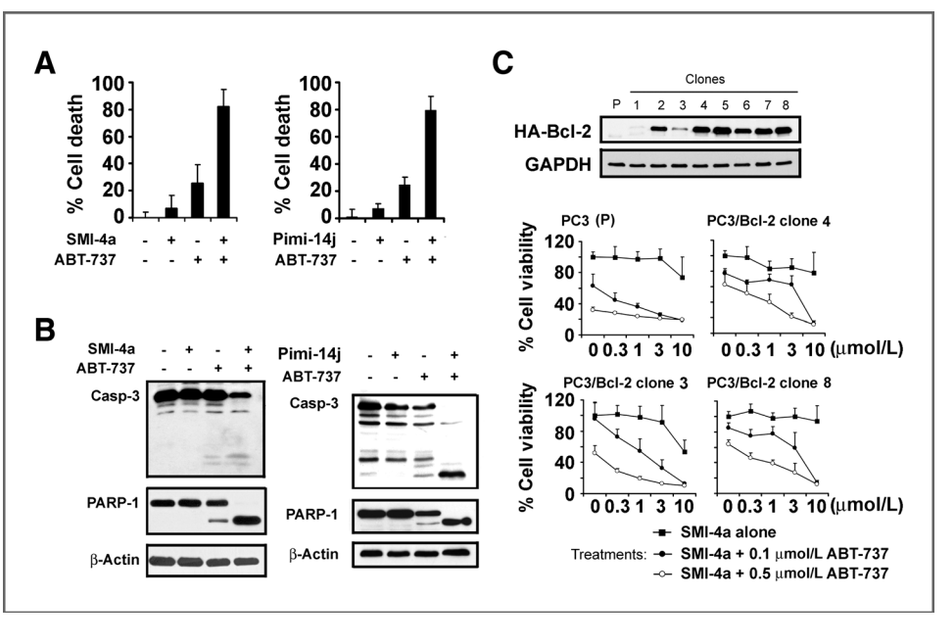

Figure 1. Bcl-2 inhibitor ABT-737 synergizes with small molecule inhibitors of Pim protein kinases to overcome cell resistance mediated by Bcl-2 overexpression. A, LNCaP cells were treated with DMSO, ABT-737 (3 μmol/L), SMI-4a (10 μmol/L), Pimi-14j (10 μmol/L), or combinations for 16 hours. The percentage of cell death was evaluated using trypan blue staining assay (mean ± SD, $n = 6$). B, whole cell extracts from the above treatments were analyzed by immunoblotting with the antibodies shown. C, PC-3 cells were transfected with HA-tagged Bcl-2 plasmid and individual clones selected with 1 mg/mL G418 treatment. Parental PC-3 (P) cells and selected individual clones were treated with DMSO, SMI-4a, ABT-737 or combinations of both agents at the indicated doses. The percentage of viable cells after 24 hours of treatment was determined by MTT assay (mean ± SD, $n = 4$).

Downloaded from cancerres.aacrjournals.org on May 22, 2012
Copyright © 2012 American Association for Cancer Research

Published OnlineFirst November 11, 2011; DOI:10.1158/0008-5472.CAN-11-3240

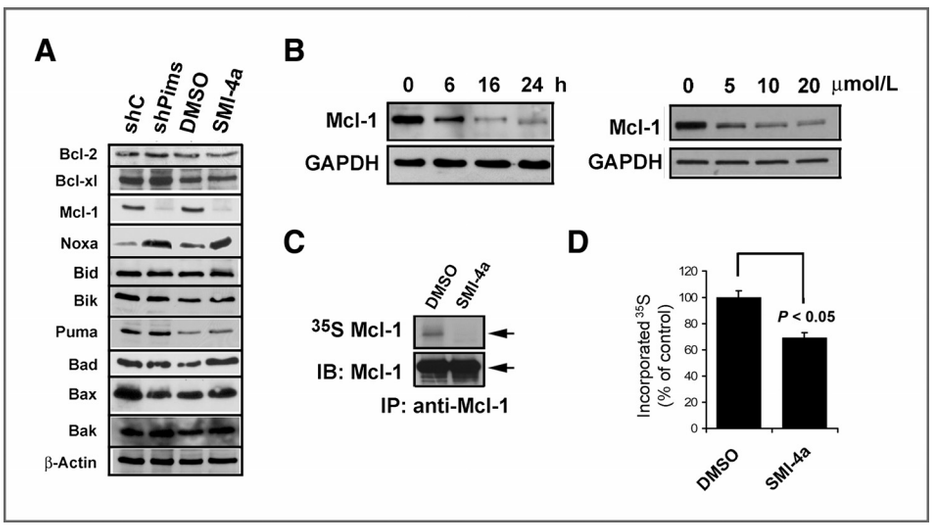

Figure 2. Pim inhibition downregulates Mcl-1 expression by blocking protein synthesis. A, LNCaP cells expressing shRNA constructs targeting Pim-1, 2, and 3, nonsilencing control (shC) or treated with SMI-4a (10 μmol/L) for 16 hours were lysed and cell extracts were analyzed by immunoblotting with the antibodies listed. B, LNCaP cells were treated with varying doses of SMI-4a for 16 hours or with SMI-4a (10 μmol/L) for different times. Cell extracts were analyzed by immunoblotting with the antibodies shown. C, LNCaP cells were methionine starved, treated with DMSO or SMI-4a for 16 hours, and incubated with ^{35}S-methionine. After labeling, the Mcl-1 protein was immunoprecipitated, and analyzed by autoradiography and immunoblotting. The arrow denotes the upper band that is identified as the Mcl-1 protein. D, aliquots of whole cell lysates obtained in C were washed with 10% TCA, the protein dried, and the proteins labeled with ^{35}S-methionine quantified by scintillation counting (mean ± SD, $n = 6$). The P value of $P < 0.05$ for differences between DMSO and SMI-4a treatment was obtained by a 2-way ANOVA.

obtained in TKO MEFs compared with wild type where decreased synthesis of proteins regulated by the 5′cap and total protein synthesis was seen (12).

Pim kinase inhibitors inhibit mTROC1-mediated protein synthesis and increase Mcl-1 degradation

To evaluate the mechanism by which inhibition of Pim kinases suppresses protein synthesis, the level of phosphorylated 4E-BP1 was measured after treatment of prostate cancer cells with either shRNAs to Pim kinases or the kinase inhibitor SMI-4a. Decreased mTORC1 activity led to increased levels of dephosphorylated 4E-BP1, which then was bound to the eIF-4E protein, blocking protein synthesis. We found that both knockdown of the 3 Pims and SMI-4a treatment decreased the phosphorylation of 4E-BP1 (Supplementary Fig. S5). Immunoprecipitation of mTORC1 followed by anti-phospho 4E-BP1 Western additionally showed that inhibition of Pim kinases decreased mTORC1 activity (Fig. 3A). To test whether Pim inhibition has an effect on the eIF4F assembly and cap structure recognition process, eIF4E and the proteins associated with it were isolated with m^7-GTP-sepharose beads, which functions by mimicking the mRNA cap structure. As shown in Fig. 3B, the amount of phosphorylated 4E-BP1 associated with eIF-4E increased markedly in Pim-depleted cells or SMI-4a treated cells, suggesting a mechanism for the inhibition of 5′cap translation. Thus, inhibition of the Pim protein kinases in these cells decreased the activity of mTORC1 kinase.

mTORC1 activity can be negatively regulated by AMP-dependent protein kinase (13), which is activated by phosphorylation on threonine 172 and increased AMP levels. We found that treatment of both LNCaP and PC-3 prostate cancer cells with SMI-4a induced increases in AMPK phosphorylation (Fig. 3C), suggesting a potential mechanism by which the Pim kinases could regulate the mTORC1 pathway. To test if AMPK is required for SMI-4a to downregulate Mcl-1 expression, LNCaP cells were treated with SMI-4a and compound C, an AMPK inhibitor (Fig. 3D). This additional treatment partially blocked the ability of SMI-4a to decrease Mcl-1 protein levels suggesting that AMPK control of mTORC1 activity contributes to this downregulation.

Because SMI-4a activity was only partially inhibited by compound C, we examined the possibility that SMI-4a also regulated the rate of destruction of the Mcl-1 protein. LNCaP cells were first treated with SMI-4a or Pimi-14j for 16 hours followed by cycloheximide treatment to block new protein synthesis in the absence of Pim inhibitors. Pretreatment with SMI-4a induced much more rapid degradation of the Mcl-1 protein than cells treated with vehicle (dimethyl sulfoxide, DMSO; Fig. 3E). To further examine whether proteasome-mediated Mcl-1 protein degradation occurs in cells treated with Pim inhibitors, LNCaP cells were pretreated with the proteasome inhibitor PS-341 (VELCADE) and then further treated with SMI-4a. In cells treated with both compounds, proteasome inhibition reversed the ability of the Pim inhibitor to induce Mcl-1 protein degradation (Fig. 3F). These results suggest that the reduction in Mcl-1 protein levels induced by Pim inhibitor treatment is mediated by regulation of both protein synthesis and protein degradation rate.

Inhibition of Pim kinase increases the level of Noxa protein

Treatment of LNCaP cells with the Pim inhibitors SMI-4a or K00135 increased the cellular levels of the BH3 protein Noxa (Fig. 4A). Small hairpin RNA-mediated knockdown of Pims in

Downloaded from cancerres.aacrjournals.org on May 22, 2012
Copyright © 2012 American Association for Cancer Research

Published OnlineFirst November 11, 2011; DOI:10.1158/0008-5472.CAN-11-3240

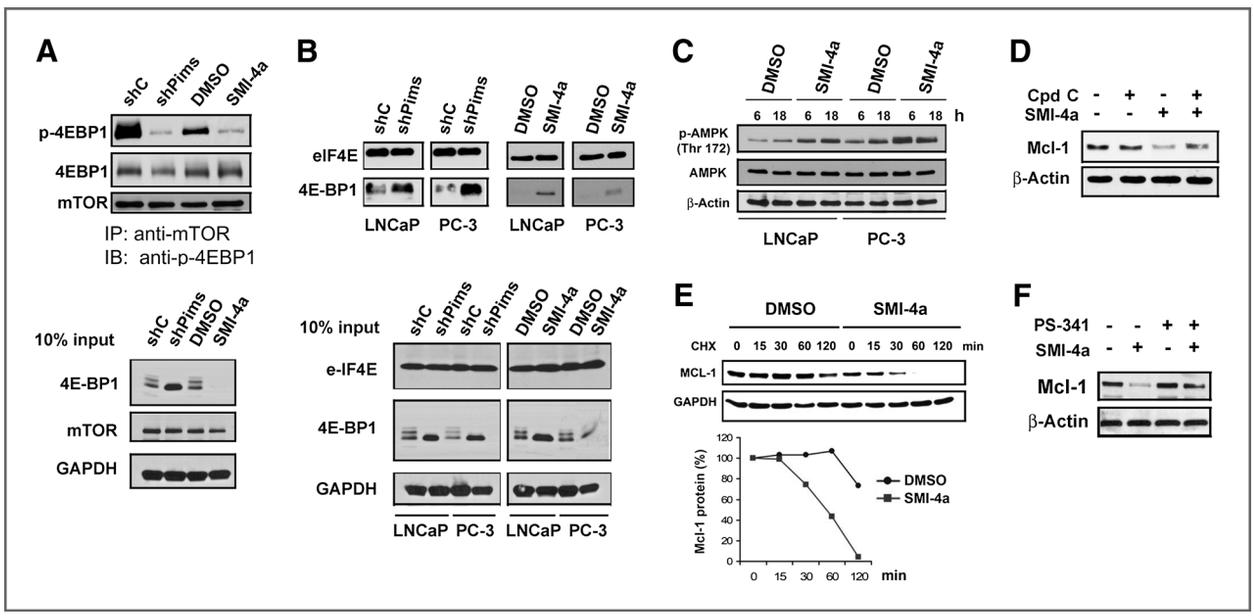

Figure 3. Pim inhibitor SMI-4a promotes Mcl-1 degradation by inhibiting mTORC1 signaling. A, LNCaP cells stably expressing shRNA constructs against Pim-1, 2, and 3 (shPims) or nonsilencing control (shC) or treated with SMI-4a for 16 hours were lysed with CHAPS buffer and resulting lysates were subjected to immunoprecipitation (IP) using an antibody to mTOR and the immunoprecipitates probed with Abs to mTOR, 4E-BP1, and phosho-4E-BP1 (Thr37/46). Cell lysates (25 μg) were also immunoblotted as a control (Input). B, cell extracts isolated after treatments described in A were incubated with m^7-GTP beads to pull down 5′cap components. After washing, proteins bound to the beads were probed by immunoblotting with antibodies to eIF4E and 4E-BP1. Cell lysates (25 μg) were also immunoblotted as a control (Input). C, LNCaP and PC-3 cells were treated with either DMSO or SMI-4a (10 μmol/L) for 6 or 18 hours. Cellular extracts were analyzed by immunoblotting with antibodies shown. D, LNCaP cells were exposed to 5 μmol/L of the AMPK inhibitor Compound C (Cpd C) prior to treatment with either DMSO or SMI-4a (10 μmol/L) for 16 hours. Cell extracts were analyzed by immunoblotting with antibodies shown. E, LNCaP cells were treated with DMSO or SMI-4a for 16 hours followed by cycloheximide (CHX) and cell samples were collected at the times indicated. Cell lysates were analyzed by immunoblotting with antibodies shown. The graph is based on densitometry scanning (NIH ImageJ software) of the above immunoblots. F, LNCaP cells were pretreated with the proteasome inhibitor PS-341 (100 nmol/L) for 1 hour and then treated with either DMSO or SMI-4a (10 μmol/L) for 16 hours. Cell extracts were analyzed by immunoblotting with antibodies shown.

LNCaP cells was also sufficient to increase Noxa protein levels (Supplementary Fig. S6A). The Noxa protein specifically binds and inhibits the Mcl-1 protein's antiapoptotic activity. Immunoprecipitation shows that the Pim inhibitor-increased Noxa protein bound to Mcl-1 (Fig. 4B). As seen on Western blot, the Pim inhibitors concurrently decreased the overall levels of the Mcl-1 protein (Fig. 4C). To determine how Pim inhibitors might regulate Noxa protein levels, we examined the unfolded protein response (UPR). In the condition of an energy deficit, activation of the endoplasmic reticulum stress response is known to stimulate the UPR by eIF-2α phosphorylation and subsequent increases in the protein levels of the ATF4 and CHOP transcription factors (39). ATF4 induces increases in the Noxa mRNA and protein (26, 27). To clarify whether induction of Noxa by Pim inhibitors is associated with the eIF-2α arm of UPR signaling, we treated LNCaP cells and evaluated protein levels of these factors. We found that SMI-4a treatment stimulates the phosphorylation of eIF-2α (Fig. 4C) and induces increases in ATF4 and CHOP protein in a dose dependent fashion (Fig. 4D and E) similarly to known activators of this pathway, tunicamycin (Tm) and thasigargen (Tg; Supplementary Fig. 6B).

Pim inhibitors induce UPR followed by ER stress

On the basis of activation of eIF-2α phosphorylation, we examined whether Pim inhibitors also induces other arms of the ER stress pathway by assessing changes in ATF6 and XBP-1 transcriptional activity. XBP-1 mRNA is increased by ATF6 and spliced by IRE1 in response to ER stress, resulting in production of a transcription factor that can induce genes associated with the UPR (28). QT-PCR analysis showed that the induction of ATF6 mRNA and XBP-1 mRNA occurs in response to Pim inhibitor treatment (Fig. 5A). The spliced version of XBP-1 is seen in this PCR assay as a larger band. This assay confirmed that SMI-4a treatment of LNCaP cells, when compared with the Tunicamycin control, is capable of inducing the splicing of XBP-1 in a dose-dependent fashion (Fig. 5B). Pim inhibitor-induced splicing was seen in PC-3, Du145, and C4–2B cell lines (Supplementary Fig. S7A–C). Moreover, we found that SMI-4a did not increase XBP-1 splicing in MEFs lacking all Pim isoforms (TKO) MEF cells (Supplementary Fig. S7D) and knockdown of Pims in LNCaP cells with shRNAs decreased the ability of Pim inhibitors to cause XBP-1 splicing (Supplementary Fig. S7E). Activation of XBP-1 is known to lead to transcription of glucose-regulated protein 78 (grp78/BiP) and its splice variant grp78*va*. We found that both grp78/Bip and grp78*va* transcripts were significantly increased by treatment of LNCaP cells with SMI-4a or K00135 (Fig. 5C). This data show that inhibition of Pim kinase pathways is sufficient to activate a second arm of the UPR response.

Downloaded from cancerres.aacrjournals.org on May 22, 2012
Copyright © 2012 American Association for Cancer Research

Published OnlineFirst November 11, 2011; DOI:10.1158/0008-5472.CAN-11-3240

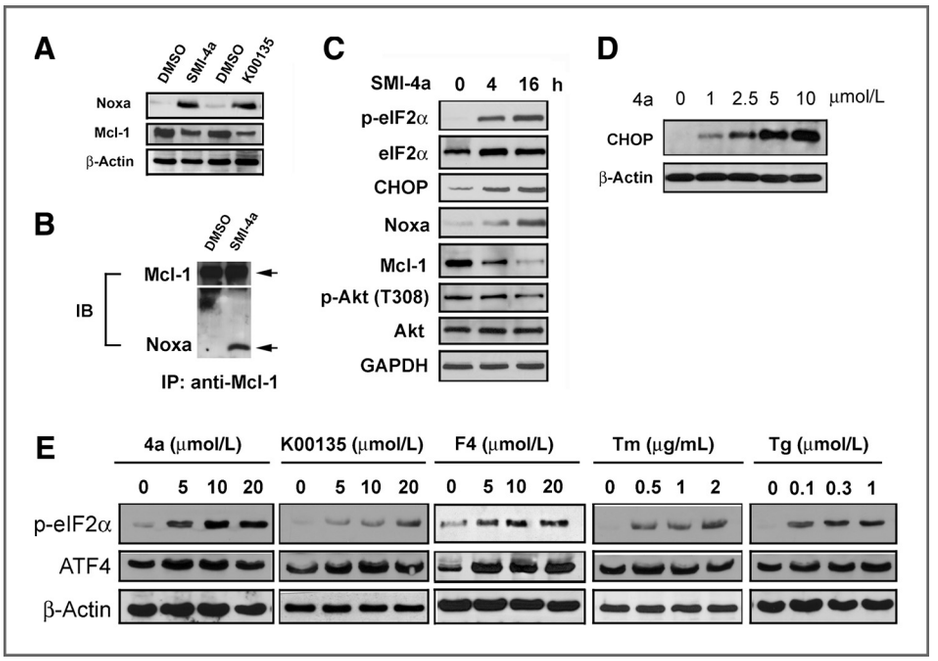

Figure 4. Noxa induction by Pim inhibitors is mediated through the endoplasmic reticulum stress response. A, LNCaP cells were treated with DMSO, 10 μmol/L SMI-4a, or 10 μmol/L K00135 for 16 hours. Cell extracts were analyzed by immunoblotting with antibodies shown. B, LNCaP cells were treated DMSO or SMI-4a for 16 hours. Aliquots of cell extracts were subjected to IP with Mcl-1 antibody and then immunoblot (IB) probed with Mcl-1 and Noxa antibodies. C, LNCaP cells were treated with 10 μmol/L SMI-4a for 0, 4, or 16 hours. Cell extracts were analyzed by immunoblotting with antibodies shown. D, LNCaP cells were treated with various doses of SMI-4a (4a) for 16 hours. Cell extracts were analyzed by immunoblotting with antibodies shown. E, LNCaP cells were treated with Pim inhibitors at the indicated doses for 16 hours. Tunicamycin (Tm) and Thapsigargin (Tg) were used as controls. Cells were treated with 10058-F4, which is of the same chemotype as SMI-4a and is an active Pim inhibitor. Cell extracts were analyzed by immunoblotting with antibodies shown.

Combination treatment of Pim inhibitor SMI-4a and ABT-737 inhibits tumor growth *in vivo*

Given the synergy of Pim inhibitors and ABT-737 in cell culture, we sought to examine anticancer efficacy of the combination treatment *in vivo* through a tumor xenograft model. Mice bearing LNCaP prostate tumors were treated with either ABT-737, SMI-4a, or a combination of both agents. Although neither individual drug treatment showed a difference from vehicle control, the combination treatment significantly suppressed tumor growth (Fig. 6A). Immunohistochemical staining of tumor tissues revealed that SMI-4a treatment markedly downregulated Mcl-1 expression (Fig. 6B) and ABT-737 increased the levels of this protein, as previously shown by others (17) whereas combination therapy seemed to increase cleaved caspase-3. In tumor samples, Western blot analysis showed that combination therapy with SMI-4a and ABT-737 decreased Mcl-1 and increased Noxa and was associated with increased levels of the apoptosis marker caspase-3 cleavages (Fig. 6C). Using PCR, we showed that SMI-4a treatment increased XBP-1 splicing in tumors (Fig. 6D), but this effect was not seen in the combination therapy. These *in vivo* results support the idea that a Pim inhibitor can be safely synergistically combined with ABT-737.

Discussion

Here, we show that Pim kinase inhibitors of varied chemical structure can be combined with the Bcl-2 family antagonist ABT-737 to induce apoptosis in prostate cancer cells and overcome cell death resistance caused by heightened expression of Bcl-2 protein. Resistance to ABT-737 in several tumor types (16, 17, 21) has been well documented to involve overexpression of the Mcl-1 protein. ABT-737 does not bind with high affinity to Mcl-1, so it cannot block Mcl-1's activity (29). Inducing changes in either the Noxa protein, Mcl-1, or both has been shown to induce the death of multiple tumor cell types (30) when incubated with ABT-737. For example, treatment with gemcitabine, a chemotherapeutic agent, increased the degradation of Mcl-1 and sensitized lung cancer cells to ABT-737 (31). In addition, combining ABT-737 with bortezomib, a proteasome inhibitor known to increase Noxa levels, inhibited the growth of lymphoma cells (32), and actinomycin D treatment of tumor cells enhanced the efficacy of ABT-737 action by downmodulating Mcl-1 expression (33). Prostate cancer cell lines express heightened levels of Mcl-1 making them resistant to the action of ABT-737 (21). However, we showed that the addition of the Pim inhibitors both decreased the cellular levels of the Mcl-1 protein and raised the level of the BH3 protein Noxa, a highly specific inhibitor of the Mcl-1 protein (34), markedly enhancing the activity of ABT-737. Previously, the application of a different Pim inhibitor, SGI-1776, to leukemic cells has been shown to decrease the levels of Mcl-1, although the mechanism was not identified (35).

Mcl-1 protein levels can be regulated by transcriptional, translational, and posttranslational mechanisms sensitize cells to ABT-737–induced death. Because the Mcl-1 protein has a

Downloaded from cancerres.aacrjournals.org on May 22, 2012
Copyright © 2012 American Association for Cancer Research

Published OnlineFirst November 11, 2011; DOI:10.1158/0008-5472.CAN-11-3240

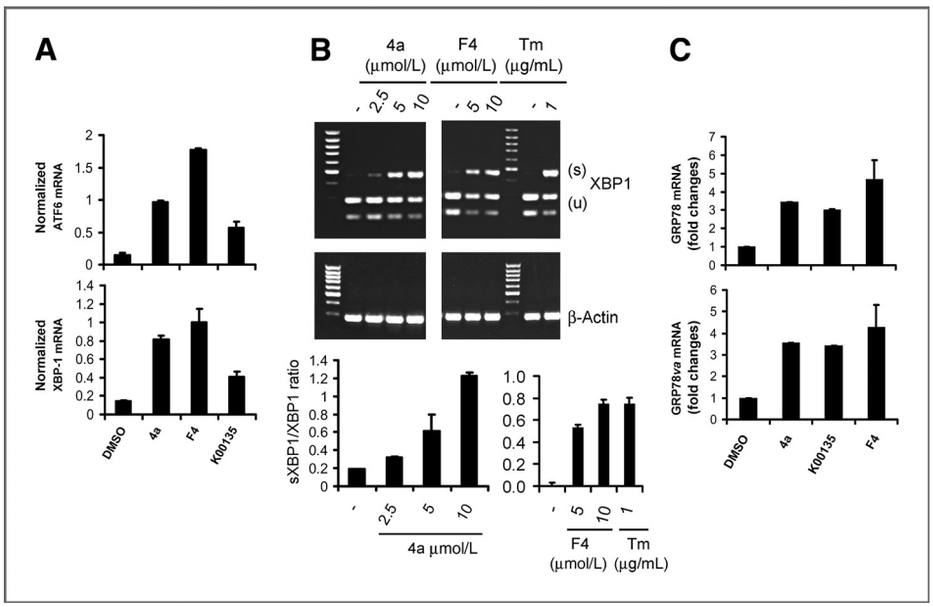

Figure 5. Pim kinase inhibitors induce XBP-1 splicing. A, LNCaP cells were treated with DMSO, 10 μmol/L SMI-4a (4a), 10 μmol/L K00135, and 10 μmol/L 10058-F4 (F4) for 16 hours. Total RNA was isolated and then subjected to qT-PCR. The levels of ATF6 or XBP-1 mRNA were normalized to the 18S mRNA. B, LNCaP cells were treated with SMI-4a (4a), 10058-F4 (F4) or Tunicamycin (Tm) at the indicated doses for 16 hours. Total RNA was isolated and then subjected to RT-PCR for detection of XBP-1 splicing (top). The ratio of the spliced (S) to the unspliced (U) XBP-1 mRNAs was assessed by qT-PCR analysis (bottom). The mean of triplicate determinations are shown ± SD. C, total RNA isolated in A was subjected to qT-PCR analysis to determine level of GRP78 and its isoform GRP78*va* using the 18S mRNA as an internal control.

short half-life, inhibitors that disturb protein synthesis, and in particular 5′cap driven translation, have the potential to decrease the cellular level of this protein (35, 36). For example, inhibition of glucose transport blocks AKT activity, inhibits the mTORC1 pathway, downregulates Mcl-1 translation and sensitizes lymphoma cells to ABT-737 treatment (37). Similarly, in other contexts, mTORC1 has been shown to be responsible for Mcl-1 protein levels (35). We find in prostate cancer cells that incubation with Pim inhibitors or knock down of Pim protein levels enhances the phosphorylation of 4E-BP-1 and as a result increases the binding of 4E-BP1 with eIF-4E inhibiting mTORC1 activity. We hypothesize that Pim inhibitors block the mTORC1 pathway based on their activation of AMPK, which we have shown plays a key role in fibroblasts in mediating the ability of Pim inhibitors to curtail protein synthesis (12). The ability of Pim kinases to modulate mTORC1 activity has been shown in lymphoma cell lines (10, 38), leukemic cells (11), and normal fibroblasts (12). Similar findings have been identified in other cell systems. For example, when glucose is withdrawn or 2-deoxyglucose applied to leukemic cells increases in AMPK activity (39), inhibition of mTOR activity, and decreases in the levels of Mcl-1 protein (40) are seen. Activation of AMP-dependent protein kinase leads to phosphorylation of both the raptor and TSC-2 proteins to block mTORC1 activity (41). The mechanism by which Pim kinases regulate AMPK is not clear, but in fibroblasts the absence of Pim kinases causes increases in the amount of cellular AMP and a drop in ATP levels secondary to regulation of mitochondrial metabolism (12). Application of the Pim inhibitor, SMI-4a, to Bcr-Abl positive K562 cells induces identical biologic effects (10).

We found that the application of Pim kinase inhibitors to prostate cancer cells also decreases the half-life of the Mcl-1 protein, an effect that is reversed by the addition of proteasome inhibitors. A number of mechanisms could explain this finding. The E3 ligase β-TrCP stimulates the degradation of Mcl-1, which has been phosphorylated by activated GSK-3β (42). GSK-3β activity is increased by agents that inhibit AKT such as by the withdrawal of growth factors like IL-3 (43). Preliminary data (unpublished results) suggests that Pim kinase inhibitors can block growth factor signaling mimicking the effects of growth factor withdrawal. Mcl-1 levels are also controlled by an interaction with Mule/ARF-BP1 E3 ubiquitin ligase (44) and this interaction can be modulated by, for example, heat shock (45). Pim kinase inhibitors by blocking mitochondrial metabolism could "stress" prostate cancer cells leading to protein degradation through a Mule/ARF-BP1 mechanism. Finally, the interaction of the Mcl-1 and its specific deubiquitinase USP9X is highly regulated (31, 46), and it is possible Pim kinases and their inhibitors could modulate this process, as well.

We show for the first time that a genetically engineered decrease in Pim kinase levels or the addition of Pim kinase inhibitors causes ER stress and activates the unfolded protein response (UPR) stimulating increases in eIF-2α phosphorylation, ATF4, CHOP proteins, cleavage of XBP-1, and increases in the Noxa protein. Although the Noxa protein was initially cloned as a p53 activated gene (47), it can be elevated transcriptionally in the absence of p53 by increases in both FoxO1 (48) and c-Myc (49). Recently, the proteasome inhibitor bortezomib was reported to activate the UPR and stimulate the formation of an ATF3 and ATF4 complex that enhances Noxa mRNA synthesis (26, 27). Previously, apoptosis and the UPR were connected by the observation that BAX and BAK were

Downloaded from cancerres.aacrjournals.org on May 22, 2012
Copyright © 2012 American Association for Cancer Research

Published OnlineFirst November 11, 2011; DOI:10.1158/0008-5472.CAN-11-3240

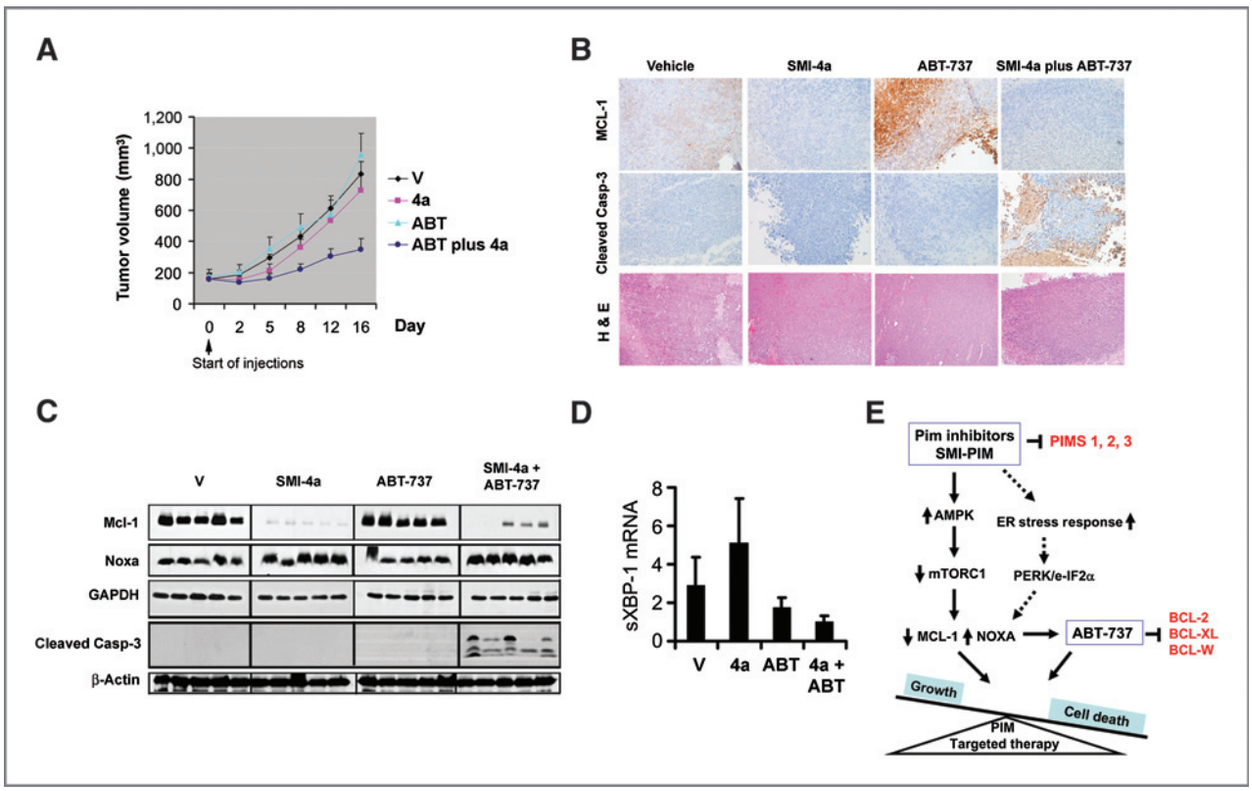

Figure 6. Tumor growth *in vivo* is inhibited by combination treatment of ABT-737 and SMI-4a. A, mice were subcutaneously inoculated with LNCaP cells. Tumor volume was monitored during the following treatments: vehicle (V), ABT-737 (ABT; 50 mg/kg; i.p., QD), SMI-4a (4a; 60 mg/kg, oral gavage, BID) or a combination of SMI-4a and ABT-737 (ABT plus 4a) for 16 days (mean ± SEM). B, immunohistochemical analysis of Mcl-1, cleaved caspase-3 (casp-3) and H&E staining. C, Western blot analysis of Noxa, Mcl-1, cleaved casp-3, β-actin, and glyceraldehydes-3-phosphate dehydrogenase (GAPDH). Five representative tumors for each treatment were examined. D, qT-PCR analysis of XBP-1 splicing in subcutaneous tumors of treatment groups. Five representative tumors for each treatment group are shown. E, proposed mechanistic model by which Pim inhibitor synergizes with ABT-737 to induce apoptosis. Pim inhibitors reduce Mcl-1 protein translation through activation of AMPK to block the mTORC1-mediated 5′cap-dependent protein translation. In addition, this treatment activates the UPR signaling to induce Noxa, thereby promoting increased Mcl-1 turnover.

needed to induce the UPR by inositol-requiring-enzyme 1α (IRE-1α; ref. 50). IRE-1α executes site-specific cleavage of XBP-1 mRNA to produce more stable transcript XBP-1 that encodes a potent transcriptional activator of UPR target genes (28). Dose dependent increases in XBP-1 splicing by Pim inhibitors confirm our finding that Pim inhibition drives cells to activate ER stress. Compared with wild MEF cells, XBP-1 splicing was not increased in Pim knock-out (TKO) MEF cells, suggesting again the potential role of Pim in regulating this pathway. Additional experiments will be necessary to determine the exact biochemical mechanism by which inhibition of the Pim kinases modulates the UPR.

On the basis of the cell culture findings that inhibition of Pim with SMI-4a increases Noxa and decreases Mcl-1 protein levels greatly enhancing the apoptotic activity of ABT-737, we combined these agents in an *in vivo* animal experiment. Results show that single agent therapy had little anticancer activity whereas combination treatment inhibited the growth of LNCaP cells grown subcutaneously. Immunohistochemistry and Western blots show that this combined therapy activates the UPR and induces apoptosis of these tumor cells (Fig. 6). On the basis of their ability to regulate protein synthesis and the UPR (see model Fig. 6E), these results suggest that Pim kinase inhibitors could be used in the clinic to enhance the anticancer activity of ABT-737.

Disclosure of Potential Conflicts of Interest

A.S. Kraft owns shares in Vortex Biotechnology.

Acknowledgments

The authors thank Abbott Laboratories and Dr. Joel Leverson for providing ABT-737 and Pim inhibitor Pimi-14j. Bcl-2 expression vector was kindly provided by Dr. Timothy C. Chambers at the University of Arkansas for Medical Sciences (Little Rock, AR). Members of the Andrew S. Kraft and Charles D. Smith laboratories (Medical University of South Carolina) have been very kind in providing research reagents, materials, and technical assistance.

Grant Support

This work was supported by the Department of Defense Grant W81XWH-08-PCRP-IDA and the NIH 1P30-CA138313.

The costs of publication of this article were defrayed in part by the payment of page charges. This article must therefore be hereby marked *advertisement* in accordance with 18 U.S.C. Section 1734 solely to indicate this fact.

Received September 27, 2011; revised November 4, 2011; accepted November 4, 2011; published OnlineFirst November 11, 2011.

Downloaded from cancerres.aacrjournals.org on May 22, 2012
Copyright © 2012 American Association for Cancer Research

Published OnlineFirst November 11, 2011; DOI:10.1158/0008-5472.CAN-11-3240

References

1. Dhanasekaran SM, Barrette TR, Ghosh D, Shah R, Varambally S, Kurachi K, et al. Delineation of prognostic biomarkers in prostate cancer. Nature 2001;412:822–6.
2. Cibull TL, Jones TD, Li L, Eble JN, Ann Baldridge L, Malott SR, et al. Overexpression of Pim-1 during progression of prostatic adenocarcinoma. J Clin Path 2006;59:285–8.
3. Dai H, Li R, Wheeler T, Diaz de Vivar A, Frolov A, Tahir S, et al. Pim-2 upregulation: biological implications associated with disease progression and perinueral invasion in prostate cancer. Prostate 2005;65: 276–86.
4. Valdman A, Fang X, Pang ST, Ekman P, Egevad L. Pim-1 expression in prostatic intraepithelial neoplasia and human prostate cancer. Prostate 2004;60:367–71.
5. Chen WW, Chan DC, Donald C, Lilly MB, Kraft AS. Pim family kinases enhance tumor growth of prostate cancer cells. Mol Cancer Res 2005;3:443–51.
6. Shah N, Pang B, Yeoh KG, Thorn S, Chen CS, Lilly MB, et al. Potential roles for the PIM1 kinase in human cancer - a molecular and therapeutic appraisal. Eur J Cancer 2008;44:2144–51.
7. Valdman A, Fang X, Pang ST, Ekman P, Egevad L. Pim-1 expression in prostatic intraepithelial neoplasia and human prostate cancer. Prostate 2004;60:367–71.
8. Zhang X, Lee C, Ng PY, Rubin M, Shabsigh A, Buttyan R. Prostatic neoplasia in transgenic mice with prostate-directed overexpression of the c-myc oncoprotein. Prostate 2000;43:278–85.
9. Xia Z, Knaak C, Ma J, Beharry ZM, McInnes C, Wang W, et al. Synthesis and evaluation of novel inhibitors of Pim-1 and Pim-2 protein kinases. J Med Chem 2009;52:74–86.
10. Beharry Z, Zemskova M, Mahajan S, Zhang F, Ma J, Xia Z, et al. Novel benzylidene-thiazolidine-2,4-diones inhibit Pim protein kinase activity and induce cell cycle arrest in leukemia and prostate cancer cells. Mol Cancer Ther 2009;8:1473–83.
11. Lin YW, Beharry ZM, Hill EG, Song JH, Wang W, Xia Z, et al. A small molecule inhibitor of Pim protein kinases blocks the growth of precursor T-cell lymphoblastic leukemia/lymphoma. Blood 2010;115: 824–33.
12. Beharry Z, Mahajan S, Zemskova M, Lin YW, Tholanikunnel BG, Xia Z, et al. The Pim protein kinases regulate energy metabolism and cell growth. Proc Natl Acad Sci U S A 2011;108:528–33.
13. Shaw RJ. LKB1 and AMP-activated protein kinase control of mTOR signalling and growth. Acta Physiol (Oxf) 2009;196:65–80.
14. Liu AY, Corey E, Bladou F, Lange PH, Vessella RL. Prostatic cell lineage markers: emergence of BCL2 +cells of human prostate cancer xenograft LuCaP 23 following castration. Int J Cancer 1996;65:85–9.
15. Fesik SW. Promoting apoptosis as a strategy for cancer drug discovery. Nat Rev Cancer 2005;5:876–85.
16. van Delft MF, Wei AH, Mason KD, Vandenberg CJ, Chen L, Czabotar PE, et al. The BH3 mimetic ABT-737 targets selective Bcl-2 proteins and efficiently induces apoptosis via Bak/Bax if Mcl-1 is neutralized. Cancer Cell 2006;10:389–99.
17. Yecies D, Carlson NE, Deng J, Letai A. Acquired resistance to ABT-737 in lymphoma cells that up-regulate MCL-1 and BFL-1. Blood;115: 3304–13.
18. Hann CL, Daniel VC, Sugar EA, Dobromilskaya I, Murphy SC, Cope L, et al. Therapeutic efficacy of ABT-737, a selective inhibitor of BCL-2, in small cell lung cancer. Cancer Res 2008;68:2321–8.
19. Certo M, Del Gaizo Moore V, Nishino M, Wei G, Korsmeyer S, Armstrong SA, et al. Mitochondria primed by death signals determine cellular addiction to antiapoptotic BCL-2 family members. Cancer Cell 2006;9:351–65.
20. Song JH, Kandasamy K, Zemskova M, Lin YW, Kraft AS. The BH3 mimetic ABT-737 induces cancer cell senescence. Cancer Res 2011;71:506–15.
21. Song JH, Kandasamy K, Kraft AS. ABT-737 induces expression of the death receptor 5 and sensitizes human cancer cells to TRAIL-induced apoptosis. J Biol Chem 2008;283:25003–13.
22. Tao ZF, Hasvold LA, Leverson JD, Han EK, Guan R, Johnson EF, et al. Discovery of 3H-benzo[4,5]thieno[3,2-d]pyrimidin-4-ones as potent, highly selective, and orally bioavailable inhibitors of the human proto-oncogene proviral insertion site in moloney murine leukemia virus (PIM) kinases. J Med Chem 2009;52:6621–36.
23. Upreti M, Chu R, Galitovskaya E, Smart SK, Chambers TC. Key role for Bak activation and Bak-Bax interaction in the apoptotic response to vinblastine. Mol Cancer Ther 2008;7:2224–32.
24. McDonnell TJ, Troncoso P, Brisbay SM, Logothetis C, Chung LW, Hsieh JT, et al. Expression of the protooncogene bcl-2 in the prostate and its association with emergence of androgen-independent prostate cancer. Cancer Res 1992;52:6940–4.
25. Banerjee PP, Banerjee S, Brown TR. Bcl-2 protein expression correlates with cell survival and androgen independence in rat prostatic lobes. Endocrinology 2002;143:1825–32.
26. Wang Q, Mora-Jensen H, Weniger MA, Perez-Galan P, Wolford C, Hai T, et al. ERAD inhibitors integrate ER stress with an epigenetic mechanism to activate BH3-only protein NOXA in cancer cells. Proc Natl Acad Sci U S A 2009;106:2200–5.
27. Armstrong JL, Flockhart R, Veal GJ, Lovat PE, Redfern CP. Regulation of endoplasmic reticulum stress-induced cell death by ATF4 in neuroectodermal tumor cells. J Biol Chem 2011;285:6091–100.
28. Yoshida H, Matsui T, Yamamoto A, Okada T, Mori K. XBP1 mRNA is induced by ATF6 and spliced by IRE1 in response to ER stress to produce a highly active transcription factor. Cell 2001;107:881–91.
29. Lin X, Morgan-Lappe S, Huang X, Li L, Zakula DM, Vernetti LA, et al. `Seed' analysis of off-target siRNAs reveals an essential role of Mcl-1 in resistance to the small-molecule Bcl-2/Bcl-XL inhibitor ABT-737. Oncogene 2007;26:3972–9.
30. Chen S, Dai Y, Harada H, Dent P, Grant S. Mcl-1 down-regulation potentiates ABT-737 lethality by cooperatively inducing Bak activation and Bax translocation. Cancer Res 2007;67:782–91.
31. Zhang C, Cai TY, Zhu H, Yang LQ, Jiang H, Dong XW, et al. Synergistic antitumor activity of gemcitabine and ABT-737 *in vitro* and *in vivo* through disrupting the interaction of USP9X and Mcl-1. Mol Cancer Ther 2011;10:1264–75.
32. Paoluzzi L, Gonen M, Bhagat G, Furman RR, Gardner JR, Scotto L, et al. The BH3-only mimetic ABT-737 synergizes the antineoplastic activity of proteasome inhibitors in lymphoid malignancies. Blood 2008;112:2906–16.
33. Olberding KE, Wang X, Zhu Y, Pan J, Rai SN, Li C. Actinomycin D synergistically enhances the efficacy of the BH3 mimetic ABT-737 by downregulating Mcl-1 expression. Cancer Bio Ther 2011;10:918–29.
34. Chen L, Willis SN, Wei A, Smith BJ, Fletcher JI, Hinds MG, et al. Differential targeting of prosurvival Bcl-2 proteins by their BH3-only ligands allows complementary apoptotic function. Mol Cell 2005;17: 393–403.
35. Chen LS, Redkar S, Taverna P, Cortes JE, Gandhi V. Mechanisms of cytotoxicity to Pim kinase inhibitor, SGI-1776, in acute myeloid leukemia. Blood 2011;118:693–702.
36. Hsieh AC, Costa M, Zollo O, Davis C, Feldman ME, Testa JR, et al. Genetic dissection of the oncogenic mTOR pathway reveals druggable addiction to translational control via 4EBP-eIF4E. Cancer Cell 2010; 17:249–61.
37. Coloff JL, Macintyre AN, Nichols AG, Liu T, Gallo CA, Plas DR, et al. Akt-dependent glucose metabolism promotes mcl-1 synthesis to maintain cell survival and resistance to bcl-2 inhibition. Cancer Res 2011;71:5204–13.
38. Schatz JH, Oricchio E, Wolfe AL, Jiang M, Linkov I, Maragulia J, et al. Targeting cap-dependent translation blocks converging survival signals by AKT and PIM kinases in lymphoma. J Exp Med 2011;208:1799–807.
39. Zhong D, Liu X, Schafer-Hales K, Marcus AI, Khuri FR, Sun SY, et al. 2-Deoxyglucose induces Akt phosphorylation via a mechanism independent of LKB1/AMP-activated protein kinase signaling activation or glycolysis inhibition. Mol Cancer Ther 2008;7:809–17.
40. Pradelli LA, Beneteau M, Chauvin C, Jacquin MA, Marchetti S, Munoz-Pinedo C, et al. Glycolysis inhibition sensitizes tumor cells to death receptors-induced apoptosis by AMP kinase activation leading to Mcl-1 block in translation. Oncogene 2010;29:1641–52.
41. Corradetti MN, Inoki K, Bardeesy N, DePinho RA, Guan KL. Regulation of the TSC pathway by LKB1: evidence of a molecular link between

Downloaded from cancerres.aacrjournals.org on May 22, 2012
Copyright © 2012 American Association for Cancer Research

Published OnlineFirst November 11, 2011; DOI:10.1158/0008-5472.CAN-11-3240

tuberous sclerosis complex and Peutz-Jeghers syndrome. Genes Dev 2004;18:1533–8.
42. Ding Q, He X, Hsu JM, Xia W, Chen CT, Li LY, et al. Degradation of Mcl-1 by beta-TrCP mediates glycogen synthase kinase 3-induced tumor suppression and chemosensitization. Mol Cell Bio 2007;27: 4006–17.
43. Maurer U, Charvet C, Wagman AS, Dejardin E, Green DR. Glycogen synthase kinase-3 regulates mitochondrial outer membrane permeabilization and apoptosis by destabilization of MCL-1. Mol Cell 2006;21:749–60.
44. Zhong Q, Gao W, Du F, Wang X. Mule/ARF-BP1, a BH3-only E3 ubiquitin ligase, catalyzes the polyubiquitination of Mcl-1 and regulates apoptosis. Cell 2005;121:1085–95.
45. Stankiewicz AR, Livingstone AM, Mohseni N, Mosser DD. Regulation of heat-induced apoptosis by Mcl-1 degradation and its inhibition by Hsp70. Cell Death Diff 2009;16:638–47.
46. Schwickart M, Huang X, Lill JR, Liu J, Ferrando R, French DM, et al. Deubiquitinase USP9X stabilizes MCL1 and promotes tumour cell survival. Nature 2010;463:103–7.
47. Oda E, Ohki R, Murasawa H, Nemoto J, Shibue T, Yamashita T, et al. Noxa, a BH3-only member of the Bcl-2 family and candidate mediator of p53-induced apoptosis. Science 2000;288:1053–8.
48. Valis K, Prochazka L, Boura E, Chladova J, Obsil T, Rohlena J, et al. Hippo/Mst1 stimulates transcription of the proapoptotic mediator NOXA in a FoxO1-dependent manner. Cancer Res 2011;71:946–54.
49. Nikiforov MA, Riblett M, Tang WH, Gratchouck V, Zhuang D, Fernandez Y, et al. Tumor cell-selective regulation of NOXA by c-MYC in response to proteasome inhibition. Proc Natl Acad Sci U S A 2007;104: 19488–93.
50. Hetz C, Bernasconi P, Fisher J, Lee AH, Bassik MC, Antonsson B, et al. Proapoptotic BAX and BAK modulate the unfolded protein response by a direct interaction with IRE1alpha. Science 2006;312:572–6.

Downloaded from cancerres.aacrjournals.org on May 22, 2012
Copyright © 2012 American Association for Cancer Research

Pim-1 Mediates the Elevation of Receptor Tyrosine Kinases Induced by Small Molecule AKT Inhibitors in Prostate Cancer Cells

Bo Cen[1*], Sandeep Mahajan[2], Wenxue Wang[2], and Andrew S. Kraft[1,2*]

[1]Department of Medicine, Medical University of South Carolina, Charleston, SC 29425, and the [2]Hollings Cancer Center, Medical University of South Carolina, Charleston, SC 29425

[*]To whom correspondence should be addressed:

1) Bo Cen, Department of Medicine, Medical University of South Carolina, 86 Jonathan Lucas Street, Charleston, SC 29425. Tel: 843-792-9366; Fax: 843-792-3200; Email: cen@musc.edu. (Communicating author)

2) Andrew S. Kraft, Department of Medicine, Hollings Cancer Center, Medical University of South Carolina, 86 Jonathan Lucas Street, Charleston, SC 29425. Tel: 843-792-8284; Fax: 843-792-9456; Email: kraft@musc.edu.

Running Head: Pim-1 regulates expression of RTKs

Abbreviations used: IRES, internal ribosome entry site; RTK, receptor tyrosine kinase; siRNA, small interfering RNA; UTR, untranslated region.

Total character count (including spaces): ~ 35,000

Abstract

The PI3K/AKT pathway is hyper-activated in many types of cancer but effective therapeutic targeting has proven difficult. The antitumor activity of AKT inhibitors is attenuated by upregulation of receptor tyrosine kinases (RTKs) through a feedback mechanism, but the molecular mechanisms underlying this upregulation are not yet fully understood. Here, we demonstrate that knockdown of Pim-1 expression or inhibition of Pim-1 activity with small molecule inhibitors curtails the AKT inhibitor-induced upregulation of RTKs in prostate cancer cells. Although Pim kinases have been implicated in cap-dependent translational control, we find that in the context of AKT inhibition the expression of RTKs is controlled by Pim-1 in a cap-independent manner through regulation of internal ribosome entry site activity. Inhibition or downregulation of AKT enhanced the expression of Pim-1 kinase as well as the RTKs, providing further evidence of the close relationship of these two pathways and potential compensatory mechanisms. Combination of a Pim inhibitor with an AKT inhibitor resulted in a highly synergistic inhibition of prostate tumor growth both *in vitro* and in a mouse model. Pim-1 is thus a novel mediator of resistance to AKT inhibition, and targeting of this protein kinase may significantly improve the efficacy of AKT inhibitors in anticancer therapy.

Introduction

The PI3K/AKT pathway is commonly activated in human cancer and controls cellular processes that contribute to the initiation and maintenance of cancer (Vivanco and Sawyers, 2002). It is activated in 40% of primary and 70% of metastatic prostate cancers secondary to mutations or deletions in the phosphatase and tensin homolog (Suzuki et al., 1998; Vivanco and Sawyers, 2002; Yoshimoto et al., 2007). Activation of the pathway can be associated with mutations in the PI3K catalytic subunit P110 alpha (Vivanco and Sawyers, 2002); point mutations in the regulatory subunit of PI3K and in each of the three AKT isoforms (Bellacosa et al., 2005; Vivanco and Sawyers, 2002); and activation of receptor tyrosine kinases (RTKs) by mutation (*e.g.*, EGFR), or gene amplification (*e.g.*, HER2), which can result in activation of downstream PI3K/AKT (Hynes and Lane, 2005; Vivanco and Sawyers, 2002). Multiple small molecules inhibitors have been developed that target PI3K/mTOR or AKT (LoPiccolo et al., 2008) but the efficacy of these drugs is compromised by the stimulation of compensatory signaling pathways that have the potential to enhance tumor growth (Chakrabarty et al., 2012; Chandarlapaty et al., 2011; Muranen et al., 2012). There is accumulating evidence that inhibition of the PI3K/AKT pathway can lead to adaptive resistance due to upregulation and activation of numerous RTKs (Chakrabarty et al., 2012; Chandarlapaty et al., 2011; Muranen et al., 2012). The mechanism underlying the AKT inhibition-induced upregulation of some of these RTKs, including HER3, INSR, and IGF1R, has been shown to involve FOXO transcription factors (Chandarlapaty et al., 2011); however, these transcription factors do not appear to be involved in the AKT inhibition-

induced upregulation of other RTKs, including MET, HER2, and RET (Chandarlapaty et al., 2011).

The Pim family of serine/threonine kinases regulates cell survival pathways and has been implicated in the progression of several human cancers, including prostate cancer (Dhanasekaran et al., 2001). Clinically, the expression of the Pim kinases are elevated in human prostate cancer (Dhanasekaran et al., 2001), in which the PI3K/AKT pathway is activated, and the levels of Pim correlate with survival of patients with certain subtypes of human lymphoma (Hsi et al., 2008), suggesting that the Pim kinases could play an important role in regulating tumor growth and, potentially, patient survival. As the Pim kinases have overlapping activity with AKT with both regulating apoptosis, cell-cycle progression, and cellular metabolism (Amaravadi and Thompson, 2005; Sussman, 2009) and AKT and the Pim kinases share substrates in common (Amaravadi and Thompson, 2005; Sussman, 2009) it has been suggested that Pim could play an important role in the activation of AKT (Muraski et al., 2007). The activity of AKT kinases is regulated by membrane recruitment and phosphorylation. In contrast, Pim kinases are thought to be constitutively active with changes in Pim kinase levels, and thus activity, being regulated for the most part by transcriptional and translational mechanisms (Amaravadi and Thompson, 2005; Nawijn et al., 2011). Reciprocal regulation of AKT and Pim-1 levels is suggested by the report that forced expression of nuclear-targeted AKT induces Pim-1 and either expression of a dominant-negative Pim-1 or genetic deletion of the enzyme increased AKT expression and phospho-AKT levels in cardiomyocytes (Muraski et al., 2007). Coexpression of AKT and Pim in the mouse

hematopoietic system has been shown to lead to additive increases in cell size, survival, and an enhanced rate of tumor formation (Hammerman et al., 2005).

Here, we demonstrate that inhibition of AKT leads to transcriptional induction of the Pim-1 protein kinase. In turn, Pim-1 can regulate the activation of RTKs by a unique cap-independent stimulation of the internal ribosome entry site (IRES) translation. A combination of small molecule AKT and Pim kinase inhibitors acts synergistically to block prostate tumor growth *in vitro* and *in vivo*, suggesting that simultaneous targeting of these two pathways could have a significant impact on cancer therapy.

RESULTS AND DISCUSSION

AKT inhibition induces Pim-1 expression

Treatment of the highly metastatic prostate cancer PC3-LN4 cells with the pan-AKT inhibitor GSK690693 markedly increased the levels of Pim-1 kinase protein in a time- and concentration-dependent fashion (Fig. 1, A and B) but had a minimal effect on the expression of Pim-3 protein and reduced the levels of Pim-2 (Fig. 1 C). Similar results were obtained using another AKT inhibitor, MK2206 (Fig. 1 C) and upon GSK690693 treatment of the prostate cancer cell line DU145, the breast cancer cell line BT474, and HeLa cells (Unpublished data). The effect of GSK690693 on Pim-1 was not secondary to an off-target effect as knockdown in PC3-LN4 cells of all three AKTs with small interfering RNAs (siRNAs) increased the levels of Pim-1 protein (Fig. 1 D).

Treatment of PC3-LN4 cells with GSK690693 and MK2206 resulted in elevations in the levels of Pim-1, but not Pim-2 or Pim-3 mRNA (Fig. 1 E). Similarly, treatment of PC3-LN4 cells with siRNAs directed at AKT1, AKT2, and AKT3 also resulted in the elevation of Pim-1 mRNA (Fig. 1 F), further suggesting that AKT controls the levels of this mRNA. To further determine whether GSK690693 regulates the transcription of the *Pim-1* gene, a 3.0 kb promoter fragment of the Pim-1 promoter was cloned upstream of a luciferase reporter and this construct was transfected into PC3-LN4 cells. Addition of GSK690693 increased the activity of this promoter (Fig. 1 G). Taken together, we identify a previously unknown feedback regulation of Pim-1 expression resulting from AKT inhibition/downregulation. The recognition of this compensatory mechanism is

potentially important to understanding the biological role of the Pim-1 and the development of unique cancer therapeutic strategies involving Pim-1 and AKT.

Upregulation of Pim-1 is required for AKT inhibitor-associated induction of RTKs

Consistent with the previous reports of upregulation of these RTKs in response to AKT inhibition by MK2206 (Chandarlapaty et al., 2011), treatment of cells with GSK690693 increased the protein levels of multiple RTKs, including MET, EPHA2, RON, EGFR, HER2, HER3, INSR, and IGF1R (Fig. S1 A). Induction of HER3, INSR, and IGF1R transcript levels were seen with MK2206 treatment and this appeared to be mediated by FOXO transcription factors (Chandarlapaty et al., 2011). However, mRNA levels of other RTKs e.g. MET and HER2 were not induced by AKT inhibitors (Chandarlapaty et al., 2011). Thus, it remains unknown how AKT inhibition induces the expression of these RTKs.

GSK690693 also completely blocked the phosphorylation of two well-known AKT substrates, GSK3β and PRAS40, demonstrating the effectiveness of this compound at inhibiting AKT activity in these cells (Fig. S1 B) and caused the paradoxical hyperphosphorylation of AKT at its two regulatory sites (Thr308 and Ser473) (Fig. S1 B), a common property of ATP-competitive AKT inhibitors and considered to be a marker of inhibition of its kinase activity (Okuzumi et al., 2009).

To determine if Pim-1 plays an important regulatory role in the ability of AKT inhibitors to modulate RTKs, we first determined the effects of Pim-directed siRNAs and small molecules inhibitors on protein levels. The use of siRNA directed at Pim-1 demonstrated that a forced reduction in Pim-1 levels markedly reduced the ability of GSK690693 to

elevate the protein levels of multiple RTKs, including MET and EPHA2, as well as HER3, HER2, INSR, and IGF1R (Fig. 2 A). GSK690693 upregulation of RTK protein levels also was reduced in both PC3-LN4 and the breast cancer cell line BT474 (Fig. 2 B) by the addition of SMI-4a, a small molecule Pim kinase inhibitor (Xia et al., 2009).

The results of phospho-RTK antibody array analysis revealed that treatment of PC3-LN4 cells with GSK690693 for 24 h increased the tyrosine phosphorylation of the RTKs tested in the assay, *i.e.*, MET, EPHA2, HER2, INSR, and EGFR (Fig. S2). This change in RTK phosphorylation is consistent with the AKT-inhibitor-induced increases in the protein levels of the RTKs; however, it cannot be ruled out that GSK690693 stimulates RTK phosphorylation through an alternative mechanism (Chandarlapaty et al., 2011). Treatment with the small molecule Pim-1 kinase inhibitor SMI-4a blocked the GSK690693-induced RTK-phosphorylation of the RTKs (Fig. S2), demonstrating that inhibition of Pim reverses the activity of this AKT inhibitor. To further evaluate the role of Pim-1 in regulating ATK-inhibitor induced upregulation of RTKs, embryonic fibroblasts were isolated from mice that are genetically engineered to knock-out expression of all three Pim isoforms (TKO). GSK690693 treatment of the cells increased the levels of the RTKs tested, *i.e.*, MET, HER3, IGF1R, and EPHA2 protein in wild-type MEFs, but not in the Pim kinase-deficient cells (Fig. 2 C). Our data suggests that Pim-1 mediates the upregulation of a number of RTKs i.e. MET, EPHA2, HER2, HER3, IGF1R, and INSR, in an AKT-inhibitor induced manner suggesting that blocking Pim-1 activity could function in tumor cells to inhibit this feedback mechanism.

Pim-1 controls RTK expression under physiological conditions

To test whether Pim-1 affects the baseline level of RTK proteins in tumor cells, we treated PC3-LN4 and BT474 cells with three different Pim kinase inhibitors, SMI-4a, SMI-16a (Xia et al., 2009), and K00135 (Pogacic et al., 2007). Treatment with these inhibitors decreased the protein levels of the RTKs tested, *i.e.*, MET, EPHA2, and HER3, in both cell lines (Fig. 2 D). Similarly, siRNA targeting of Pim-1 decreased the levels of MET and HER3 as well as HER2 and EGFR protein in PC3-LN4 cells (Fig. 2 E). Conversely, overexpression of human Pim-1 in PC3-LN4 increased the levels of the RTKs tested, *i.e*., MET, HER3, and EPHA2 as well as HER2 and EGFR protein (Fig. 2 E). These findings demonstrate that Pim-1 is capable of regulating RTK expression under physiological conditions.

Pim-1 regulates RTK expression through cap-independent translation

Expression of human Pim-1 in PC3-LN4 cells did not affect the levels of RTK mRNAs (Fig. S3, A and B) or the half-life of the RTKs (Fig. S3 C), suggesting that Pim-1 may control the levels of these proteins through a translational mechanism. Pim-2 has been shown to control cap-dependent translation independent of mTORC1 through indirect phosphorylation of 4E-BP1, and this activity is not shared with Pim-1 (Fox et al., 2005; Hammerman et al., 2005). To define the role of cap-dependent translation in the mechanism regulating RTK increase by AKT inhibitors, GSK690693 was combined with two potent inhibitors of mTORC1/mTORC2, PP242 and AZD8055 (Chresta et al., 2010; Feldman et al., 2009), which are both inhibitors of cap-dependent translation. The phosphorylation of 4E-BP1 was markedly reduced and the phosphorylation of eIF2α was increased when these inhibitors were combined with the GSK690693 treatment (Fig. 3 A), suggesting that 5'-cap dependent translation is suppressed. Similarly,

treatment with either PP242 or AZD8055 in combination with GSK690693 strongly reduced the binding of eIF4G and increased the binding of 4E-BP1 to m^7GTP-sepharose, while GSK690693 alone had only a minor effect (Fig. S4). However, as seen on western blotting, even though these compounds markedly inhibited cap-dependent translation, they did not affect the GSK690693-induced elevation of the levels of either Pim-1 protein or of the RTKs tested, *i.e.*, MET, EPHA2, HER3, HER2, and IGF1R (Fig. 3 A). These results were consistent with the results of a recent study (Thoreen et al., 2012) in which other investigators utilized treatment with Torin 1, an ATP competitive mTOR inhibitor, to identify mRNAs whose translation is controlled by mTORC1. This group identified MET, IGF1R, and INSR as mRNAs that do not depend on mTORC1 activity for their translation (Thoreen et al., 2012). Together, these data suggest that the upregulation of the RTKs induced by AKT inhibitors could be controlled, at least in part, by a cap-independent mechanism.

To determine whether GSK690693 can regulate IRES-mediated translation, we transduced PC3-LN4 cells with a dual vector containing the SV-40 promoter driving the production of *Renilla* luciferase protein and an IRES controlling the level of firefly luciferase and quantitated the ratio of firefly to *Renilla* luciferase. Using the cells transduced with this vector, we found that treatment with GSK690693 induced an increase in IRES activity in constructs containing either cellular, *i.e.*, HIF1α, Myc, and VEGF (Lang et al., 2002), or viral, *i.e.*, cricket paralysis virus, CrPV, and hepatitis C virus, HCV (Landry et al., 2009) IRES sequences (Fig. 3 B). Our results are consistent with the hypothesis put forward by Muranen and colleagues that inhibition of

PI3K/mTOR could lead to enhanced cap-independent translation mediated by an IRES (Muranen et al., 2012).

To examine whether the translation of RTKs may use a cap-independent mechanism, we first determined whether the MET 5' untranslated region (UTR) contained an IRES that could be stimulated by either GSK690693 or Pim-1. The MET 5'UTR is relatively long (408 nt) and is GC-rich (Gambarotta et al., 1994), which are two common properties of IRES-containing 5'UTRs. The 5'UTR of MET was cloned and inserted in front of firefly luciferase in the dicistronic vector pRF (Stoneley et al., 1998). Upon transfection of PC3-LN4 cells, the presence of the MET 5'UTR sequence increased the expression of downstream firefly luciferase relative to *Renilla* by 38-fold compared to the negative control vector (Fig. 3 C), suggesting that it could function as an IRES. In comparison, the IRESs of encephalomyocarditis virus (EMCV), HIF1α, and VEGF produced 18-, 9-, and 13-fold increases, respectively. In PC3LN4 cells transfected with the pRF vector containing the MET IRES, overexpression of Pim-1 resulted in an increase in firefly luciferase as compared to control treatment. (Fig. 3 C). Collectively, these results indicated that Pim-1 can potentially regulate translation of MET in a cap-independent fashion.

To determine whether the MET 5'UTR is sufficient to drive translation by acting as an IRES and to rule out the possibility of a cryptic promoter in the 5'UTR of MET, we *in vitro* transcribed the pRF vector containing the MET IRES capped the dicistronic mRNA, and then transfected this mRNA directly into PC3-LN4 cells. Insertion of the MET or VEGF 5'UTR resulted in a 7- or 5-fold increase in the firefly/*Renilla* ratio, respectively, demonstrating that these sequences could function as an IRES. In

comparison, when a dual luciferase construct containing the viral EMCV IRES was transcribed, capped, and transduced into these cells, the firefly/*Renilla* ratio increased by 114-fold (Fig. 3 D). Thus, in comparison to a viral IRES, both the MET and VEGF sequences were relatively weak stimulators of protein translation. Besides MET, other RTKs including IGF1R have been reported to have IRES elements in their 5'UTRs (Giraud et al., 2001). As shown in Fig. 3 E, the IRES activity of the 5'UTR of IGF1R represented by the firefly/*Renilla* ratio was increased on treatment of the cells with GSK690693 or Pim-1 overexpression and, conversely, was decreased on knockdown of endogenous Pim-1 protein levels. Additionally, knockdown of Pim-1 in PC3-LN4 cells led to a reduction of IRES activities of viral, CrPVand HCV, and cellular, HIF1α and Myc, IRESs (Fig. 3 F). This data suggests that Pim-1 could be a more general regulator of IRES-mediated translation. This concept is further supported by our finding that the upregulation of proteins whose translation can be controlled by an IRES-mediated mechanism under cellular stress, Bcl-2, Myc, VEGF, and HIF1α, is stimulated by GSK690693 and requires Pim-1 expression (Fig. 3 G).

Combination treatment with an AKT and a Pim inhibitor synergistically blocks prostate tumor growth *in vitro* and *in vivo*

As a preliminary test of whether combined inhibition of AKT and Pim kinases might provide synergistic antitumor efficacy, we tested the effects of the inhibitors on the proliferation of PC3-LN4 cells *in vitro*. Treatment of PC3-LN4 cells with the Pim inhibitor SMI-4a in combination with the AKT inhibitor GSK690693 resulted in a synergistic enhancement of the inhibition of proliferation as demonstrated by combination index of less than 0.5 (Fig. 4 A and unpublished data). Treatment of PC3-LN4 cells with SMI-4a

in combination with GSK690693 also resulted in a markedly greater reduction in both the numbers and the size of colonies seen in a soft-agar colony formation assay than when either drug was used alone (Fig. 4 B).

To test the activity of these agents *in vivo,* PC3-LN4 cells were injected into mice and treated with GSK690693 alone, SMI-4a alone, or both drugs in combination on a daily basis for 21 days starting at 15 days after tumor implantation**.** When used alone, treatment these drugs caused a modest inhibition of tumor growth whereas the combined treatment resulted in a markedly greater inhibition of tumor growth (Fig. 4 C). As shown in Fig. 4 D, immunoblot analysis of lysates of tumors harvested at the termination of the experiment on day 36 indicated that the levels of MET, EPHA2, and HER3 protein were upregulated in the tumors from mice treated with GSK690693 alone as compared with the tumors from mice treated with vehicle alone (Fig. 4 D). This upregulation of the RTKs was reduced in the tumors from mice treated with a combination of GSK690693 and SMI-4a (Fig. 4 D).

The results of these experiments provide insights into the mechanisms underlying the compensatory interplay between AKT and Pim-1 in the regulation of tumor cell behavior influenced by the expression of RTKs. They suggest a model in which reduction in AKT activity is associated with an increase in the levels of Pim-1 protein kinase that occurs through a transcriptional mechanism. This increase in Pim-1 kinase is associated, in turn, with promotion of the expression of RTKs through a cap-independent mechanism. Downregulation of Pim-1 either by genetic means or by small molecule inhibitors blocks the feedback elevation in RTKs associated with inhibition of AKT (Fig. 4 E). Likewise inhibitors of Pim synergize with small molecule AKT inhibitors to inhibit the growth of

prostate cancer cells. Because both these kinase pathways are highly activated in human prostate cancer, dual inhibitor treatment of these tumors could be a particularly attractive strategy.

MATERIALS AND METHODS

Antibodies, drugs, and reagents. Anti-Pim-1 (Cat#3247), anti-MET (Cat#3127), anti-RON (Cat#2654), Anti-EGFR (Cat#2646), anti-IGF1R (Cat#3018), anti-INSR (Cat#3020), anti-AKT (pan, Cat#4691), anti-phospho-AKT (S473, Cat#4058), anti-phospho-AKT (T308, Cat#3127), anti-AKT1 (Cat#2938), anti-AKT2 (Cat#3063), anti-AKT3 (Cat#3788), anti-PRAS40 (Cat#2610), anti-phospho-PRAS40 (Cat#2997), anti-GSK3β (Cat#9315), anti-phospho-GSK3β (Cat#9322), anti-phospho-eIF2α (Cat#3398), anti-eIF2 α (Cat#2103) , anti-phospho-4E-BP1 (Cat#2855), anti-4E-BP1 (Cat#9452), anti-phospho-S6 (Cat#2215), anti-S6 (Cat#2317), anti-Pim-2 (Cat#4730), anti-Pim-3 (Cat#4165), and anti-Myc (Cat#9402) antibodies were purchased from Cell Signaling Technology. Anti-EPHA2 (Cat#sc-924), anti-HER3 (Cat#sc-7390), anti-HIF1α (Cat#sc-10790), anti-VEGF (Cat#sc-7269) antibodies were obtained from Santa Cruz Biotechnology. Anti-Bcl-2 antibody was from BD Transduction Laboratories (Cat#610539). Anti-β-actin (Cat#A3854) and anti-GAPDH (Cat#G9295) antibodies were bought from Sigma.

GSK690693 was kindly provided by GlaxoSmithKline for *in vitro* and *in vivo* studies.

MK2206, PP242, AZD8055 were purchased from Selleck Biochemicals.

Plasmids and siRNAs. A Pim-1 siRNA plasmid and the control plasmid were described previously (Zemskova et al., 2008). A second Pim-1 siRNA plasmid was made by using the following primers and restriction sites *Bam*HI and *Hind*III of the pSilence3.1H1puro vector: F, GATCCGATATGGTGTGTGGAGATATTCAAGAGATATCTCCACACACCATATCTTTTT

TGGAAA; R, AGCTTTTCCAAAAAAGATATGGTGTGTGGAGATATCTCTTGAATATCTCCACACACC ATATCG. A scrambled sequence was obtained based on this sequence to construct a negative control plasmid. A human Pim-1 construct, pcDNA3-Pim-1 was described elsewhere (Zemskova et al., 2008). Dicistronic luciferase plasmids containing CrPV and HCV IRES were described (Landry et al., 2009). Dicistronic luciferase plasmids containing HIF, VEGF and Myc IRES and the control plasmid pRF were described previously (Lang et al., 2002). A dicistronic luciferase plasmid containing the IGF1R IRES was described elsewhere (Meng et al., 2005).

siRNA for Pim-1 and a negative control were from Dharmacon. siRNA for AKT1/2 was were from Cell Signaling Technology. siRNA for AKT3 was from Origene.

Immunoblotting. Cells were harvested in lysis buffer A consisting of 50 mM Tris pH 7.4, 150 mM NaCl, 1% NP-40, 5 mM EDTA. Following 30 min incubation in lysis buffer at 4°C, lysates were cleared by centrifugation at 13k RPM 10 min 4°C, then protein concentrations were determined by DC Protein Assay (BioRad, Hercules, CA).

7-Methyl-GTP cap binding assay. After treatment, 5×10^5 cells were washed in phosphate-buffered saline then resuspended in lysis buffer A. After centrifugation (16,000 *g* for 10 min at 4 °C), 200 µg of protein was applied to 20 µl of m^7-GTP-sepharose 4B beads (GE Healthcare) and incubated for 3 h at 4 °C. The beads were then washed with lysis buffer A three times followed by boiling in Laemmli sample buffer.

Cell Culture and transfections. Cell lines were grown in RPMI (PC3-LN4, DU145, BT474) or DMEM (Hela, MEFs) in 5% CO2. The mouse embryo fibroblasts (MEFs)

which were triple knock-out for all Pim genes were previously described (2). Cells were transfected with lipofectamine 2000 reagent for both plasmids and siRNAs according to manufacturer's instructions.

Real-time PCR analyses. SYBR Green reactions were done using a BioRad iQ5 real-time quantitative PCR system. For data analysis, raw counts were normalized to the housekeeping gene average for the same time point and condition (ΔCt). Counts are reported as fold change relative to the untreated control ($2^{-\Delta\Delta Ct}$). All primers were designed and synthesized by Integrated DNA Technologies (IDT). The following is a list of primers used: MET-F, GCC CAA ACC ATT TCA ACT GAG; MET-R, ACC TGT TAT TGT GCT CCC AC. EPHA2-F, ACT GCC AGT GTC AGC ATC AAC C; EPHA2-R, GTG ACC TCG TAC TTC CAC ACT C. HER3-F, CGA TGC TGA GAA CCA ATA CCA G; HER3-R, ATA GCC TGT CAC TTC TCG AAT C. INSR-F, GGA AGT TAC GTC TGA TTC GAG G; INSR-R, TGA GTG ATG GTG AGG TTG TG. IGF1R-F, CCT GCA CAA CTC CAT CTT CGT G; IGF1R-R, CGG TGA TGT TGT AGG TGT CTG C. EGFR-F, AAG CCA TAT GAC GGA ATC CC; EGFR-R, GGA ACT TTG GGC GAC TAT CTG. Pim-1-F, CGA CAT CAA GGA CGA AAA CAT C; Pim-1-R, ACT CTG GAG GGC TAT ACA CTC. AKT1-F, TGG ACT ACC TGC ACT CGG AGA A; AKT1-R, GTG CCG CAA AAG GTC TTC ATG G. AKT2-F, CAT CCT CAT GGA AGA GAT CCG C; AKT2-R, GAG GAA GAA CCT GTG CTC CAT G. AKT3-F, CGG AAA GAT TGT GTA CCG TGA TC; AKT3-R: CTT CAT GGT GGC TGC ATC TGT G. β-Actin-F, CAT TGC TGA CAG GAT GCA GAA GG; β-ACTIN-R, TGC TGG AAG GTG GAC AGT GAG G.

Soft-agar colony formation assays. The soft-agar assay was performed on 6-well plates in duplicate. For each well, 5,000 cells were mixed thoroughly in cell growth

medium containing 0.7% agarose (Cat#A9045, Sigma) and GSK690693 or SMI-4a. Cells were then plated onto bottom layers prepared with 1% agarose in regular medium. Medium containing GSK690693 or SMI-4a was added to each well every four days. The assays were terminated after 21 days and colonies were stained with crystal violet and counted under a microscope.

Phospho-RTK arrays. Human Phospho-RTK arrays (R&D Systems) were utilized according to the manufacturer's instructions. Briefly, cells were washed with cold PBS and lysed in 1% Igepal CA-630 lysis buffer and 500 µg of lysates incubated with blocked membranes overnight at 4°C. Membranes were subsequently washed and exposed to chemiluminescent reagent and exposed to X-ray film. Quantification was performed by densitometry using ImageJ software.

***In vitro* transcription and RNA transfection.** The mRNAs were purified with MEGA clear kit (Ambion), quantified spectrophotometrically and their qualities were verified on a denaturing agarose gel. RNA transfection was performed with *Trans*IT®-mRNA Transfection Kit (Mirus) according to the manufacturer's suggestion. An aliquot of 1 µg of capped mRNAs and 2 µl of TransIT mRNA reagent together with 1 µl of mRNA boost reagent were used to transfect 80% confluent cells grown in 12-well plates. At 16 h after transfection cells were harvested and lysed for luciferase activity assay.

Luciferase Assays. Firefly luciferase and *Renilla* luciferase activities were measured in a luminometer (Model TD 20/20; Turner Designs) using the reagents provided with the dual luciferase reporter kit (Promega). Transfection efficiency was normalized to the corresponding *Renilla* luciferase activity for each construct. When a dicistronic vector

was used, transfection efficiency was corrected by normalizing the data to the β-galactosidase activity from a cotransfected plasmid carrying this enzyme.

Cell Proliferation Measurement. Cells were plated in 96-well plates at 3000 cells/well in 100 µl of 10% FBS-containing medium. After 72 hr incubation, the medium was replaced with 0.2% FBS medium with GSK690693, SMI-4a or DMSO. Cells viability was measured using a MTT assay. The absorbance was read at 590 nm with a reference filter of 620 nm. The Combination index was calculated using the software CalcuSyn version2.1 (Biosoft).

Animal Experiments. 4-6 week old nu/nu nude male mice were obtained from Charles River Laboratories and maintained in pressurized ventilated caging. All studies were performed in compliance with institutional guidelines under an IACUC approved protocol (MUSC#3081). For efficacy studies, mice with well-established tumors were selected and randomized approximately fourteen days post-implantation (Size > 150mm^3); PC3-LN4 xenograft tumors were established in nude mice by subcutaneously injecting 5 × 10^6 cells suspended in PBS into the right flank. Mice were treated with vehicle, GSK690693, or SMI-4a, or GSK690693 + SMI-4a at the indicated doses. GSK690693 was dissolved in 30% propylene glycol, 5% Tween-80, 65% of 5% dextrose in water(pH 4–5), and administered intraperitoneally daily while SMI-4a was dissolved in the same solvent and administered by oral gavage twice daily. Tumor dimensions were measured with a caliper and tumor volumes calculated (tumor volume (mm^3) = (length × $width^2$)/2.).

Statistical Analysis- The results of quantitative studies are reported as mean ±SD or mean ±SEM (for animal experiments).

Online supplemental materials. Contains additional data supporting the concepts presented in this paper. Fig. S1 shows upregulation of RTKs induced by GSK690693 as well as effect of GSK690693 on phosphorylation of PRAS40, GSK3β, and AKT. Fig. S2 presents results of phospho-RTK array. Fig. S3 shows Pim-1 controls neither mRNA expression of RTKs nor half-life of RTKs. Fig. S4 shows 7-Methyl-GTP cap binding analysis of cells treated with GSK690693, PP242, and AZD8055.

ACKNOWLEDGEMENTS. This work is supported by NIH Grant 1K01DK085196 (to B.C.), NIH/NCRR Grant UL1RR029882, DOD W81XWH-09-1-0300 (to A.S.K.), DOD W81XWH-10-1-0249 (to A.S.K.), and in part by pilot research funding, Hollings Cancer Center's Cancer Center Support Grant P30 CA138313 at the Medical University of South Carolina. We thank members of the Kraft laboratory, including Drs. Zanna Beharry for critical reading of the manuscript, Jin Song for helping to carry out experiments, and Marina Zemskova for providing the luciferase construct containing the human Pim-1 promoter. We are grateful to GlaxoSmithKline for supplying GSK690693. Dicistronic plasmids were kindly provided by Drs. Scott Blume, University of Alabama at Birmingham, Birmingham, AL (IGF1R); Gregory Goodall, Institute of Medical and Veterinary Science, Adelaide SA 5000, Australia (HIF, c-Myc, and VEGF); Gregg Johannes, Drexel University, Philadelphia, PA (EMCV); and Robert Gemmill, Medical University of South Carolina, Charleston, SC (CrPV and HCV).

REFERENCES

Amaravadi, R., and C.B. Thompson. 2005. The survival kinases Akt and Pim as potential pharmacological targets. *J Clin Invest* 115:2618-2624.

Bellacosa, A., C.C. Kumar, A. Di Cristofano, and J.R. Testa. 2005. Activation of AKT kinases in cancer: implications for therapeutic targeting. *Adv Cancer Res* 94:29-86.

Chakrabarty, A., V. Sanchez, M.G. Kuba, C. Rinehart, and C.L. Arteaga. 2012. Feedback upregulation of HER3 (ErbB3) expression and activity attenuates antitumor effect of PI3K inhibitors. *Proc Natl Acad Sci U S A* 109:2718-2723.

Chandarlapaty, S., A. Sawai, M. Scaltriti, V. Rodrik-Outmezguine, O. Grbovic-Huezo, V. Serra, P.K. Majumder, J. Baselga, and N. Rosen. 2011. AKT inhibition relieves feedback suppression of receptor tyrosine kinase expression and activity. *Cancer Cell* 19:58-71.

Chresta, C.M., B.R. Davies, I. Hickson, T. Harding, S. Cosulich, S.E. Critchlow, J.P. Vincent, R. Ellston, D. Jones, P. Sini, D. James, Z. Howard, P. Dudley, G. Hughes, L. Smith, S. Maguire, M. Hummersone, K. Malagu, K. Menear, R. Jenkins, M. Jacobsen, G.C. Smith, S. Guichard, and M. Pass. 2010. AZD8055 is a potent, selective, and orally bioavailable ATP-competitive mammalian target of rapamycin kinase inhibitor with in vitro and in vivo antitumor activity. *Cancer Res* 70:288-298.

Dhanasekaran, S.M., T.R. Barrette, D. Ghosh, R. Shah, S. Varambally, K. Kurachi, K.J. Pienta, M.A. Rubin, and A.M. Chinnaiyan. 2001. Delineation of prognostic biomarkers in prostate cancer. *Nature* 412:822-826.

Feldman, M.E., B. Apsel, A. Uotila, R. Loewith, Z.A. Knight, D. Ruggero, and K.M. Shokat. 2009. Active-site inhibitors of mTOR target rapamycin-resistant outputs of mTORC1 and mTORC2. *PLoS Biol* 7:e38.

Fox, C.J., P.S. Hammerman, and C.B. Thompson. 2005. The Pim kinases control rapamycin-resistant T cell survival and activation. *J Exp Med* 201:259-266.

Gambarotta, G., S. Pistoi, S. Giordano, P.M. Comoglio, and C. Santoro. 1994. Structure and inducible regulation of the human MET promoter. *J Biol Chem* 269:12852-12857.

Giraud, S., A. Greco, M. Brink, J.J. Diaz, and P. Delafontaine. 2001. Translation initiation of the insulin-like growth factor I receptor mRNA is mediated by an internal ribosome entry site. *J Biol Chem* 276:5668-5675.

Hammerman, P.S., C.J. Fox, M.J. Birnbaum, and C.B. Thompson. 2005. Pim and Akt oncogenes are independent regulators of hematopoietic cell growth and survival. *Blood* 105:4477-4483.

Hsi, E.D., S.H. Jung, R. Lai, J.L. Johnson, J.R. Cook, D. Jones, S. Devos, B.D. Cheson, L.E. Damon, and J. Said. 2008. Ki67 and PIM1 expression predict outcome in mantle cell lymphoma treated with high dose therapy, stem cell transplantation and rituximab: a Cancer and Leukemia Group B 59909 correlative science study. *Leuk Lymphoma* 49:2081-2090.

Hynes, N.E., and H.A. Lane. 2005. ERBB receptors and cancer: the complexity of targeted inhibitors. *Nat Rev Cancer* 5:341-354.

Landry, D.M., M.I. Hertz, and S.R. Thompson. 2009. RPS25 is essential for translation initiation by the Dicistroviridae and hepatitis C viral IRESs. *Genes Dev* 23:2753-2764.

Lang, K.J., A. Kappel, and G.J. Goodall. 2002. Hypoxia-inducible factor-1alpha mRNA contains an internal ribosome entry site that allows efficient translation during normoxia and hypoxia. *Mol Biol Cell* 13:1792-1801.

LoPiccolo, J., G.M. Blumenthal, W.B. Bernstein, and P.A. Dennis. 2008. Targeting the PI3K/Akt/mTOR pathway: effective combinations and clinical considerations. *Drug Resist Updat* 11:32-50.

Meng, Z., P.H. King, L.B. Nabors, N.L. Jackson, C.Y. Chen, P.D. Emanuel, and S.W. Blume. 2005. The ELAV RNA-stability factor HuR binds the 5'-untranslated region of the human IGF-IR transcript and

differentially represses cap-dependent and IRES-mediated translation. *Nucleic Acids Res* 33:2962-2979.

Muranen, T., L.M. Selfors, D.T. Worster, M.P. Iwanicki, L. Song, F.C. Morales, S. Gao, G.B. Mills, and J.S. Brugge. 2012. Inhibition of PI3K/mTOR Leads to Adaptive Resistance in Matrix-Attached Cancer Cells. *Cancer Cell* 21:227-239.

Muraski, J.A., M. Rota, Y. Misao, J. Fransioli, C. Cottage, N. Gude, G. Esposito, F. Delucchi, M. Arcarese, R. Alvarez, S. Siddiqi, G.N. Emmanuel, W. Wu, K. Fischer, J.J. Martindale, C.C. Glembotski, A. Leri, J. Kajstura, N. Magnuson, A. Berns, R.M. Beretta, S.R. Houser, E.M. Schaefer, P. Anversa, and M.A. Sussman. 2007. Pim-1 regulates cardiomyocyte survival downstream of Akt. *Nat Med* 13:1467-1475.

Nawijn, M.C., A. Alendar, and A. Berns. 2011. For better or for worse: the role of Pim oncogenes in tumorigenesis. *Nat Rev Cancer* 11:23-34.

Okuzumi, T., D. Fiedler, C. Zhang, D.C. Gray, B. Aizenstein, R. Hoffman, and K.M. Shokat. 2009. Inhibitor hijacking of Akt activation. *Nat Chem Biol* 5:484-493.

Pogacic, V., A.N. Bullock, O. Fedorov, P. Filippakopoulos, C. Gasser, A. Biondi, S. Meyer-Monard, S. Knapp, and J. Schwaller. 2007. Structural analysis identifies imidazo[1,2-b]pyridazines as PIM kinase inhibitors with in vitro antileukemic activity. *Cancer Res* 67:6916-6924.

Stoneley, M., F.E. Paulin, J.P. Le Quesne, S.A. Chappell, and A.E. Willis. 1998. C-Myc 5' untranslated region contains an internal ribosome entry segment. *Oncogene* 16:423-428.

Sussman, M.A. 2009. Mitochondrial integrity: preservation through Akt/Pim-1 kinase signaling in the cardiomyocyte. *Expert Rev Cardiovasc Ther* 7:929-938.

Suzuki, H., D. Freije, D.R. Nusskern, K. Okami, P. Cairns, D. Sidransky, W.B. Isaacs, and G.S. Bova. 1998. Interfocal heterogeneity of PTEN/MMAC1 gene alterations in multiple metastatic prostate cancer tissues. *Cancer Res* 58:204-209.

Thoreen, C.C., L. Chantranupong, H.R. Keys, T. Wang, N.S. Gray, and D.M. Sabatini. 2012. A unifying model for mTORC1-mediated regulation of mRNA translation. *Nature* 485:109-113.

Vivanco, I., and C.L. Sawyers. 2002. The phosphatidylinositol 3-Kinase AKT pathway in human cancer. *Nat Rev Cancer* 2:489-501.

Xia, Z., C. Knaak, J. Ma, Z.M. Beharry, C. McInnes, W. Wang, A.S. Kraft, and C.D. Smith. 2009. Synthesis and evaluation of novel inhibitors of Pim-1 and Pim-2 protein kinases. *J Med Chem* 52:74-86.

Yoshimoto, M., I.W. Cunha, R.A. Coudry, F.P. Fonseca, C.H. Torres, F.A. Soares, and J.A. Squire. 2007. FISH analysis of 107 prostate cancers shows that PTEN genomic deletion is associated with poor clinical outcome. *Br J Cancer* 97:678-685.

Zemskova, M., E. Sahakian, S. Bashkirova, and M. Lilly. 2008. The PIM1 kinase is a critical component of a survival pathway activated by docetaxel and promotes survival of docetaxel-treated prostate cancer cells. *J Biol Chem* 283:20635-20644.

Figure Legends

Fig. 1. AKT inhibition induces expression of Pim-1. PC3-LN4 cells were treated with (A) 5 μM GSK690693 for the times indicated, (B) increasing doses of GSK690693 as indicated for 24 h, (C) 5 μM GSK690693 or 2 μM MK2206 for 24 h, and (D) siRNAs against AKT1, AKT2, and AKT3 or a negative control siRNA for 72 h. Whole cell lysates were subjected to immunoblot analyses with the indicated antibodies. (E) Cells as in (C) were harvested and total RNA was isolated. Real-time qPCR analyses were performed with Pim-1, Pim-2, Pim-3-specific primers. Results were normalized to the expression of β-actin. (F) PC3-LN4 cells were treated with siRNAs against AKT1,2 (siA1,2), AKT3 (siA3), AKT1,2,3 (siA1,2,3), or a nontargeting control siRNA (siC) for 72 h and then RNA isolated, and real-time qPCR with indicated primers perfomred. (G) PC3-LN4 cells were transfected with a luciferase reporter containing a 3.0 kb human Pim-1 promoter. After 24 h, cells were treated with DMSO or two different doses of GSK690693 (GSK) as indicated for additional 24 h before harvesting for luciferase assays. Results were normalized to *Renilla* luciferase activity by a co-transfected plasmid carrying this enzyme. Data in A, B, C, and D are representative of at least three independent experiments. Data in E, F, and G are mean ±SD of three independent experiments.

Fig. 2. Pim-1 is required for elevated expression of RTKs induced by AKT inhibition. Immunoblot analyses were carried out with the indicated antibodies in (A) PC3-LN4 cells were treated with two different siRNAs (1 & 2) against Pim-1 as well as a nontargeting control siRNA (two left lanes) for 48 h followed by adding GSK690693 (5 μM) for additional 24 h, (B) PC3-LN4 cells and BT474 cells were treated with GSK690693 (GSK, 5 μM), or SMI-4a (4a, 10 μM), or the combination of the two

compounds for 24 h, (C) Wild-type (WT), Pim kinase triple-knockout (TKO) murine embryonic fibroblast cells were treated with 5 μM GSK690693 for 24 h, (D) PC3-LN4 cells and BT474 cells were treated with three different Pim inhibitors SMI-4a (4a, 10 μM), or SMI-16a (16a, 10 μM), or K00135 (K, 5 μM) for 24 h, (E) PC3-LN4 cells were transfected with a nontargeting control siRNA, siRNA against Pim-1, an empty vector, or a Pim-1 expressing plasmid for 72 h. Data are representative of at least two independent experiments.

Fig. 3. Pim-1 regulates RTK translation through controlling IRES activity. (A) PC3-LN4 cells were treated with GSK690693 (5 μM) alone, or in combination with PP242 (2 μM) or AZD8055 (1 μM) for 24 h, and immunoblotting performed. (B) Dicistronic luciferase plasmids containing viral (CrPV and HCV) or cellular (HIF1α, VEGF, and Myc) IRESs were transfected into PC3-LN4 cells. GSK690693 (5 μM) was added 6 h after transfection for additional 24 h. Luciferase activities were determined. (C) Dicistronic plasmids pRF, pR-EMCV-F, pR-HIF-F, pR-VEGF-F, and pR-MET-F were transfected into PC3-LN4 cells. A Pim-1 expressing plasmid was cotransfected with pR-MET-F as indicated. GSK690693 (GSK, 5 μM) was added 6 h after transfection as indicated. Luciferase activities were determined 24 h after transfection. (D) Capped, polyadenylated dicistronic mRNAs as indicated were transfected into PC3-LN4 cells. Luciferase activities were determined 16 h after transfection. The ratios of firefly/*Renilla* activities are shown relative to the ratio for RF, which was given a value of 1. (E) A dicistronic plasmid containing IGF1R IRES was transfected into PC3-LN4 cells. A Pim-1 expressing plasmid or siRNA against Pim-1 was cotransfected. GSK690693 (GSK, 5 μM) was added 6 h after transfection. Luciferase activities were determined 48 h after

transfection. (F) Dicistronic luciferase plasmids containing viral (CrPV and HCV) or cellular (HIF1α and Myc) IRESs were transfected into PC3-LN4 cells together with siRNA against Pim-1 or a nontargeting control siRNA as indicated. Luciferase activities were determined 48h after transfection. (G) PC3-LN4 cells were treated with two different siRNAs (1 & 2) against Pim-1 as well as a nontargeting control siRNA (two left lanes) for 48h followed by adding GSK690693 (5 μM) for additional 24h as indicated. Whole cell lysates were subjected to immunoblot analyses with the indicated antibodies. Data in A and G are representative of at least two independent experiments. Data in B, C, D, E, and F are mean ±SD of four independent experiments and are shown as the ratio of firefly/*Renilla* luciferase activities.

Fig. 4. Combined inhibition of AKT and Pim demonstrates synergistic antitumor activity. (A) PC3-LN4 cells were treated with increasing doses of GSK690693 and SMI-4a (4a) as indicated in media containing 0.2% serum for 72 h followed by a MTT assay. Similar results were obtained from three independent experiments. One representative experiment is shown. (B) PC3-LN4 cells were plated in 10% serum and 0.7% agarose-containing medium with 10 μM of GSK690693 or 4a alone or in combination. Colonies were stained with crystal violet and counted after 21 days. Data are mean ±SD of three independent experiments. Bar, 200 μM. (C) Nu/Nu nude mice bearing PC3-LN4 tumors were randomized into four groups: vehicle, GSK690693 (30 mg/kg i.p. daily), 4a (60 mg/kg oral twice/day), and the combination of GSK690693 and 4a. Tumor size was measured every three days. The results are presented as the mean tumor volume ±SEM (n = 6 mice/group). (D) Immunoblot analyses of tumors in (C) with the indicated antibodies. Tumors were harvested 6 h after the last dose of therapy on Day 36. The

numbers above each lane represent individual tumors of that treatment group. (E) A model for feedback upregulation of RTK expression mediated by Pim-1 kinase. AKTi, AKT inhibitors; Pimi, Pim inhibitors.

Supplemental Figure Legends

Fig.S1. AKT inhibition induces expression of RTKs. (A) PC3-LN4 cells were treated with GSK690693 as indicated for 24 h. Whole cell lysates were subjected to immunoblot analyses with the indicated antibodies. (B) Extracts from (A) were probed by Western blotting for the AKT substrates and AKT phosphorylation. Data are representative of at least two independent experiments.

Fig.S2. Phospho-RTK array analysis of cells treated with AKT and Pim inhibitors. PC3-LN4 cells were treated with GSK690693 (GSK, 5 μM), or SMI-4a (4a, 10 μM), or the combination of the two compounds for 24 h. 500 μg of whole cell lysates was applied to each blot for phospho-RTK array analyses. Data are representative of two independent experiments.

Fig.S3. Pim-1 does not control RTK mRNA expression or protein half-life. (A) A Pim-1 expressing construct or a vector control was transfected into PC3-LN4 cells for 48 h before RNA isolation and real-time qPCR was carried out. (B) A siRNA against Pim-1 or a nontargrting control siRNA was transfected into PC3-LN4 cells for 72h. RNA was isolated and real-time qPCR performed. Data in A and B are mean ±SD of three independent experiments. (C) A Pim-1 expressing construct or the vector control was transfected into PC3-LN4 cells for 48h before cycloheximide (CHX, 100 μg/ml) was

added. Cells were harvested at the indicated time points for immunoblot analyses with the indicated antibodies. Data are representative of two independent experiments.

Fig.S4. mTORC inhibitors suppress cap-dependent initiation. PC3-LN4 cells were treated with GSK690693 (5 μM), PP242 (2 μM), and AZD8055 (1 μM) for 24 h. Cell lysates were incubated with m7-GTP-Sepharose. Elutes and whole cell lysates (WCL) were subject to immunoblot analyses with the indicated antibodies. Data are representative of three independent experiments.

Fig. 1

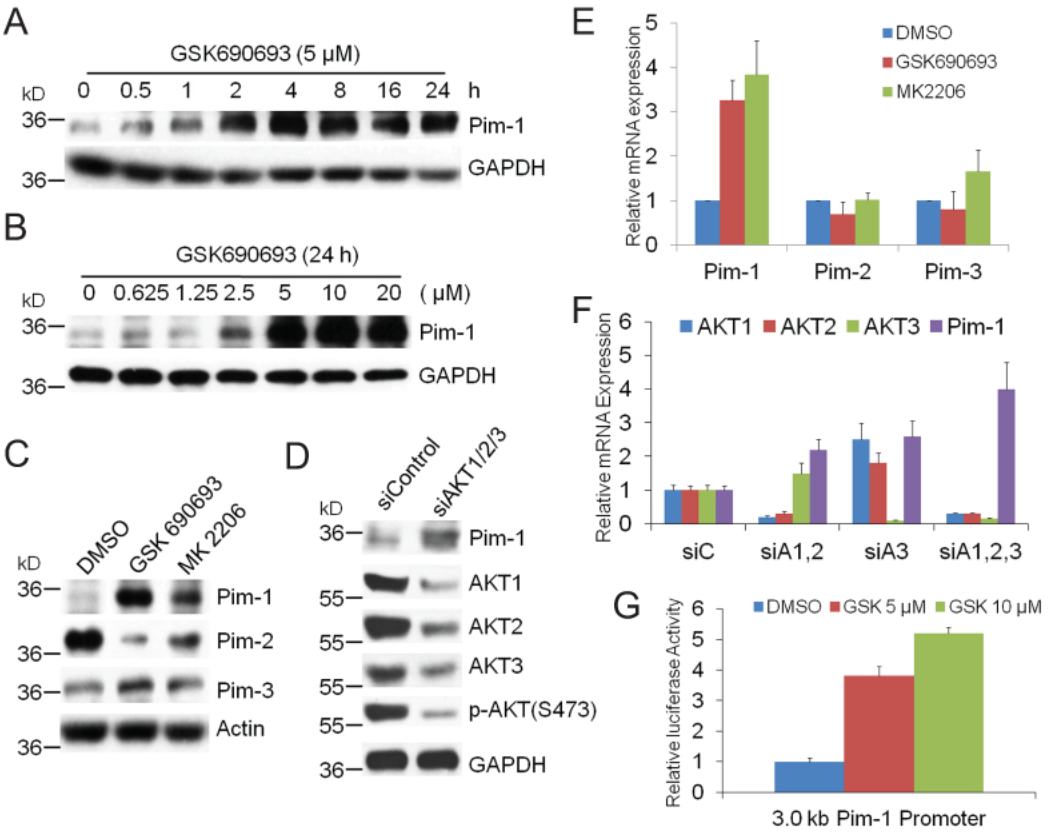
A
GSK690693 (5 μM)
kD
0 0.5 1 2 4 8 16 24 h
36
Pim-1
36
GAPDH
B
GSK690693 (24 h)
kD
0 0.625 1.25 2.5 5 10 20 (μM)
36
Pim-1
36
GAPDH
C
DMSO
GSK 690693
MK 2206
kD
36
Pim-1
36
Pim-2
36
Pim-3
36
Actin
D
siControl
siAKT1/2/3
kD
36
Pim-1
55
AKT1
55
AKT2
55
AKT3
55
p-AKT(S473)
36
GAPDH
E
Relative mRNA expression
0 1 2 3 4 5
DMSO
GSK690693
MK2206
Pim-1
Pim-2
Pim-3
F
Relative mRNA Expression
0 1 2 3 4 5 6
AKT1
AKT2
AKT3
Pim-1
siC
siA1,2
siA3
siA1,2,3
G
Relative luciferase Activity
0 1 2 3 4 5 6
DMSO
GSK 5 μM
GSK 10 μM
3.0 kb Pim-1 Promoter

Fig. 2

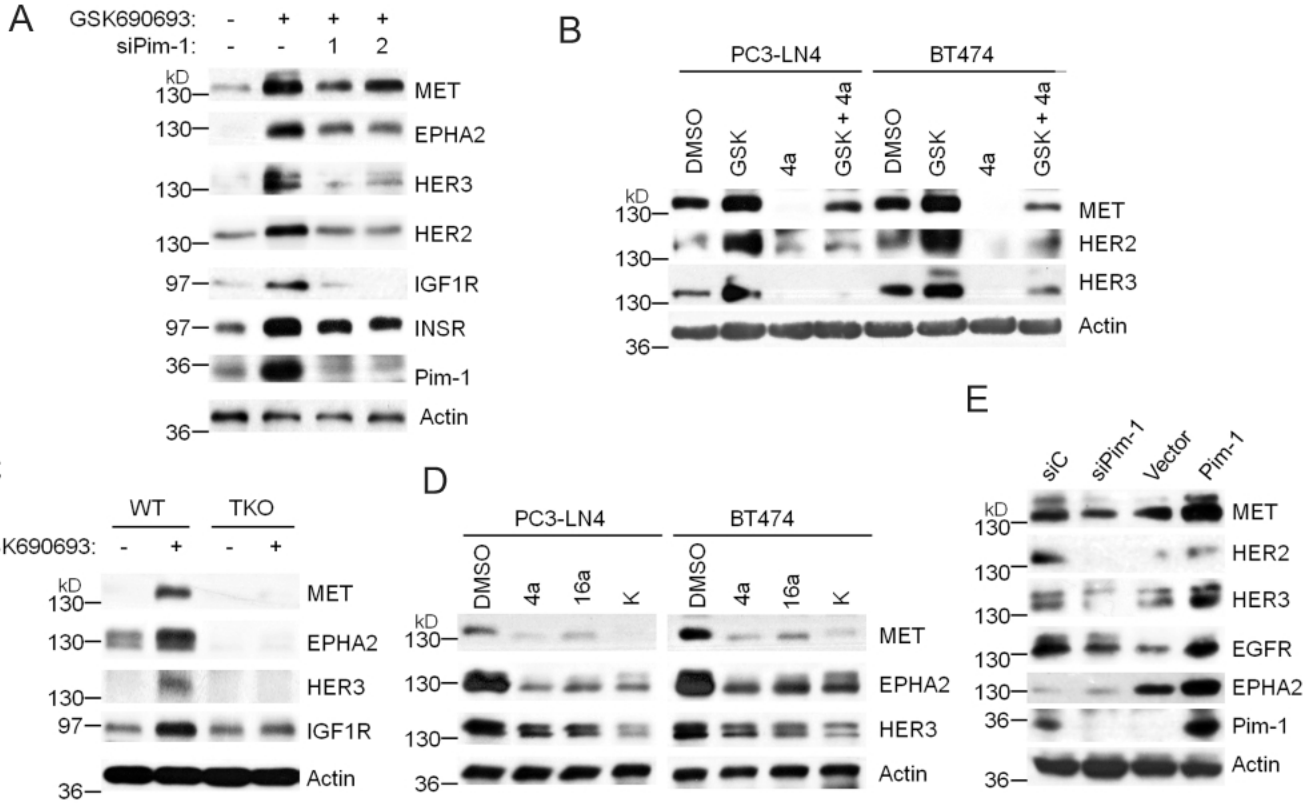
A
GSK690693: - + + +
siPim-1: - - 1 2
kD
130
MET
EPHA2
HER3
HER2
97
IGF1R
INSR
36
Pim-1
Actin
B
PC3-LN4
BT474
DMSO
GSK
4a
GSK + 4a
MET
HER2
HER3
Actin
C
WT
TKO
GSK690693: - + - +
D
PC3-LN4
BT474
DMSO
4a
16a
K
E
siC
siPim-1
Vector
Pim-1
HER2
HER3
EGFR
EPHA2

Fig. 3

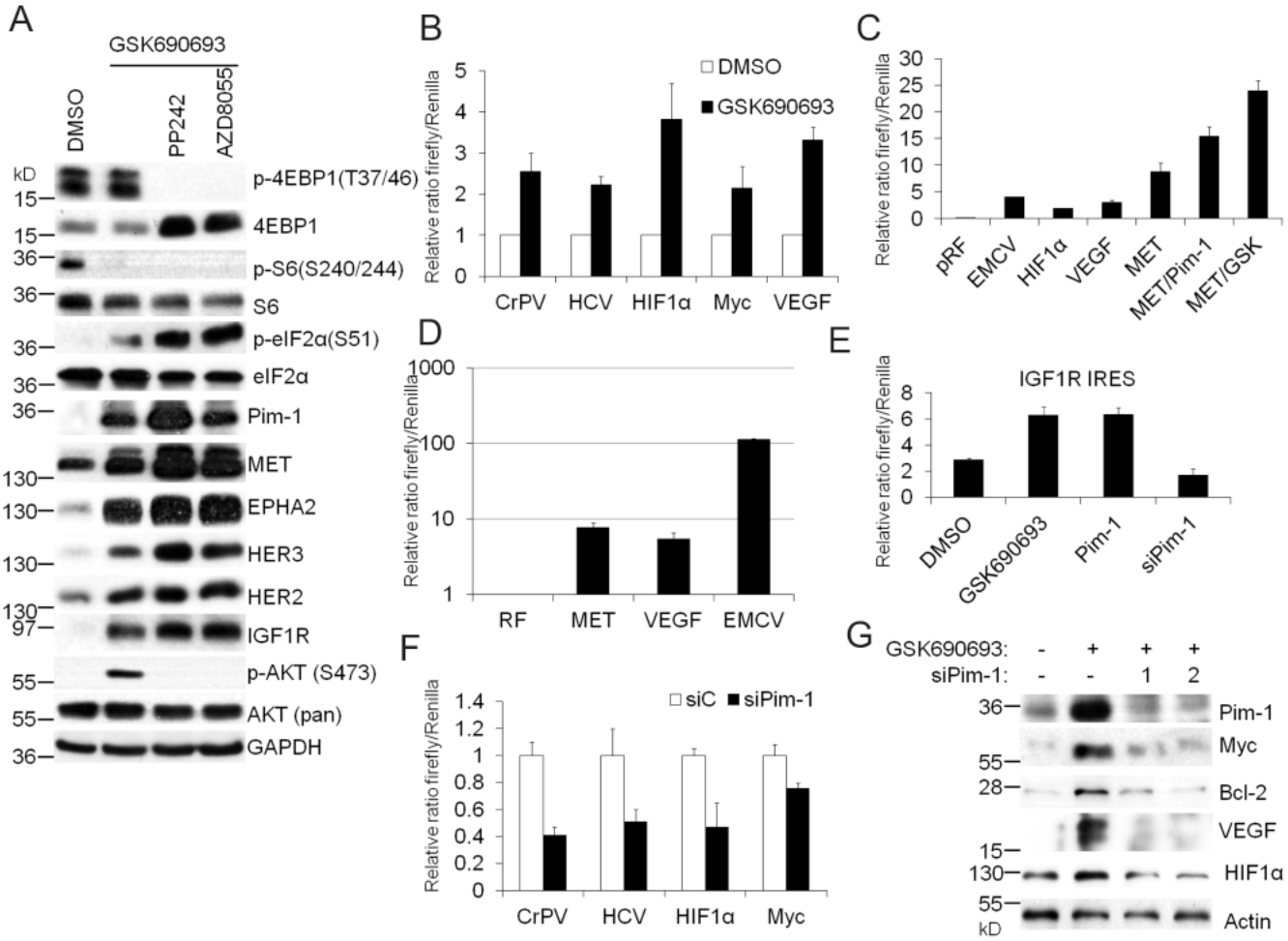
A
GSK690693
DMSO
PP242
AZD8055
kD
p-4EBP1(T37/46)
4EBP1
p-S6(S240/244)
S6
p-eIF2α(S51)
eIF2α
Pim-1
MET
EPHA2
HER3
HER2
IGF1R
p-AKT (S473)
AKT (pan)
GAPDH
B
DMSO
GSK690693
Relative ratio firefly/Renilla
CrPV
HCV
HIF1α
Myc
VEGF
C
Relative ratio firefly/Renilla
pRF
EMCV
HIF1α
VEGF
MET
MET/Pim-1
MET/GSK
D
Relative ratio firefly/Renilla
RF
MET
VEGF
EMCV
E
IGF1R IRES
Relative ratio firefly/Renilla
DMSO
GSK690693
Pim-1
siPim-1
F
siC
siPim-1
Relative ratio firefly/Renilla
CrPV
HCV
HIF1α
Myc
G
GSK690693:
siPim-1:
Pim-1
Myc
Bcl-2
VEGF
HIF1α
Actin
kD

Fig. 4

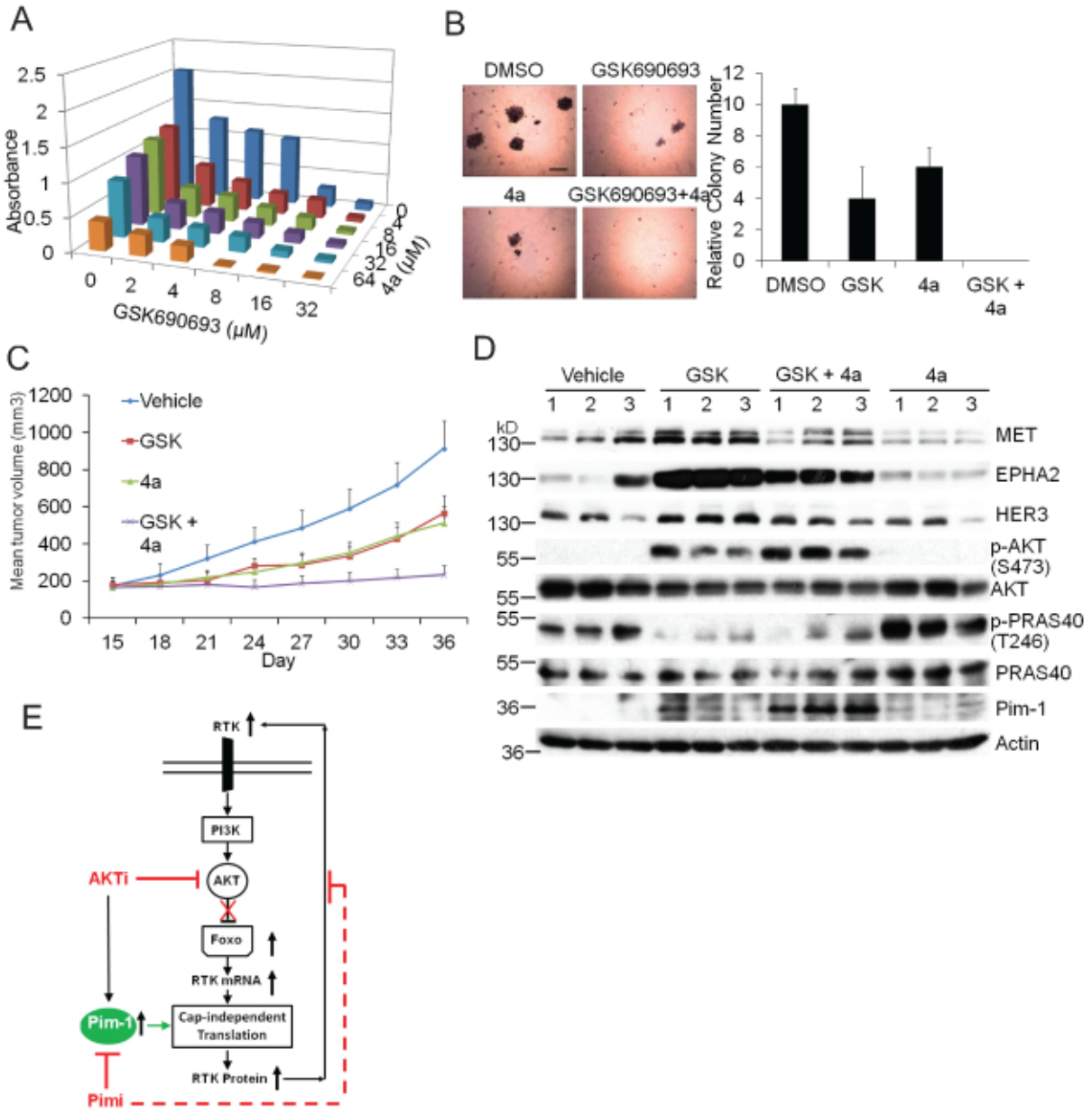
A
Absorbance
2.5
2
1.5
1
0.5
0
0
2
4
8
16
32
GSK690693 (μM)
4a (μM)
B
DMSO
GSK690693
4a
GSK690693+4a
Relative Colony Number
12
10
8
6
4
2
0
DMSO
GSK
4a
GSK + 4a
C
Mean tumor volume (mm3)
1200
1000
800
600
400
200
0
Vehicle
GSK
4a
GSK + 4a
15
18
21
24
27
30
33
36
Day
D
Vehicle
GSK
GSK + 4a
4a
1 2 3 1 2 3 1 2 3 1 2 3
kD
130
130
130
55
55
55
55
36
36
MET
EPHA2
HER3
p-AKT (S473)
AKT
p-PRAS40 (T246)
PRAS40
Pim-1
Actin
E
RTK
PI3K
AKT
AKTi
Foxo
RTK mRNA
Pim-1
Cap-independent Translation
RTK Protein
Pimi

Fig. S1

A

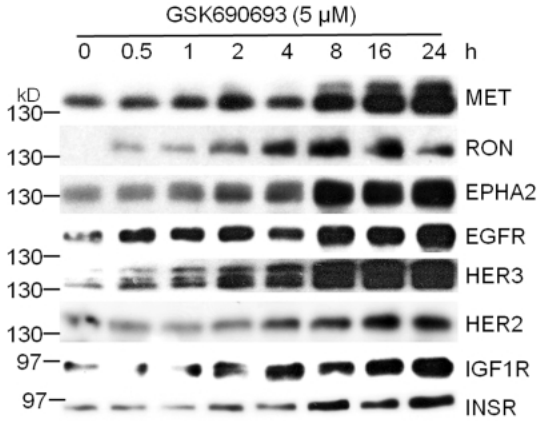
GSK690693 (5 μM)
0 0.5 1 2 4 8 16 24 h
kD
130
MET
130
RON
130
EPHA2
EGFR
130
HER3
130
HER2
130
97
IGF1R
97
INSR

B

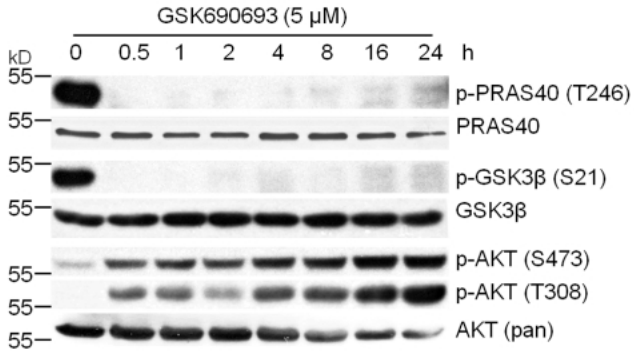
GSK690693 (5 μM)
kD
0 0.5 1 2 4 8 16 24 h
55
p-PRAS40 (T246)
55
PRAS40
55
p-GSK3β (S21)
55
GSK3β
55
p-AKT (S473)
55
p-AKT (T308)
55
AKT (pan)

Fig. S2

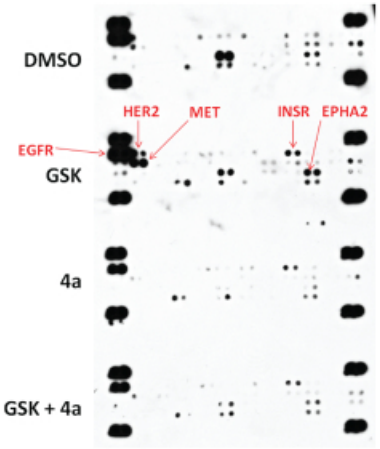

Fig. S3

A

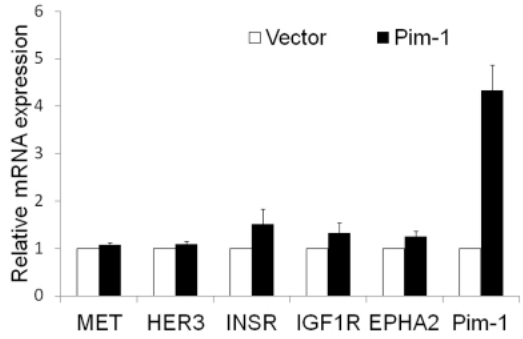
Relative mRNA expression
Vector
Pim-1
0
1
2
3
4
5
6
MET
HER3
INSR
IGF1R
EPHA2
Pim-1

B

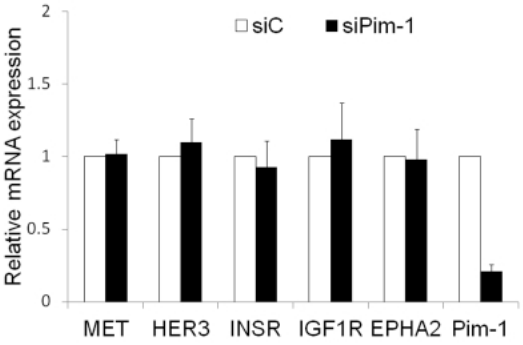
Relative mRNA expression
siC
siPim-1
0
0.5
1
1.5
2
MET
HER3
INSR
IGF1R
EPHA2
Pim-1

C

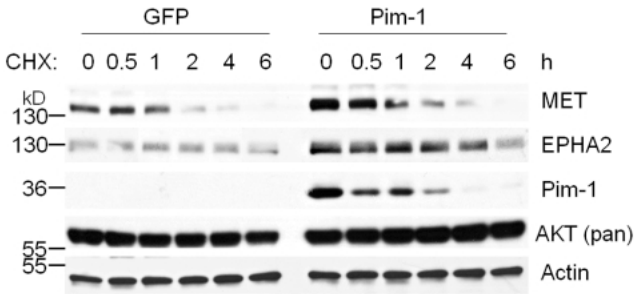
GFP
Pim-1
CHX:
0 0.5 1 2 4 6
0 0.5 1 2 4 6
h
kD
130
130
36
55
55
MET
EPHA2
Pim-1
AKT (pan)
Actin

Fig. S4

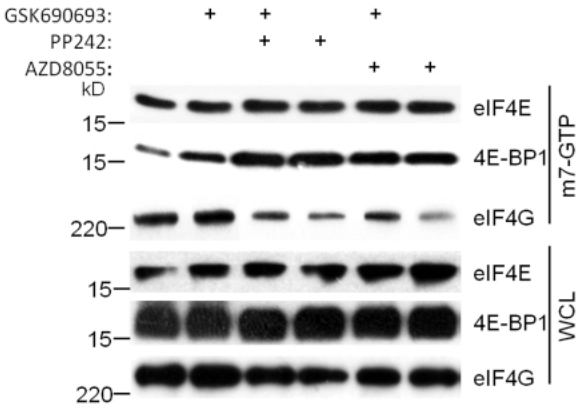
GSK690693:
PP242:
AZD8055:
kD
15
15
220
15
15
220
eIF4E
4E-BP1
eIF4G
eIF4E
4E-BP1
eIF4G
m7-GTP
WCL